

Distribution Agreement

In presenting this thesis as a partial fulfillment of the requirements for a degree from Emory University, I hereby grant to Emory University and its agents the non-exclusive license to archive, make accessible, and display my thesis in whole or in part in all forms of media, now or hereafter now, including display on the World Wide Web. I understand that I may select some access restrictions as part of the online submission of this thesis. I retain all ownership rights to the copyright of the thesis. I also retain the right to use in future works (such as articles or books) all or part of this thesis.

Ruohan Chen

April 7, 2023

Synthesis of alkyl analogues of 1,4-dihydropyridine for developing novel treatment
against chemoresistance in prostate cancer

By

Ruhan Chen

Frank McDonald
Adviser

Chemistry

Frank McDonald
Adviser

Soria Jose
Committee Member

James Kindt
Committee Member

2023

Synthesis of alkyl analogues of 1,4-dihydropyridine for developing novel treatment
against chemoresistance in prostate cancer

By

Ruohan Chen

Frank McDonald

Adviser

An abstract of a thesis submitted to the Faculty of Emory College of Arts and Sciences
of Emory University in partial fulfillment
of the requirements of the degree of
Bachelor of Science with Honors

Chemistry

2023

Abstract

Synthesis of alkyl analogues of 1,4-dihydropyridine for developing novel treatment against chemoresistance in prostate cancer

By Ruohan Chen

Prostate cancer is the leading cancer-related cause of death among male patients in the United States. The development of chemoresistance in prostate cancer calls for urgent emphasis in development of novel treatment to address this medical need. Recent studies have revealed that cancer cells are highly dependent on the EED-EZH2 signaling pathway as a mechanism of chemoresistance, and EED protein inhibition may be the key to target chemoresistance by disrupting EED-EZH2 protein interaction. Nicardipine, among all of the existing known EED inhibitors, constitutes the most ideal candidate due to its advanced known drug profile. This thesis presents the synthesis and characterization of a novel class of analogues for screening and selecting optimal clinical candidates for cancer treatment development. Since the antihypertensive effect is undesirable and the nitrophenyl ring attached to the C4 position of nicardipine is suspected to be an active calcium channel-blocking component, the rational design consists of replacing the nitrophenyl ring with other substituents—specifically, cyclic and acyclic alkyl groups. Overall, the 1,4-dihydropyridine analogues were synthesized using the Hantzsch condensation, and most entries gave adequate overall yields of 30% to 40%. Significant effort was invested into optimizing the purification process to ensure substantial purity of all analogues for biological screening assay. All compounds were thoroughly characterized prior to biological testing for structural activity relationships, and future direction of synthesis were determined based on preliminary SAR results. We have successfully identified multiple candidates with optimal cellular activities with great potential to proceed into the clinical trials.

Synthesis of alkyl analogues of 1,4-dihydropyridine for developing novel treatment
against chemoresistance in prostate cancer

By

Ruohan Chen

Frank McDonald

Adviser

A thesis submitted to the Faculty of Emory College of Arts and Sciences
of Emory University in partial fulfillment
of the requirements of the degree of
Bachelor of Science with Honors

Chemistry

2023

Acknowledgements

Special thanks to Dr. Frank McDonald and 2nd year graduate student San Pham for mentorship and guidance through this project and thesis

Huge appreciation for:

All members of the McDonald Laboratory:

Paul Beasley, PhD Candidate;

Emily Williamson, 3rd year graduate student;

Taehee Kim, 3rd year graduate student;

Erika Diosdado Castro, 3rd year graduate student;

Nyasha Musoni, Sophomore undergraduate student

Honors Thesis committee members

Dr. Jose Soria and Dr. James Kindt

Project collaborator

Dr. Daqing Wu Laboratory and Dr. Paul Xie Laboratory

Table of Contents

Introduction/Background	1
Review of existing literature	5
Methods	10
Result and analysis	
---General discussion of experimental outcome	13
---Spectroscopic analysis	18
---SAR result and other aims	24
Conclusion	27
References	29
Supporting information	
---Experimental procedure	32
---Mass spectrometry	36
---Nuclear magnetic resonance spectra	44

Introduction/Background

Prostate cancer is one of the most common types of cancer, as well as one of the leading cancer-related causes of death among men, occurring in the prostate gland where seminal fluid is produced. Prostate cancer has a slow growth rate and is usually confined in the prostate gland; it is usually asymptomatic during early stages, making early detection and treatment difficult. Many symptoms, such as dysuria, bladder blockage, and urinary frequency, start to develop when the cancer enters an advanced stage, and is often controlled with treatment that reduces testosterone level. Castration-resistant prostate cancer (CRPC) is a type of advanced prostate cancer that minimally responds to the treatment, which means signs of growth are still evident in the physical environment even though the testosterone level is low. As the disease progresses, they are capable of spreading to the other organ systems, starting with adjacent lymph nodes, and eventually making their way to the liver, lungs, and even the brain (Urology Care Foundation, 2020).

Treatment of metastatic castration-resistant prostate cancer has been a challenge in the history of therapeutic development. Docetaxel, one of the earliest and most promising cytotoxic therapy, is often used in chemotherapy for patients with advanced prostate cancer as a standard of care. Docetaxel is usually administered weekly or every three weeks, with significant decline in prostate-specific antigen (PSA) levels in patients during clinical trials. However, Docetaxel treatment can ultimately lead to development of resistance against the treatment. This may be caused by autophagy, a highly conserved lysosome-dependent mechanism that can perform ordered degradation and recycling to maintain cellular homeostasis and survival under stressful

environments--in this case, chemotherapy. Therefore, relevant research attention is needed to address such urgent medical needs for current and future patients who suffer from prostate cancer.

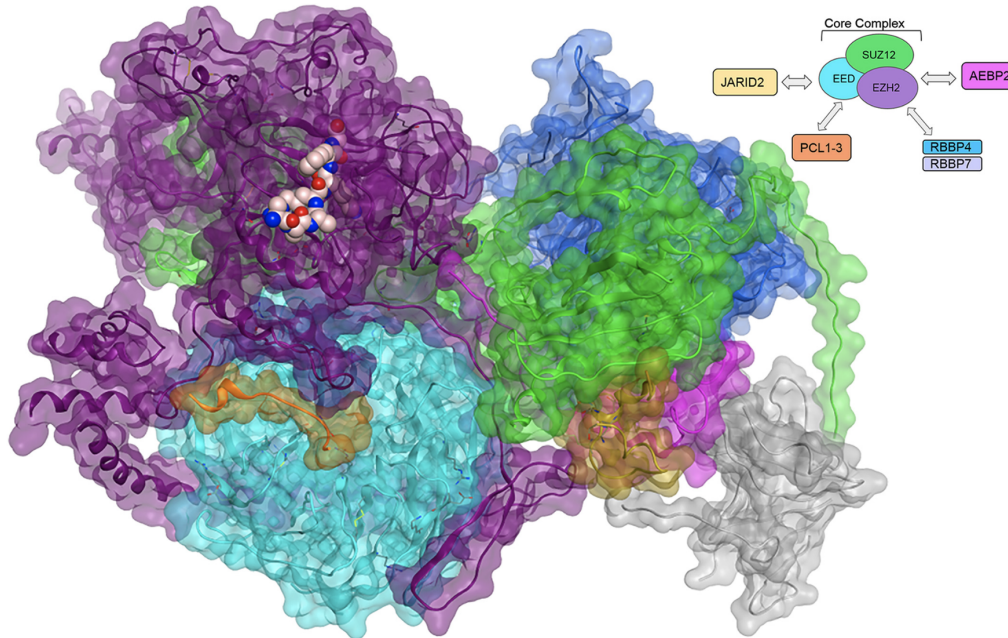


Figure 1. A surface structure of polycomb repressive complex 2 (PRC2, PDB ID 6C23). The core structural feature of PRC2 contains EED, EZH2, and SUZ12 (Kouznetsova *et al*, 2019).

Figure reference: Kouznetsova, V. L., Tchekhanov, A., Li, X., Yan, X., & Tsigelny, I. F. Polycomb repressive 2 complex—molecular mechanisms of function. *Protein Science*, **2019**; 28(8), 1387-1399.

Recent studies revealed that cancer cells are highly dependent on the EED-EZH2 signaling pathway as a mechanism of chemoresistance for the enhancement of survival (Li *et al*, 2021). The enhancer of zeste homolog 2 (EZH2), catalytic subunit of polycomb repressive complex 2 (PRC2), functions as an initial activator of the survival signaling cascade, which includes the activation of signal transducer and activator of transcription 3 (Stat3), S-phase kinase-associated protein 2 (SKP2), ATP binding cassette B 1 (ABCB1) and survivin. However, the embryonic ectoderm development (EED) protein that closely interacts with EZH2 is a possible control switch for the process. When other small molecules bind EED, interaction

between EZH2 and EED is disrupted. This results in ubiquitin-mediated EZH2 degradation, and hence suppresses the survival signaling cascade. This finding lays prospective novel strategy for developing treatment for chemoresistance in castration-resistant prostate cancer, with a specific aim of EED inhibition with competent small molecules.

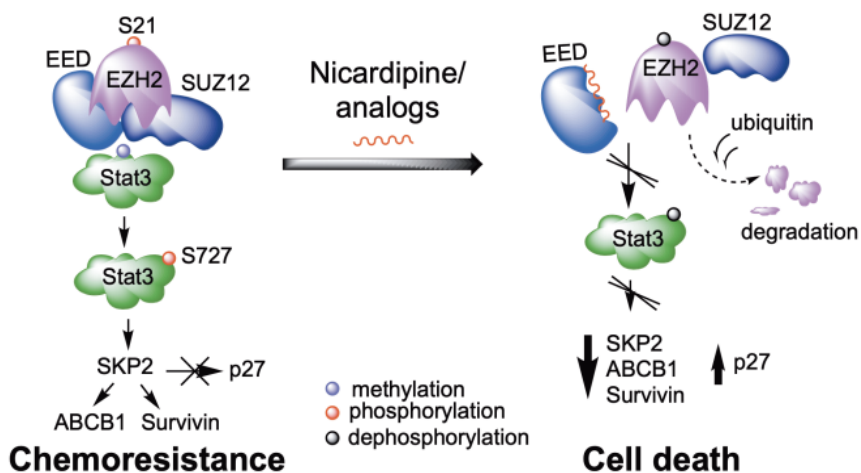


Figure 2. Demonstration of nicardipine analogs as inhibitors of cancer cell survival signaling cascade, through disruption of EED-EZH2 protein-protein interaction that results in the degradation of EZH2 and termination of the signaling pathway (Wu *et al*, accepted with minor revision, *Br. J. Cancer*, 2023).

The FDA-approved anti-hypertensive medication, nicardipine HCl acts as a calcium channel blocker, which achieves its function by blocking the influx of calcium ions into the circulatory system, thereby reducing a patient's blood pressure by inducing vasodilation and decreasing cardiac output. Recently, nicardipine has recently been identified as a potential competent candidate for treating chemoresistant prostate cancer, due to its ability to selectively and potently inhibit the EED (embryonic ectoderm development) protein associated with histone methylation (Wu *et al*, accepted with minor revision, *Br. J. Cancer*, 2023), which induces cell cycle arrest and apoptosis of target cancer cells.

A concern with implementing nicardipine as a part of the cancer therapeutic treatment is the undesirable antihypertensive side effect that the compound was originally designed for.

According to preliminary studies done by Dr. Daqing Wu's laboratory at Clark Atlanta University, the nitrophenyl ring substituent in the nicardipine compound is associated with calcium channel blocker activity, which is a key component to target under the circumstance that antihypertensive activity is unwanted. However, with respect to the core purpose of the project, it is also vital to ensuring that alteration of the nitrophenyl ring does not reduce the EED inhibiting activity of the resulting analogue.

To test the hypothesis that the nitrophenyl ring substituent in the nicardipine compound does not affect biological activity towards EED protein binding, a series of nicardipine derivative synthesis to replace the nitrophenyl substituent with other functional groups was carried out through rational design. This project is a structure-activity relationship study, in collaboration with Dr. Daqing Wu's lab, to identify structural requirements to maintain nicardipine's function towards treating prostate cancer while minimizing its calcium channel blocking activity responsible for treating hypertension.

Review of Existing Literature

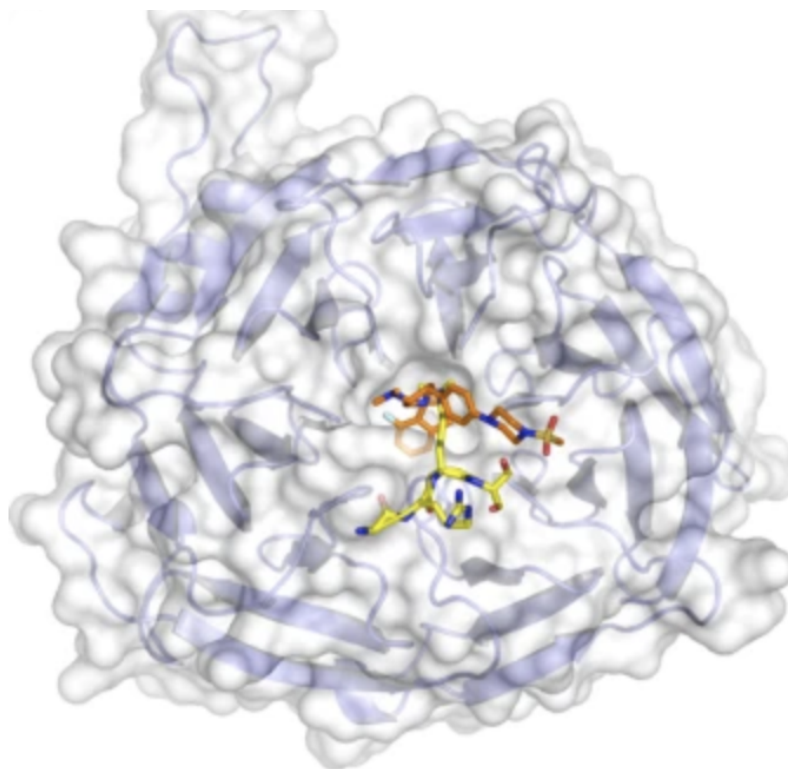


Figure 3. Crystal structure of A-395 binds to EED, with stick structure representing the A-395 and blue ribbon with white surface representing the EED protein (He *et al*, 2017).

Figure reference: He, Y., Selvaraju, S., Curtin, M. L., Jakob, C. G., Zhu, H., Comess, K. M., ... & Pappano, W. N. The EED protein–protein interaction inhibitor A-395 inactivates the PRC2 complex. *Nature chemical biology*, **2017**; 13(4), 389-395.

Prior to the current interest in nicardipine as a novel EED inhibitor, many studies have uncovered mechanisms and compounds with EED-inhibiting activity that contribute to the big picture. Huang and colleagues proposed the potential viable strategy of development of anticancer treatment through methyltransferase activity of PRC2 through binding to the K27Me3 pocket of EED (Huang *et al*, 2017). During the same year, He and colleagues discovered that the allosterically activated catalytic activity of PCR2 is adequately inhibited when identified A-395, an antagonist of H3K27me3 substrate (He *et al*, 2017), binds to EED in the H3K27me3-binding

pocket that plays a vital role in repressive gene silencing (Margueron *et al*, 2009). More recently, Huang's group identified a new clinical candidate, MAK683 (N-((5-fluoro-2, 3-dihydrobenzofuran-4-yl)methyl)-8- (2-methylpyridin-3-yl)-[1,2,4]triazolo [4,3-c] pyrimidin -5-amine), which is an optimized candidate from previously discovered EED226 that showed undesirable mild to moderate adrenal reticularis degeneration during a two-week toxicology study in mice (Qi *et al*, 2017; Huang *et al*, 2022). MAK683 achieves EED inhibition through binding of the EED Me3 pocket with remarkable selectivity and requirement of lower dosage during clinical trial; furthermore, preclinical pharmacokinetic and metabolism studies of MAK683 demonstrated its predicted high oral bioavailability, low potential for drug-drug interaction with common co-administered medication, and favorable metabolism and excretion pathway (Zhang *et al*, 2022).

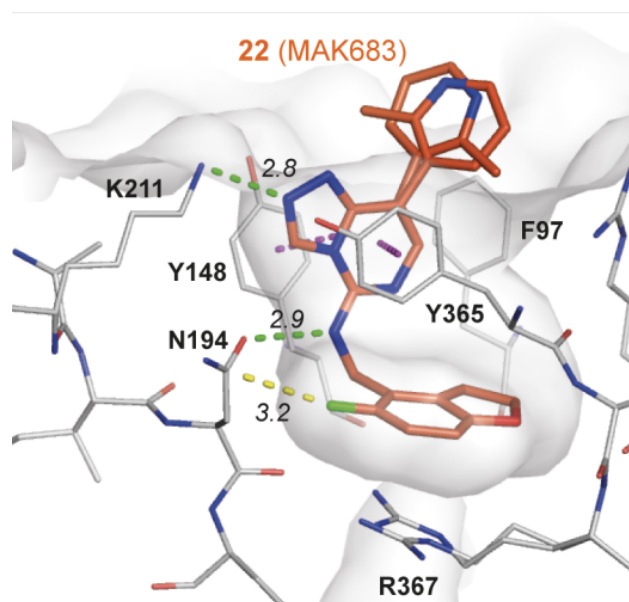


Figure 4. X-ray structure of MAK683 binds to EED, with orange and blue stick structure representing the MAK683 (Huang *et al*, 2022).

Figure reference: Huang, Y., Sendzik, M., Zhang, J., Gao, Z., Sun, Y., Wang, L., ... & Oyang, C. Discovery of the clinical candidate MAK683: An EED-directed, allosteric, and selective PRC2 inhibitor for the treatment of advanced malignancies. *Journal of medicinal chemistry*, **2022**; 65(7), 5317-5333.

Dr. Daqing Wu's lab, in collaboration with Dr. Haiyan Fu's group at Emory University, discovered exciting features of nicardipine with potentiality to act against chemoresistance in prostate cancer. When testing nicardipine activity in cancer cells, not only did it demonstrate ability to induce cell cycle arrest and apoptosis, there is also a presence of selectivity to act upon chemoresistant cells when compared to chemosensitive lines, showing a greater cytotoxicity and lower IC₅₀ value when interacting with target cells. In addition, nicardipine was shown to be a competent EED inhibitor through molecular docking analyses, in which multiple structural features of nicardipine directly interact with and bind to EED protein with optimal binding affinity. Hence, the disturbance in EED-EZH2 interaction by nicardipine leads to a serial inhibition of the survival signaling cascade, which means the cell concentrations of transcription 3 (Stat3), S-phase kinase-associated protein 2 (SKP2), ATP binding cassette B 1 (ABCB1) and survivin are further reduced.

Although multiple EED-inhibitor candidates have been discovered in recent years, nicardipine has a significant advantage with regards to developing novel treatments compared to other identified inhibitors such as MAK683, which require thorough experimental and clinical trials starting from scratch. Repurposing an existing FDA-approved medication like nicardipine is promising, since nicardipine analogue has a known drug profile with minimal concerns for toxicity and adverse reaction. With the above preliminary results, this project orients to dig deeper into the in vitro and in vivo efficacy of nicardipine as a candidate for treating chemoresistant prostate cancer. Through in vitro screening of nicardipine analogue activities in PCa cells, the project aims to identify specific mechanisms of action, including specific EED binding site, effect on EED-EZH2 protein interactions, and noncanonical EZH2 signaling pathway. In the future, in vivo experiments will be done to examine correlations among selected

analogues in treatment, tumor regression, and cancer cell survival rate. This will also address the concern of possible toxicity and adverse reactions that some nicardipine analogues may exhibit when functioning in living organisms, which is an important consideration for therapeutic development.

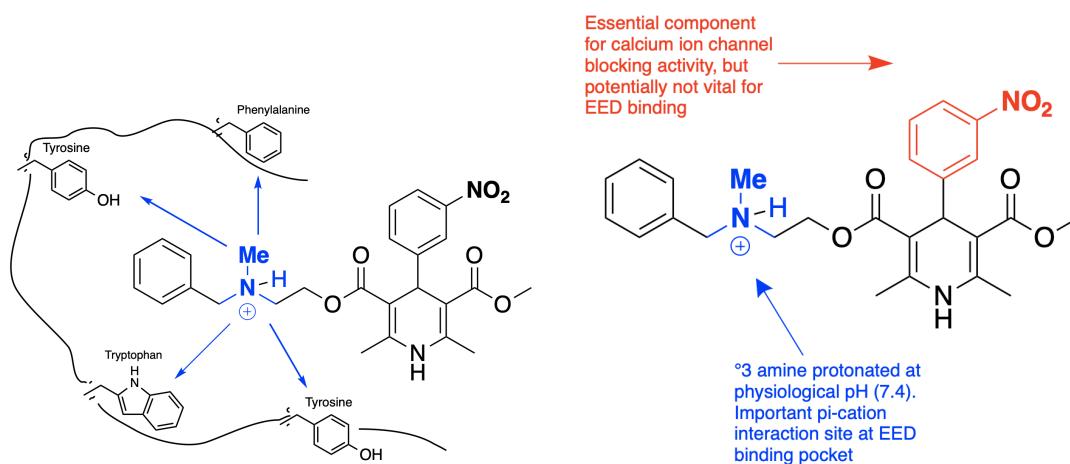


Figure 5. Structural features and functions of protonated nicardipine and interaction with aromatic amino acid side chains (phenylalanine, tyrosine, and tryptophan) in EED binding pocket.

The preliminary rational design of nicardipine-derived analogues consists of two major classes. First generation analogues maintain the structure of the core 1,4-dihydropyridine and vary the linker and tertiary amine, which manipulates the distance and dihedral angle between the ammonium cation and EED binding pocket, which graduate student, San Pham, is currently preparing. This Honors thesis describes an initial family of second generation analogues that replace the presumably active calcium channel blocking component nitrophenyl ring located on chiral carbon 4 position (C4) introduced through the three-component Hantzsch dihydropyridine synthesis. More specifically, the work aims to replace nitrophenyl ring with other cycloalkyl and branched acyclic alkyl substituents, to identify promising nicardipine-derived analogues to carry forward into future clinical stages of metastatic castrate-resistant prostate cancer treatment. I also

invested efforts in synthesizing other compounds of similar features, such as amlodipine, for the possibility of equal, or even better, activity in chemoresistant PCa cells.

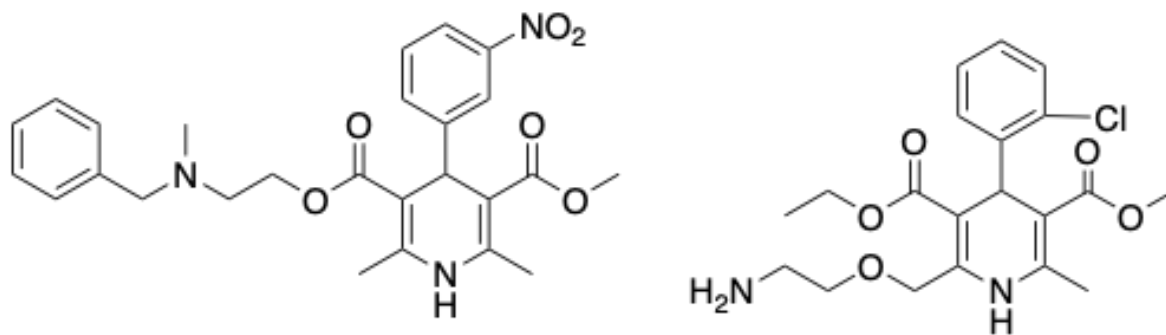
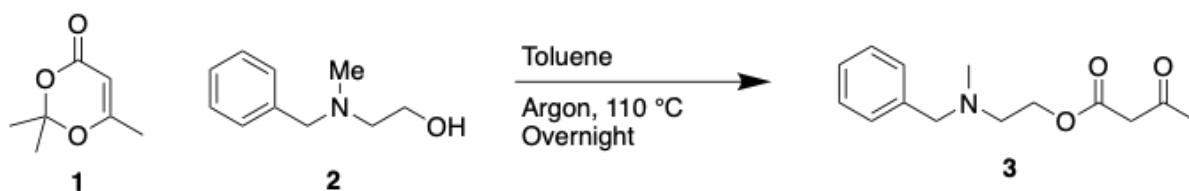


Figure 6. Comparison of molecular structures of nicardipine (left) and amlodipine (right).

Methods

All of the 1,4 dihydropyridines were prepared following the Hantzsch dihydropyridine synthesis, using precursor 2-(Benzylmethylamino) ethyl acetoacetate, methyl-3-aminocrotonate, and an aldehyde species with target substituent R. This is a three-component, one-step cyclocondensation reaction that is optimal for generation of analogue library, since the diversity can be achieved by simply varying the reacting component, in this case, the functional group on the aldehyde starting material. Reaction progress of all steps depicted below can be conveniently monitored using thin layer chromatography.

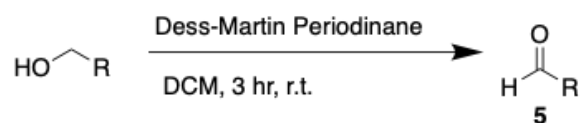
Scheme 1. 1,4 dihydropyridine precursor 2-(Benzylmethylamino) ethyl acetoacetate (compound **3**) synthesis



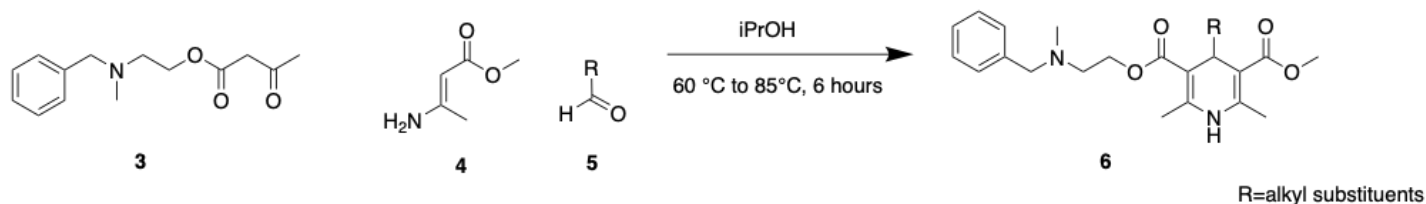
In the first step, commercially available 2,2,6-trimethyl-4H-1,3-dioxin-4-one (compound **1**) and 2-benzyl(methyl)amino ethanol (compound **2**) was utilized to synthesize the precursor 2-(Benzylmethylamino) ethyl acetoacetate (compound **3**), following existing experimental procedures (Mao *et al*, 2013; Lacotte *et al*, 2013). The synthesis was a convenient one-pot reaction, and the resulting product was easily separated from a small residual unreacted alcohol starting reagent. Purification of crude products through column chromatography using 50%:50%

ethyl acetate to hexane showed excellent separation and proceeded with no complication, giving a promising final yield of 85% consistently with changes in scales from 5 mmol to 20 mmol.

Scheme 2. Dess-Martin oxidation



Aldehydes (compound 5) that were of interest but are too expensive or commercially unavailable (cyclopentyl acetaldehyde and cyclobutylacetaldehyde) were synthesized by oxidizing the primary alcohol precursor (Liebeschuetz *et al*, 2000) using commercially available Dess–Martin periodinane (DMP). Although formation of aldehyde products was prominent as indicated by TLC and NMR, there is consistent difficulty in separation of iodo-compound byproduct of the Dess-Martin oxidation reaction during workup. Due to the volatility of aldehyde compounds, impurities present in the crude was not removed using column chromatography secondary to the potential alteration of products by the acidic silica gel; instead, the crude material was used directly in the following 1,4-dihydropyridine synthesis with no associated complication.

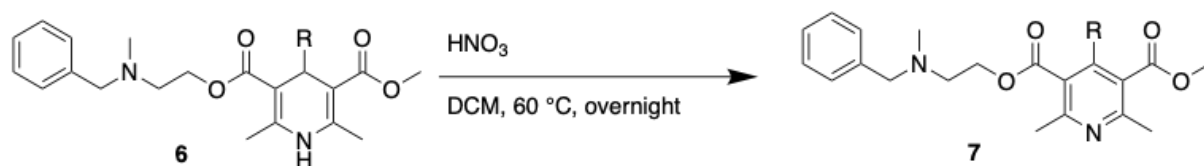


Scheme 3. Nicardipine dihydropyridine analog synthesis.

Next, the targeted 1,4 dihydropyridine analogues (compound 6) were prepared through the Hantzsch synthesis (Iqbal & Knaus, 1996) using commercially available methyl-3-aminocrotonate (compound 4), commercially available aldehyde species (or aldehyde obtained

from in-lab oxidation of commercially available alcohol species in scheme 2, compound **5**), and the beta-ketoester precursor (compound **3**) synthesized in **Scheme 1**.

Scheme 4. Nicardipine pyridine analog transformation from dihydropyridine through oxidation.



In the attempt of limiting the variability at the C4 chiral carbon location and potentially increasing the potency of the analogue, oxidation of 1,4 dihydropyridine analogues to pyridine using nitric acid (Shibanuma *et al*, 1980) was performed to examine the effect of removing the chirality at the location where substituents are introduced.

All of the 1,4-dihydropyridine analogues were synthesized using the Hantzsch condensation, with most entries giving adequate overall yields of 30% to 40%. Mild deviation in reaction temperature (compare entry 1 and entry 9, Table 1.) and extension in reaction time from 6 hours to overnight (compare entry 1 and entry 12, Table 1.) exert no significant changes to the experimental outcome.

Column chromatography as a purification method initially proceed using solvent system of 50%:50% ethyl acetate to hexane (entries 1-3, Table 1.); however, ¹H NMR analysis of some compounds showed presence of small impurity, which required performing a second column chromatography to remove the residual impurity to eliminate any potential confounding variables or cellular damage during the following in vitro cellular screening process. Using 40%:60% ethyl acetate to hexane as a generalized solvent system seems to be sufficient for the 6 of the compounds (entries 1b, 2, 3, 4, 5, 8, Table 1.), giving clean products with no need for further purification. Few exceptions are longer and branched substituents (entries 6, 7, 9, Table 1.) that show poor separation between product and residual starting material, which required additional adjustment in the solvent system to 30%:70% ethyl acetate to hexane for adequate separation and purification.

Table 1. Results of reaction and purification conditions evaluated for the preparation of 1,4-dihydropyridine analogues using various cycloalkyl and branched acyclic alkyl aldehydes.

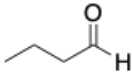
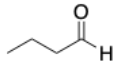
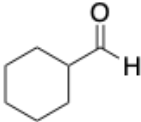
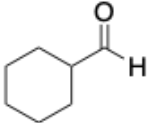
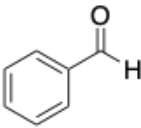
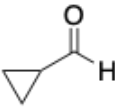
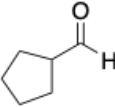
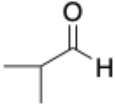
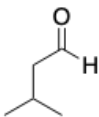
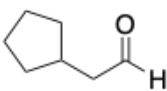
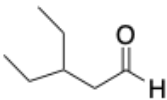
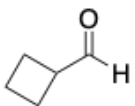
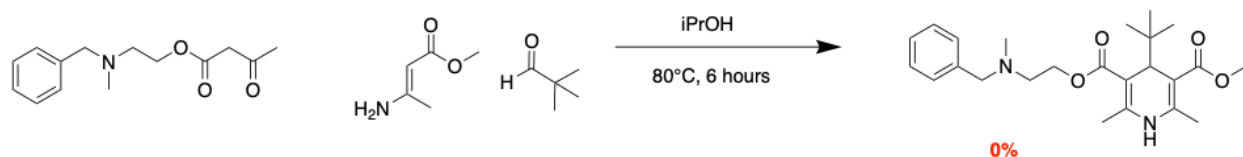
Entry	Exp #	Aldehyde	Experimental Condition	Eluent Solvent ratio	Isolated Yield
1a	RHC-57		Argon, 75°C, 5.5 hrs iPrOH	50%:50% EtOAc: Hexane	40%
**1b	RHC-77		Argon, 80°C, overnight iPrOH	40%:60% EtOAc: Hexane	45%
2a	RHC-58		Argon, 75°C, 5.5 hr iPrOH	50%:50% EtOAc: Hexane; 40%:60% EtOAc: Hexane	35%
**2b	RHC-78		Argon, 80°C, overnight iPrOH	40%:60% EtOAc: Hexane	40%
3	RHC-59		Argon, 75°C, 5.5 hr iPrOH	50%:50% EtOAc: Hexane; 40%:60% EtOAc: Hexane	30%
4	RHC-71		Argon, 80°C, 6 hr iPrOH	40%:60% EtOAc: Hexane	45%
5	RHC-72		Argon, 80°C, 6 hr iPrOH	40%:60% EtOAc: Hexane	45%
6	RHC-73		Argon, 80°C, 6 hr iPrOH	40%:60% EtOAc: Hexane 30%:70% EtOAc: Hexane	20%
7	RHC-75		Argon, 80°C, 6 hr iPrOH	40%:60% EtOAc: Hexane 30%:70% EtOAc: Hexane	35%

Table 1. Continued.

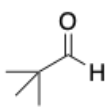
Entry	Exp #	Aldehyde	Experimental Condition	Eluent Solvent ratio	Isolated Yield
8	RHC-88		Argon, 85°C, 6 hr iPrOH	40%:60% EtOAc: Hexane	UND
9	RHC-89		Argon, 85°C, overnight iPrOH	40%:60% EtOAc: Hexane 30%:70% EtOAc: Hexane	35%
10	RHC-90		Argon, 85°C, overnight iPrOH	40%:60% EtOAc: Hexane 30%:70% EtOAc: Hexane	In-progress

Entries marked with ** are compounds that were previously synthesized and later repeated.

Scheme 5. Reaction of pivaldehyde 1,4-dihydropyridine analogue synthesis (RHC-74).

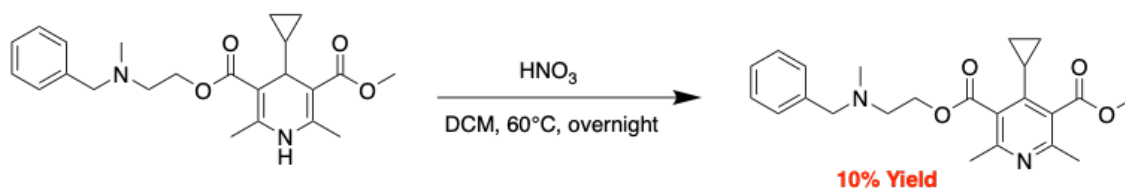
On a special note, the reaction using pivaldehyde showed no evidence of reaction progress and no formation of product--¹H NMR showed mainly unreacted starting materials. The hypothesized reason is that the reaction site is severely hindered by the bulky tert-butyl group.

Table 2. Pivaldehyde analogue synthesis.

Entry	Exp #	Aldehyde	Experimental Condition	Eluent Solvent ratio	Isolated Yield
1	RHC-74		Argon, 80°C, 6 hr iPrOH	--	0%

To answer the question raised regarding the effect of chirality at the C4 position on EED protein binding activity, oxidation reaction was performed on the 1,4-dihydropyridine analogues for transformation into corresponding pyridine, which is a metabolic product from nicardipine. The experimental protocol closely follows the procedure by Shibamura's group, who performed the oxidation on similar 1,4-dihydropyridine without the terminal benzyl methylamino group and with a nitrophenyl substituent.

Scheme 6. Oxidation of cyclopropyl 1,4-dihydropyridine analogue (RHC-76).



Initial oxidation reaction of cyclopropyl dihydropyridine analogue was successful, although with a low overall yield of 10%. However, the proceeding oxidation reactions conducted on cyclopentyl, isopropyl, and isobutyl dihydropyridine analogues did not yield desired products. Crude NMR showed starting material along with other impurities, and column chromatography using a solvent system of 5:5 ethyl acetate to hexane recovered around 30% of starting material. Further efforts to synthesize the pyridine analogues were terminated after preliminary SAR proved the pyridine compound RHC-76 was biologically inactive.

Table 3. Results of reaction and purification conditions evaluated for the nitric acid oxidation of 1,4-dihydropyridine analogues to pyridine.

Entry	Exp #	DHP	Reaction Condition	Eluent Solvent ratio	Isolated Yield
1	RHC-76		Room air, 60 °C, overnight DCM	50%:50% EtOAc: Hexane	10%

Spectroscopic Analysis

All ten synthesized 1,4-dihydropyridine compounds were characterized using ^1H NMR after synthesis. For six of the analogues, we also obtained ^{13}C NMR, 2D NMR (COSY, HSQC, and HMBC), and high-resolution mass spectra. Assignments of carbons and protons were consistent across all synthesized derivatives, with a few interesting findings that are worth highlighting. Thorough data collection, analyses, and assignments of the cyclopropyl derivative (RHC-71) and isobutyl derivative (RHC-75) are provided below as examples.

The combination of ^1H NMR and HSQC gives valuable insight into the assignment of para versus ortho/meta position on the benzene ring. By taking a closer look at the 600 MHz ^1H NMR, the apparent multiplet in the aromatic region can be separated into an overlapping multiplet at 7.37 to 7.28 ppm integrating to 4H and a triplet of triplet at 7.23 ppm that integrates to 1H (**Figure 18**). With this information in hand, the proton at the para position is apparent; with careful examination of the corresponding region in HSQC, the carbon peak at the 127 ppm region can be correlated with the para proton (**Figure 24**). Unfortunately, not much information can be inferred from the spectra regarding meta versus ortho positions at this point due to them being too close in proximity on both the ^1H NMR and ^{13}C NMR.

Quaternary carbons were assigned using additional two-bond and three-bond correlations provided by HMBC (**Figure. 8** and **Figure. 9**). Specifically, two carbonyl positions in the 168 ppm region were easily distinguished by looking at correlation with methoxy group versus the methylene group; C1/C2 versus C3/C5 of dihydropyridine ring were correlated with C-H bond at the C4 position and the alkyl substituents; quaternary carbon on the benzene ring was sorted out using correlation with the NMe protons. However, there is no definitive evidence found for

distinguishing C1 from C2 and C3 from C5 due to the close proximity of the ^{13}C chemical shifts. Similarly, carbon pairs of the alkyl substituents (T/U, **Figure 8**; S/T, **Figure 9**.) and the two methyl groups directly attached to the dihydropyridine cannot be separated from one another due to near-identical characteristics and close proximity of chemical shifts of both carbons and protons.

Table 4. Nuclear magnetic resonance spectroscopic analysis of cyclopropyl derivative of 1,4-dihydropyridine (RHC-71). Diastereotopic atoms labeled with *.

Chemical shift ^{13}C	^1H (Determined by HSQC)	Assignment
A, 168.78 ppm	--	Carbonyl
B, 168.21 ppm	--	Carbonyl
C, 144.93 ppm	--	Dihydropyridine
D, 144.88 ppm	--	Dihydropyridine
E, 138.93 ppm	--	Ipsso, phenyl
F, 128.95 ppm	7.28-7.37 ppm, overlapping m, 4H	Ortho/Meta, phenyl
G, 128.24 ppm	7.28-7.37 ppm, overlapping m, 4H	Ortho/Meta, phenyl
H, 127.02 ppm	7.23 ppm, tt, J=1.6 Hz, 7.0 Hz, 1H	Para, phenyl
I, 102.48 ppm	--	Dihydropyridine
J, 102.45 ppm	--	Dihydropyridine
K, 62.55 ppm	*3.57 ppm, s, 2H	N-benzylic CH_2
L, 61.62 ppm	*4.29 ppm, d of apparent dt, J= 6.0 Hz, 11 Hz, 2H	O- CH_2
M, 55.73 ppm	*2.74 ppm, apparent t, J=6.0 Hz, 2H	N- CH_2
N, 50.89 ppm	3.67 ppm, s, 3H	O- CH_3
O, 42.36 ppm	2.27 ppm, s, 3H	N- CH_3
P, 35.08 ppm	3.65 ppm, d, J=7.6 Hz, 1H	CH (C4)
Q, 19.57 ppm	2.31/2.30 ppm, s, 3H	C- CH_3 (dihydropyridine)
R, 19.42 ppm	2.31/2.30 ppm, s, 3H	C- CH_3 (dihydropyridine)
S, 17.92 ppm	0.81 ppm, m, 1H	CH (cyclopropyl)
T, 1.90 ppm	*0.23 ppm, overlapping m, 4H	C-(CH_2 - CH_2 -)
U, 1.86 ppm		C-(CH_2 - CH_2 -)
--	5.75 ppm, broad singlet, 1H	N-H

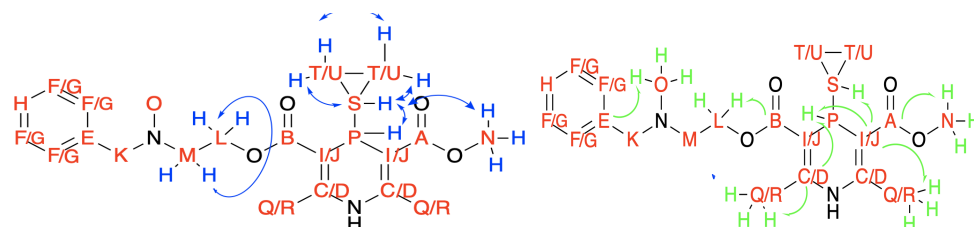


Figure 8. COSY correlation of cyclopropyl dihydropyridine derivative (left). Carbons letter-coded in red; protons involved and respective COSY correlation shown in blue. HMBC correlation of cyclopropyl dihydropyridine derivative (right). Carbons letter-coded in red; protons involved and respective HMBC correlation shown in green.

The presence of a chiral center at the C4 position of dihydropyridine gives rise to diastereotopic atoms, which can complicate coupling patterns of protons that are affected. In the cyclopropyl derivative, diastereotopic atoms are seen in the 4.29 ppm region in the ^1H NMR, showing two overlapping doublet of triplet integrating to 2H (**Figure 19.**). Although the multiplet at 0.23 ppm with 4H integration (**Figure. 20**) can not be deduced any further, they correspond to the two methylene diastereotopic in the cyclopropyl substituent. The alkyl diastereotopic protons are seen in the 1.14 ppm region of the isobutyl derivative, showing two overlapping multiplets (**Figure 34.**), however, the diastereotopic proton in the 4.30 ppm in the cyclopropyl derivative shows up as an apparent triplet in the isobutyl derivative (**Figure 35.**).

Following the diastereotopic discussion, the comparison between the dihydropyridine with its oxidized form--pyridine--is rather interesting secondary to the absence of the previous chiral center at C4. The alkyl region in the ^1H NMR of the cyclopropyl dihydropyridine derivative (**Figure. 20**) is compared against that of its oxidized pyridine form (**Figure 41.**). Not only are alkyl protons more deshielded in the pyridine compound, the resolution of the previous multiplet into a triplet of doublet is evident, each integrating to 2H, corresponding with the two methylene groups.

While characterizing the cyclopentyl dihydropyridine derivative (RHC-72), minor impurities in the ^{13}C NMR, most evidently in the 165-170 ppm region (**Figure 28.**) complicates the assignment process. The same obstacle was encountered by Szeleszczuk's group when attempting to characterize nicardipine. They concluded that nitro-analogues and halogen-analogues of 1,4-dihydropyridine compounds are UV-sensitive and can undergo light-induced aerobic oxidation of pyridine aromatization, which gives rise to a minor impurity in the spectrum (Szeleszczuk *et al*, 2018). Due to alkyl analogues of dihydropyridine compounds being a

relatively novel class of compounds that have barely been studied before, the light-induced aerobic oxidation mechanism has not been validated in this class of compounds; however, we can reasonably hypothesize that the light-induced aerobic oxidation has also occurred secondary to the similarity in relative chemical shifts of the dihydropyridine compound and the minor impurity.

Table 5. Nuclear magnetic resonance spectroscopic analysis of isobutyl derivative of 1,4-dihydropyridine (RHC-75). Diastereotopic labeled with *.

Chemical shift ^{13}C	^1H (Determined by HSQC)	Assignment
A, 168.67 ppm	--	Carbonyl
B, 167.97 ppm	--	Carbonyl
C, 144.94 ppm	--	Dihydropyridine
D, 144.74 ppm	--	Dihydropyridine
E, 141.07 ppm	--	Ipso, phenyl
F, 128.98 ppm	7.30-7.37 ppm, overlapping m, 4H	Ortho/Meta, phenyl
G, 128.25 ppm	7.30-7.37 ppm, overlapping m, 4H	Ortho/Meta, phenyl
H, 127.16 ppm	7.26 ppm, tt, J=1.5 Hz, 6.8 Hz, 1H	Para, phenyl
I, 103.97 ppm	--	Dihydropyridine
J, 103.92 ppm	--	Dihydropyridine
K, 62.53 ppm	*3.57 ppm, s, 2H	N-benzylic CH_2
L, 61.54 ppm	*4.29 ppm, apparent t, J= 6.0 Hz, 2H	O- CH_2
M, 55.68 ppm	*2.74 ppm, m, 2H	N- CH_2
N, 50.83 ppm	3.70 ppm, s, 3H	O- CH_3
O, 46.67 ppm	1.14 ppm, overlapping m, 2H	CH_2 (isobutyl)
P, 42.38 ppm	2.29 ppm, s, 3H	N- CH_3
Q, 30.82 PPM	3.98 ppm, t, J=6.7 Hz, 1H	CH (C4)
R, 23.76 ppm	1.48 ppm, apparent heptet, J=6.5 Hz, 1H	CH (isobutyl)
S, 23.26 ppm	*0.88 ppm, d, J=6.5 Hz, 9.5 Hz, 3H	CH_3 (isobutyl)
T, 22.74 ppm	*0.86 ppm, d, J=6.5 Hz, 3H	CH_3 (isobutyl)
U, 19.54 ppm	2.31/2.30 ppm, s, 3H	C- CH_3 (dihydropyridine)
V, 19.38 ppm	2.31/2.30 ppm, s, 3H	C- CH_3 (dihydropyridine)
--	5.75 ppm, broad singlet, 1H	N-H

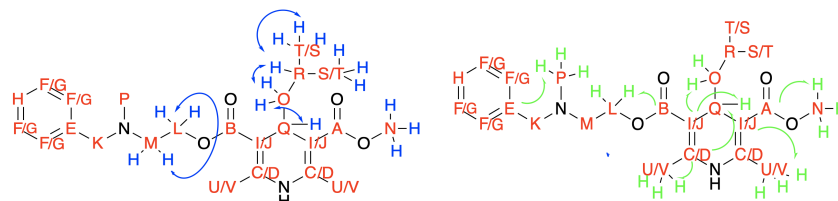


Figure 9. COSY correlation of the isobutyl dihydropyridine derivative (left). Carbons letter-coded in red; protons involved and respective COSY correlation shown in blue. HMBC correlation of cyclopropyl dihydropyridine derivative(right). Carbons letter-coded in red; protons involved and respective HMBC correlation shown in green.

A final note in this section is made with respect to the mass spectrometry. The data obtained from mass spectrometry well-align with the characterization of all compounds with the exception of the 3-methylpentane derivative (RHC-89), which shows a peak mass at 357.18056 ppm in the positive atmospheric pressure chemical ionization (APCI) study instead of its exact mass of 428.27 g/mol. In addition, negative APCI, positive ESI, and negative ESI were used in addition to positive APCI, with no identity of molecular ion in the 428 ppm region. Although the data does not indicate the presence of the molecular ion, the peak mass is consistent with the fragmentation of the 3-methylpentane substituent from the synthesized compound followed by a protonation after rearrangement to form aromaticity, which is a mechanism that was evident in other analogues as well. Another vital information obtained from the mass spectra that consolidates the characterization is the presence of peaks that are one value greater than all the $[M+H]^+$ with a relative percentages of 24% to 28%. This information corresponds to the number of carbons in the formula of these analogues and the natural abundance of the ^{13}C isotope.

SAR Results and Other Aims

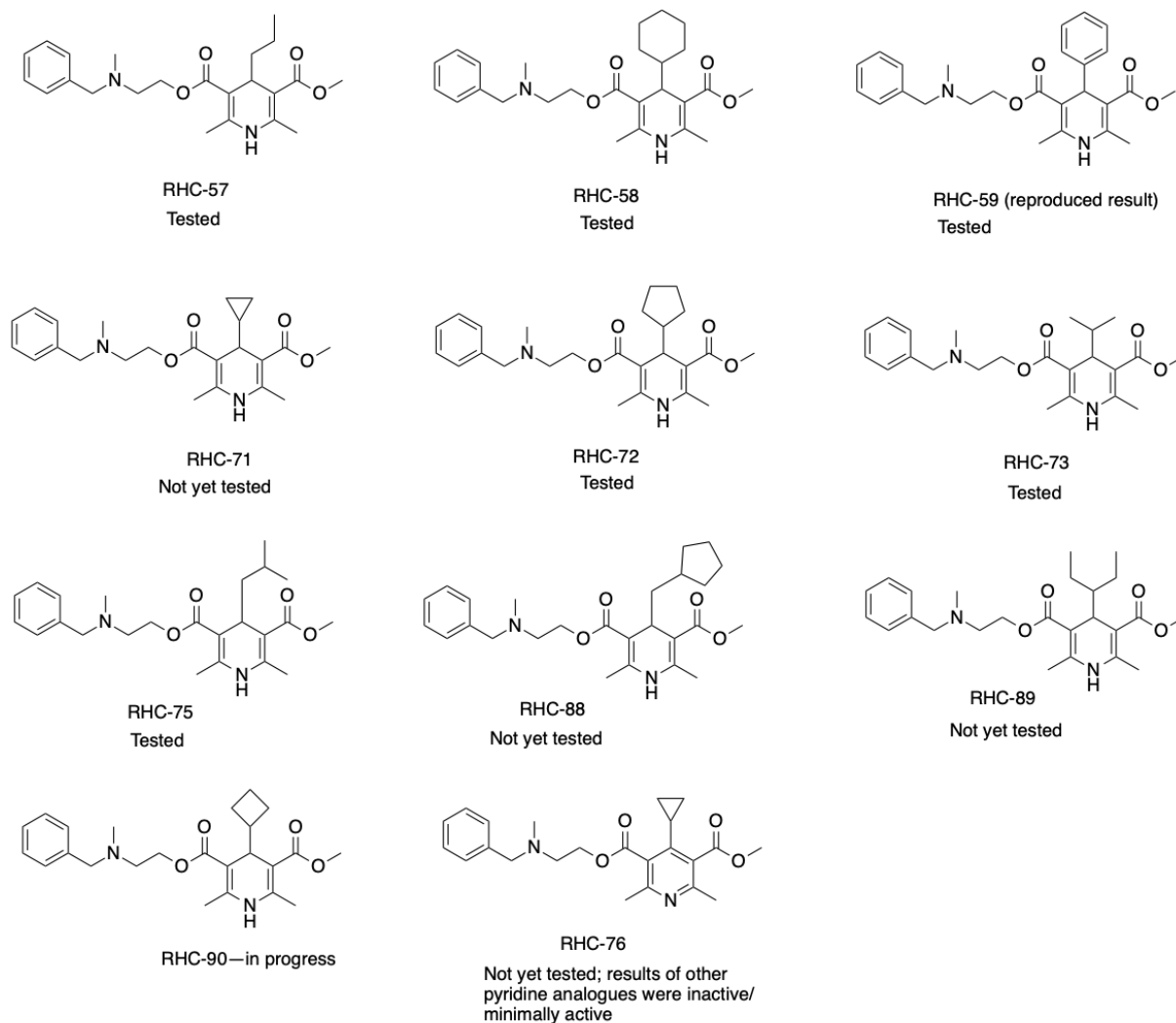


Figure 12. Synthesized compounds with status of structure-activity relationship assay.

Synthesized analogues were delivered to Dr. Daqing Wu's laboratory for cellular biological assay to evaluate IC_{50} for determination of cytotoxicity in comparison to daily nicardipine. The above figure displays the available preliminary structure-activity relationship analysis result, with nicardipine used as a control with IC_{50} standardized to 1, and novel

compounds with calculated IC_{50} with respect to nicardipine, greater than 1 representing greater activity/cytotoxicity and less than 1 representing less activity/cytotoxicity. For acyclic analogues, the general trend observed is that activity is enhanced with longer, branched substituent (**Figure 12**, RHC-57, RHC-73, RHC-75). While not all cyclic substituents have been tested at this moment, the cyclopentyl analogue exhibits the highest activity by far in the second generation compound and constitutes a competent candidate for further development. Regarding the above trends, synthesis of methylcyclopentyl analogue (RHC-88) and 3-methylpentyl analogue (RHC-89) were done with hypotheses of high activity levels.

Besides the novel second generation compounds synthesized above, our second-year graduate student San Pham has been targeting the first-generation analogues altering the amino group, as well as in-progress synthesis of single enantiomers. SAR results of synthesized first generation analogues shows the trend that higher activity levels seem to correlate with greater distances between the tertiary ammonium cation and the dihydropyridine core.

The above results with associated trends provide valuable information regarding future synthesis directions as well as potential mechanistic proposals during later stages of the project. Other analogue classes including amlodipine derivatives and aromatic substituents in the second-generation analogues are of great interest as well.

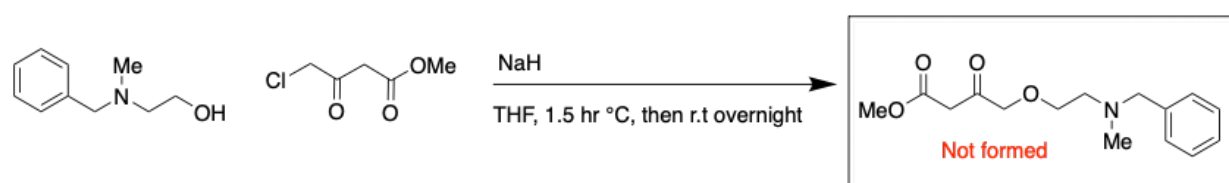
Conclusion

The development of chemoresistance of existing treatment in castration-resistant prostate cancer in the patient population called for urgent research effort and pharmacological development of novel treatments to address the medical need. Although a few other candidates such as A-395 and MAK683 have been identified as EED inhibitors, the pathway from current understanding of their novel structural types to potential development of adequate treatment can present potential possibilities of complications and uncertainties at multiple stages. Nicardipine and other 1,4-dihydropyridines, on the other hand, constitutes a more ideal candidate that rides an accelerated path secondary to more advanced understanding in both the synthetic and application aspects.

In the light of preliminary study done by Dr. Daqing Wu's laboratory, the current novel projects targets the known antihypertensive medication, nicardipine, with the aim to reduce its side effect of calcium ion channel blocking activity while maintaining its desired EED-inhibiting ability, thereby inducing apoptosis and suppressing survival signaling cascades of cancer cells. Through rational design of multiple analogue classes, synthesis of nicardipine-derived analogue library and in-vitro biological SAR assay analyses were performed to select candidates with superior cytotoxicity to carry forward.

Amlodipine, another popular antihypertensive medication in the calcium ion channel blocker class with similar structural features compared to those of nicardipine, can be a future direction of interest. The synthesis of its precursor methyl 4-(2-(benzyl(methyl)amino) ethoxy)-3-oxobutanoate was actually attempted through S_N2 nucleophilic substitution reaction using sodium hydride, following experimental protocol proposed by Legeay *et al*, 2007 and

Arrowsmith *et al*, 1986. The first attempt utilized 3.06 equivalent of sodium hydride (Legeay *et al*, 2017) and the second attempt utilized 1 equivalent of sodium hydride (Arrowsmith *et al*, 1986). Although both attempts did not yield sufficient results, the synthesis of amlodipine analogue still remains to be a valuable future perspective that awaits to be optimized. Based on the reaction mechanism and structural electronics, we can propose using 2 equivalents of NaH as a future direction. While one equivalent of NaH is responsible for deprotonation of the nucleophile, the residual active NaH can interact with the chloroacetate ester, deprotonation of the carbon at the alpha position generates a delocalized negative charge that repels nucleophilic attack and increases selectivity of substitution reaction at the terminal halide.



Scheme 7. Attempted amlodipine precursor methyl 4-(2-(benzyl(methyl)amino)ethoxy)-3-oxobutanoate synthesis.

While this project is still at its early stage, existing theories and results suggest inherent potential in the repurposing of nicardipine to target chemoresistance in castration-resistant prostate cancer. With continuing progress in the near future, we aim to diversify the analogue library for biological assay to expand the existing knowledge on structure-activity relationship trend, enrich the member of available competent candidates, and dig deeper into the specific mechanism of action for carrying forward into the clinical trials.

References

1. Arrowsmith, J. E., Campbell, S. F., Cross, P. E., Stubbs, J. K., Burges, R. A., Gardiner, D. G., & Blackburn, K. J. Long-acting dihydropyridine calcium antagonists. 1. 2-Alkoxyethyl derivatives incorporating basic substituents. *J. Med. Chem.*, **1986**; 29(9), 1696-1702.
2. Iqbal, N., & Knaus, E. E. Synthesis of 3-(2-guanidinoethyl) and 3-[2-(S-methylisothioureidoethyl)] analogs of 5-isopropyl 2, 6-dimethyl-1, 4-dihydro-4-(2, 3-dichlorophenyl) pyridine-3, 5-dicarboxylate as a respective releaser of nitric oxide and inhibitor of nitric oxide synthase. *J. Heterocycl. Chem.*, **1996**; 33(1), 157-160.
3. He, Y., Selvaraju, S., Curtin, M. L., Jakob, C. G., Zhu, H., Comess, K. M., ... & Pappano, W. N. The EED protein–protein interaction inhibitor A-395 inactivates the PRC2 complex. *Nat. Chem. Biol.*, **2017**; 13(4), 389-395.
4. Huang, Y., Zhang, J., Yu, Z., Zhang, H., Wang, Y., Lingel, A., ... & Oyang, C. Discovery of first-in-class, potent, and orally bioavailable embryonic ectoderm development (EED) inhibitor with robust anticancer efficacy. *J. Med. Chem.*, **2017**; 60(6), 2215-2226.
5. Huang, Y., Sendzik, M., Zhang, J., Gao, Z., Sun, Y., Wang, L., ... & Oyang, C. Discovery of the clinical candidate MAK683: An EED-directed, allosteric, and selective PRC2 inhibitor for the treatment of advanced malignancies. *J. Med. Chem.*, **2022**; 65(7), 5317-5333.
6. Kouznetsova, V. L., Tchekanov, A., Li, X., Yan, X., & Tsigelny, I. F. Polycomb repressive 2 complex—molecular mechanisms of function. *Protein Sci.*, **2019**; 28(8), 1387-1399.

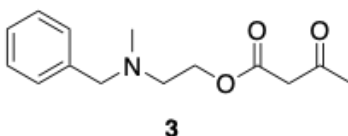
7. Lacotte, P., Puente, C., & Ambroise, Y. Synthesis and Evaluation of 3, 4-Dihydropyrimidin-2 (1H)-ones as Sodium Iodide Symporter Inhibitors. *ChemMedChem*, **2013**; 8(1), 104-111.
8. Legeay, J. C., Eynde, J. J. V., & Bazureau, J. P. Sequential synthesis of a new analogue of amlodipine bearing a short amino polyethyleneglycol chain. *Tetrahedron*, **2007**; 63(48), 12081-12086.
9. Li X, Gera L, Zhang S, Chen Y, Lou L, Wilson LM, Xie ZR, Sautto G, Liu D, Danaher A, Mamouni M, Yang Y, Du Y, Fu H, Kucuk O, Osunkoya AO, Zhou J, Wu D. Pharmacological inhibition of noncanonical EED-EZH2 signaling overcomes chemoresistance in prostate cancer. *Theranostics* **2021**; 11(14): 6873-90.
10. Li, X., Chen, Y., Bai, L., Zhao, R., ... & Wu, D. Nicardipine is a Putative EED Inhibitor and Has High Selectivity and Potency against Chemoresistant Prostate Cancer in Preclinical Models. Accepted with minor revision, *Br. J. Cancer*, 2023
11. Liebeschuetz, J, Lyons, A, Murray, C, Rimmer, A; Young, S, Camp, N, Jones, S, Morgan, P, Richards, S, Wylie, W, Masters, J, & Wiley, M. Preparation of amino acid derivatives as serine protease inhibitors. WO2000076971. Protherics Molecular Design Limited, United States. **2000**.
12. Mao, H., Lin, A., Shi, Y., Mao, Z., Zhu, X., Li, W., ... & Zhu, C. Construction of enantiomerically enriched diazo compounds using diazo esters as nucleophiles: Chiral Lewis base catalysis. *Angew. Chem., Int. Ed.*, **2013**; 52(24), 6288-6292.
13. Shibamura, T., Iwanami, M., Fujimoto, M., Takenaka, T., & Murakami, M. Synthesis of the metabolites of 2-(N-benzyl-N-methylamino) ethyl methyl 2, 6-dimethyl-4-(m-

- nitrophenyl)-1, 4-dihydropyridine-3, 5-dicarboxylate hydrochloride (nicardipine hydrochloride, YC-93). *Chem. Pharm. Bull.*, **1980**; 28(9), 2609-2613.
14. Szeleszczuk, Ł., Zielińska-Pisklak, M., & Pisklak, D. M. Structural studies of calcium channel blockers used in the treatment of hypertension-¹H and ¹³C NMR characteristics of nifedipine analogues. *MRC*. **2018**.
15. Urology Care Foundation. What you should know fact-sheet. *Urology Health*. 2020.
16. Zhang, J. Y., Zhang, J., Kiffe, M., Walles, M., Jin, Y., Blanz, J., ... & Oyang, C. Preclinical pharmacokinetics and metabolism of MAK683, a clinical stage selective oral embryonic ectoderm development (EED) inhibitor for cancer treatment. *Xenobiotica*, **2022**; 52(1), 65-78.

Supporting Information

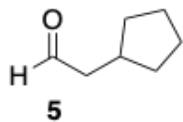
Experimental Procedures

2-(Benzylmethylamino) ethyl acetoacetate (**3**).



2,2,6-trimethyl-4H-1,3-dioxin-4-one (1.33 mL, 10 mmol, 1 equiv.) and 2-benzyl(methyl)amino ethanol (1.65 g, 10 mmol, 1 equiv.) were combined in a 15 mL tube equipped with a stir bar. The content is purged with argon for 10 minutes followed by addition of 10 mL dry toluene freshly obtained from the dispenser. The mixture is purged with argon for 5 more minutes, then capped, sealed, and allowed for stirring at 150 °C overnight. Solvent is removed through vacuum to obtain a crude of dark brown oil. Column chromatography is used for purification to obtain pure compound in a yellow oil at a consistent 70 to 80% yield of 4.56 grams. ¹H NMR (600 MHz, CDCl₃) δ 7.33 – 7.24 (m, 5H), 4.29 (t, J = 5.9 Hz, 2H), 3.57 (s, 2H), 3.48 (s, 2H), 2.70 (t, J = 5.8 Hz, 2H), 2.29 (d, J = 1.9 Hz, 5H), 1.59 (s, 4H).

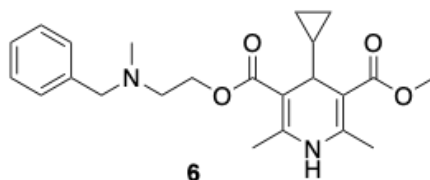
2-cyclopentylacetaldehyde (**5**)



Dess-Martin periodinane (5.4 g, 12.7 mmol) was suspended in dichloromethane (45 mL) in a 250 mL round bottom flask. Cyclopentylethanol (1.29 g, 11.6 mmol) dissolved in dichloromethane (35 mL) was added slowly over a five-minute period. The mixture stirred for 3 hours at room temperature. (mixture remained cloudy the whole time). The mixture was diluted with saturated aqueous NaHCO_3 and ether (approximately 20 mL each was used). The mixture was stirred for 10 min and diluted with sodium thiosulfate and stirred until the solids dissolved. The mixture was transferred to a separatory funnel. The layers were separated, and the aqueous layer was extracted with ether. The organic layers were combined, washed with water and brine, dried (Na_2SO_4), filtered and concentrated to provide product. Due to difficulty of purification, the crude mixture was carried forward directly into the 1,4-dihydropyridine synthesis.

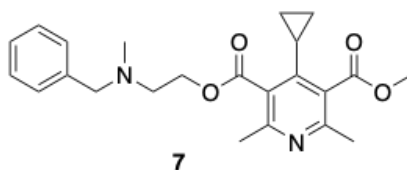
Identification of aldehyde based on appearance of ^1H NMR (400 MHz, CDCl_3) δ 9.76 (t, $J = 2.5$ Hz, 1H) in the crude spectrum and complete disappearance of ^1H NMR (400 MHz, CDCl_3) δ 3.69 (td, $J = 7.8, 5.3$ Hz, 2H).

(3-(2-(benzyl(methyl)amino)ethyl) 5-methyl 4-cyclopropyl-2,6-dimethyl-1,4-dihydropyridine - 3,5-dicarboxylate) (**6**).



Combine 2-(Benzylmethylamino) ethyl acetoacetate (175 mg, 0.7 mmol, 1 equiv.), methyl-3-aminocrotonate (85 mg, 0.7 mmol, 1 equiv.), and cyclopropylacetaldehyde (76 microliter, 0.7 mmol, 1 equiv.) into a 4 mL vial. Reaction mixture is purged under argon and dissolved in isopropanol. The reaction content is then purged under argon for an additional 10 minutes, then capped and sealed. The reaction is kept in an 80 °C sand bath and stirred for 6 hours, after which the mixture is cooled to room temperature. Solvent is removed under vacuum to obtain a crude mixture of clear orange oil. Crude mixture then undergo column chromatography to afford a pure product of clear, light yellow oil, with consistent yields of 30% to 40% (120 mg). ¹H NMR (600 MHz, CDCl₃) δ 7.37 – 7.28 (m, 4H), 7.23 (tt, J = 1.6, 7.0 Hz, 1H), 5.75 (broad s, 1H), 4.29 (ddt, J = 2.0, 6.0, 11 Hz, 2H), 3.67 (s, 3H), 3.65 (d, J = 7.6 Hz, 1H), 3.57 (s, 2H), 2.74 (t, J = 6.0 Hz, 2H), 2.31 (s, 3H), 2.30 (s, 3H), 2.27 (s, 3H), 0.85 – 0.77 (m, 1H), 0.29 – 0.17 (m, 4H).

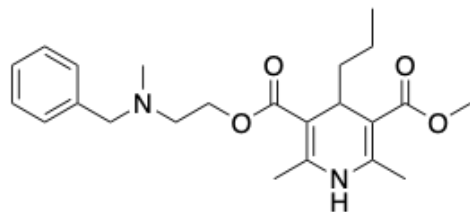
3-(2-(benzyl(methyl)amino)ethyl) 5-methyl 4-cyclopropyl-2,6-dimethylpyridine-3,5-dicarboxylate (7).



3-(2-(benzyl(methyl)amino)ethyl) 5-methyl 4-cyclopropyl-2,6-dimethyl-1,4-dihydropyridine-3,5-dicarboxylate is transferred to a 8 mL vial using DCM, and solvent is removed under vacuum. Concentrated nitric acid is diluted to 2M with DI water, and added to the reaction content (0.3M of the reaction). Reaction is stirred at 65 °C overnight, after which reaction is cooled down to room temperature, and transferred to a septum funnel using deionized water and dichloromethane. Extractions with dichloromethane (10 mL) performed three times, followed by washes with deionized water, sodium bicarbonate, water, and brine. Resulting content is dried over sodium sulfite and the solvent is removed under vacuum to obtain a crude mixture of dark orange oil. Column chromatography was performed to purify the crude to afford a pure product of clear, light yellow oil with a yield of 10% (8.7 mg). ¹H NMR (400 MHz, CDCl₃) δ 7.35 – 7.23 (m, 5H), 4.51 (d, J = 7.0 Hz, 2H), 3.96 (s, 3H), 3.63 (s, 2H), 2.83 (s, 2H), 2.53 (d, J = 1.3 Hz, 6H), 2.34 (s, 3H), 2.08 (tt, J = 8.8, 5.9 Hz, 1H), 1.27 (s, 0H), 0.86 – 0.75 (m, 2H), 0.57 (td, J = 6.0, 4.4 Hz, 2H).

Mass Spectrometry

3-(2-(benzyl(methyl)amino)ethyl) 5-methyl 2,6-dimethyl-4-propyl-1,4-dihydropyridine-3,5-dicarboxylate (RHC-57)



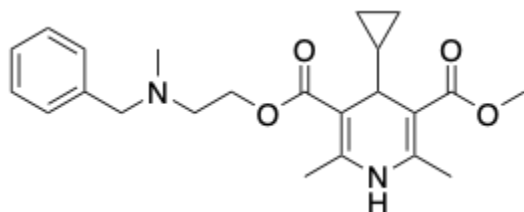
Calculated for $[C_{23}H_{33}N_2O_4]^+$, 401.2362, found, 401.2436.

Peak Mass	Display Formula	RD B	Delta [ppm]	Delta [mmu]	Theo. mass	Combined Score	MS Cov. [%]
401.24355	$C_{23}H_{33}N_2O_4$	8.5	0.16	0.07	401.2435	97.02	99.77

Molecular Ion peaks:

m/z	Intensity	Relative
401.2435	1.8E+09	100
402.2467	4.44E+08	24.64751

3-(2-(benzyl(methyl)amino)ethyl) 5-methyl 4-cyclopropyl-2,6-dimethyl-1,4-dihydropyridine-3,5-dicarboxylate (RHC-71).



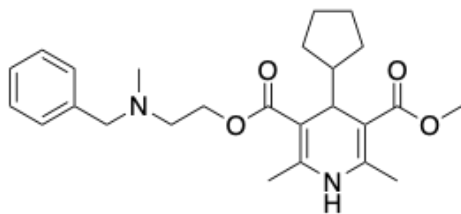
Calculated for $[C_{23}H_{31}N_2O_4]^+$, 399.2206, found, 399.2278

Peak Mass	Display Formula	RDB	Delta [ppm]	Delta [mmu]	Theo. mass	Combined Score	MS Cov. [%]
399.22781	$C_{23}H_{31}N_2O_4$	9.5	-0.07	-0.02	399.22783	98.07	99.94

Molecular Ion peaks:

m/z	Intensity	Relative
399.2278	1.48E+09	100
400.231	3.71E+08	25.01197

3-(2-(benzyl(methyl)amino)ethyl) 5-methyl 4-cyclopentyl-2,6-dimethyl-1,4-dihydropyridine-3,5-dicarboxylate (RHC-72).



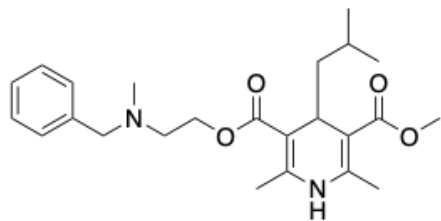
Calculated for $[C_{25}H_{35}N_2O_4]^+$, 427.2519, found, 427.2594.

Peak Mass	Display Formula	RDB	Delta [ppm]	Delta [mmu]	Theo. mass	Combined Score	MS Cov. [%]
427.25938	$C_{25}H_{35}N_2O_4$	9.5	0.57	0.25	427.25913	97.02	99.21

Molecular Ion peaks:

m/z	Intensity	Relative
427.2594	1.96E+08	53.94288
428.2627	50448463	13.90956

3-(2-(benzyl(methyl)amino)ethyl) 5-methyl 4-isobutyl-2,6-dimethyl-1,4-dihydropyridine- 3,5-dicarboxylate (RHC-75).



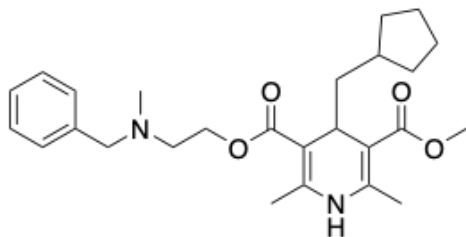
Calculated for $[C_{24}H_{35}N_2O_4]^+$, 415.2519, found, 415.2588.

Peak Mass	Display Formula	RDB	Delta [ppm]	Delta [mmu]	Theo. Mass	Combined Score	MS Cov. [%]
415.25882	$C_{24}H_{35}N_2O_4$	8.5	-0.76	-0.31	415.25913	96.87	99.75

Molecular Ion peaks:

m/z	Intensity	Relative
415.2588	1.55E+09	100
416.2621	4E+08	25.81475

3-(2-(benzyl(methyl)amino)ethyl) 5-methyl 4-(cyclopentylmethyl)-2,6-dimethyl-1,4-dihydropyridine-3,5-dicarboxylate (RHC-88).



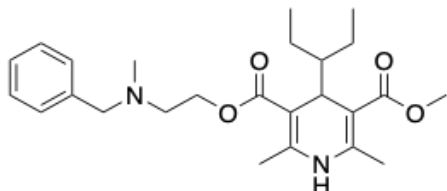
Calculated for $[C_{26}H_{37}N_2O_4]^+$, 441.2675, found, 441.2746.

Peak Mass	Display Formula	RDB	Delta [ppm]	Delta [mmu]	Theo. Mass	Combined Score	MS Cov. [%]
441.27463	$C_{26}H_{37}N_2O_4$	9.5	-0.35	-0.15	441.27478	98.32	99.96

Molecular Ion peaks:

m/z	Intensity	Relative
441.2746	1.81E+09	100
442.2778	5.06E+08	28.01621

3-(2-(benzyl(methyl)amino)ethyl) 5-methyl 2,6-dimethyl-4-(pentan-3-yl)-1,4-dihydropyridine - 3,5-dicarboxylate (RHC-89).



Calculated for fragment $[C_{20}H_{25}N_2O_4]^+$, 357.1803, found, 357.1806.

Positive APCI

Peak Mass	Display Formula	RDB	Delta [ppm]	Delta [mmu]	Theo. Mass	Combined Score	MS Cov. [%]
357.18056	$C_{20}H_{25}N_2O_4$	9.5	-0.9	-0.32	357.18088	96.19	99.79

Fragment Ion peaks:

m/z	Intensity	Relative
357.1806	2.03E+09	100
358.1838	4.31E+08	21.17373

APCI Negative

Peak Mass	Display Formula	RDB	Delta [ppm]	Delta [mmu]	Theo. mass	Combined Score	MS Cov. [%]
355.16526	C ₁₆ H ₁₉ O ₂ N ₈	11.5	4.53	1.61	355.16365	94.3	98.83

Peak Mass	Display Formula	RDB	Delta [ppm]	Delta [mmu]	Theo. mass	Combined Score	MS Cov. [%]
371.15785	C ₁₅ H ₂₃ O ₇ N ₄	6.5	1.7	0.63	371.15722	95.29	99.38

Molecular Ion peaks:

m/z	Intensity	Relative
355.1653	6.91E+08	100
356.1678	1.3E+08	18.77097

ESI Positive

Peak Mass	Display Formula	RDB	Delta [ppm]	Delta [mmu]	Theo. mass	Combined Score	MS Cov. [%]
357.18158	C ₂₀ H ₂₅ O ₄ N ₂	9.5	1.95	0.7	357.18088	94.69	98.81

Peak Mass	Display Formula	RDB	Delta [ppm]	Delta [mmu]	Theo. mass	Combined Score	MS Cov. [%]
373.17661	C ₂₀ H ₂₅ O ₅ N ₂	9.5	2.18	0.81	373.1758	94.7	98.83

m/z	Intensity	Relative
357.1816	40301.47	80.36167
358.1849	8285.904	16.5222

Negative ESI

m/z	Intensity	Relative
208.0617	29564580	100
209.0648	2801311	9.475227

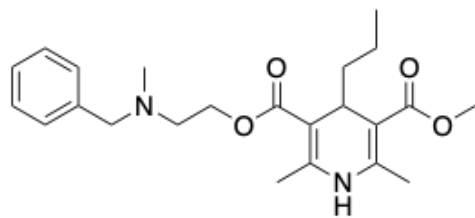
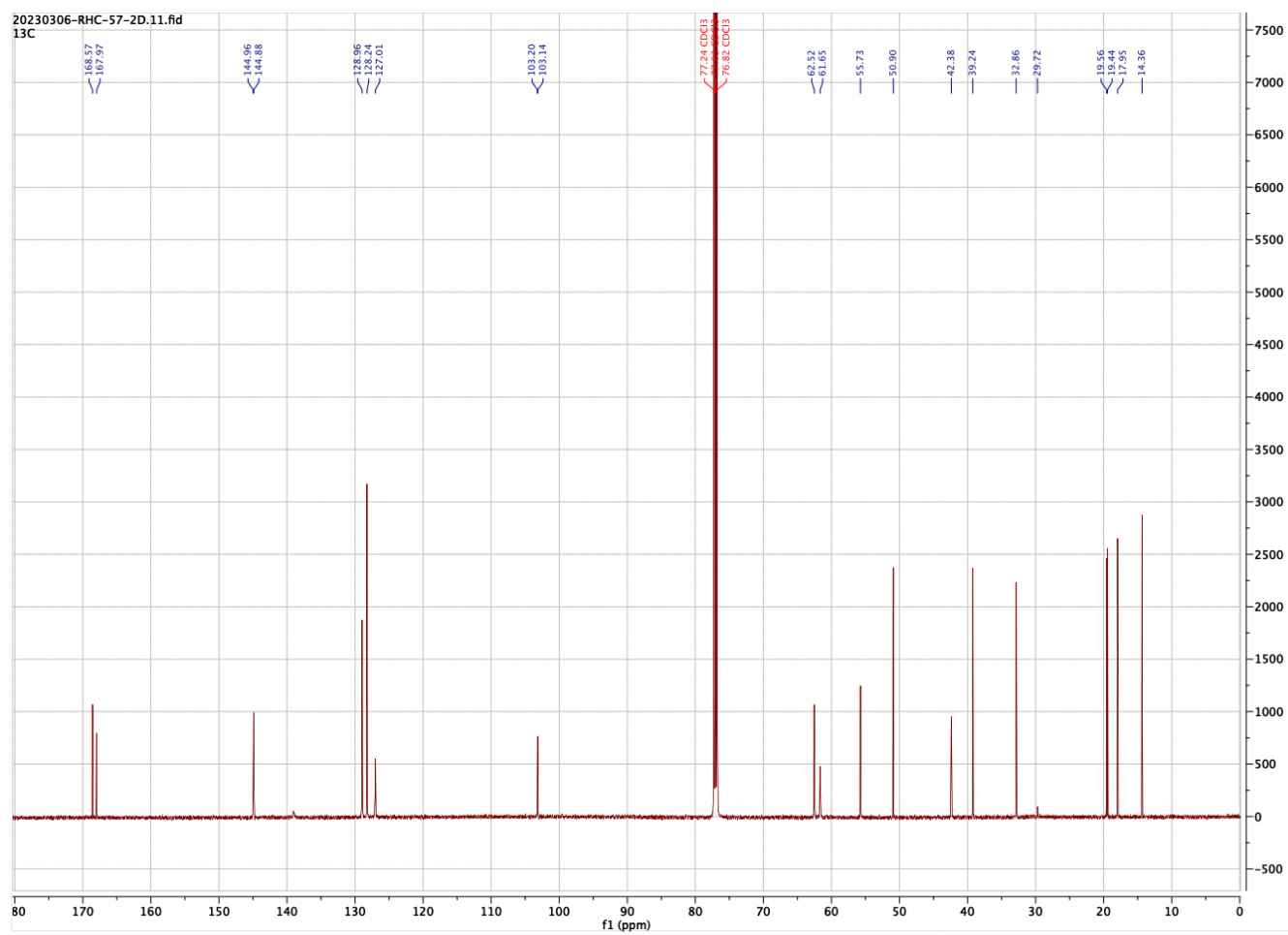


Figure 11. ^{13}C NMR (600 MHz, CDCl_3)



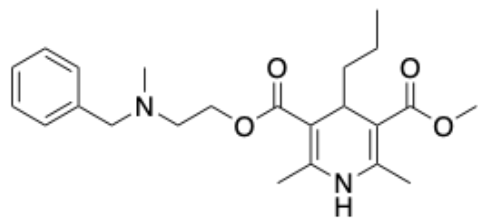
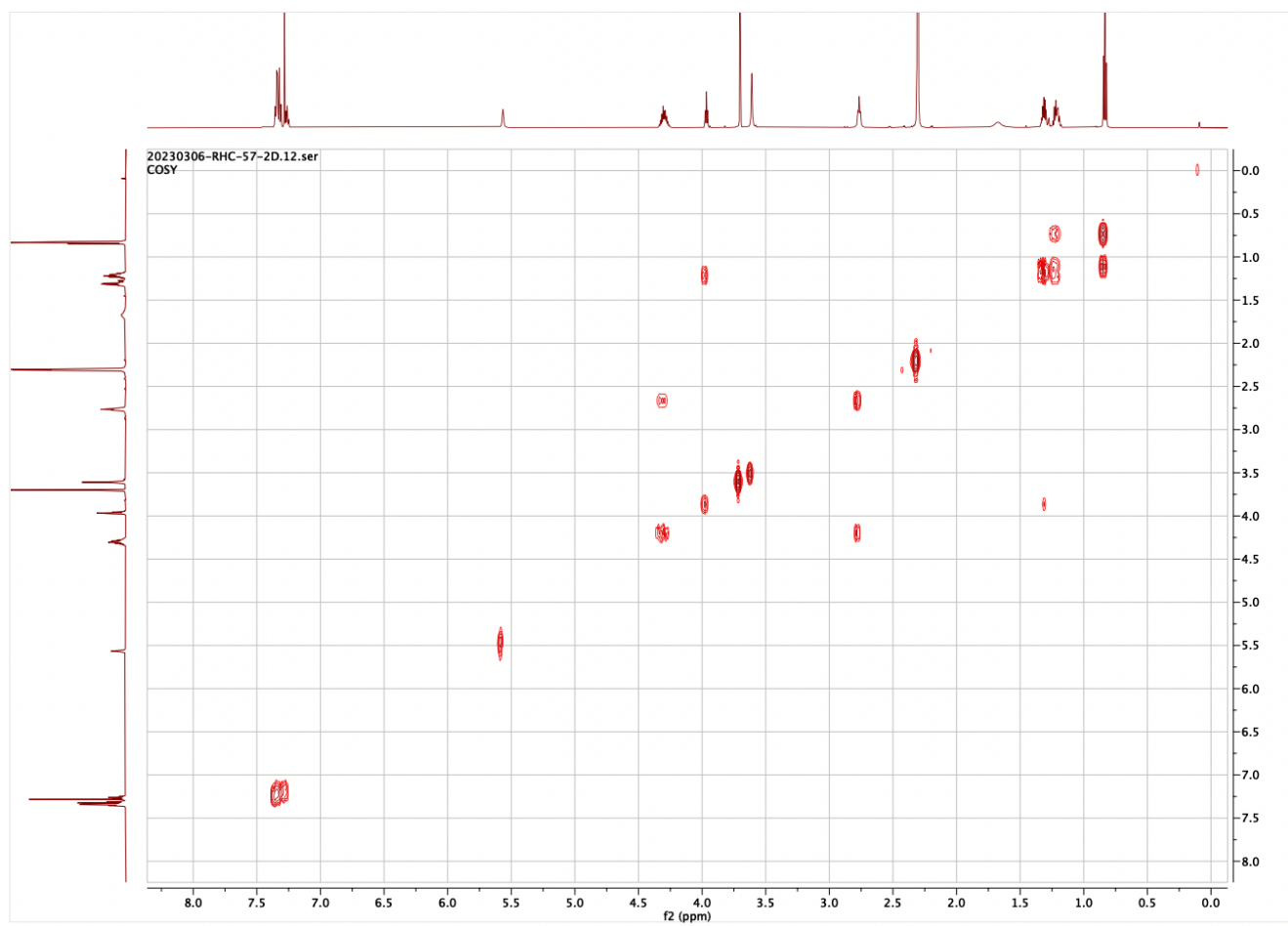


Figure 12. COSY NMR (600 MHz, CDCl₃)



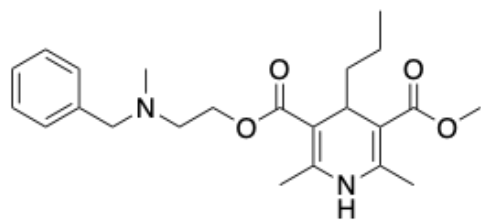
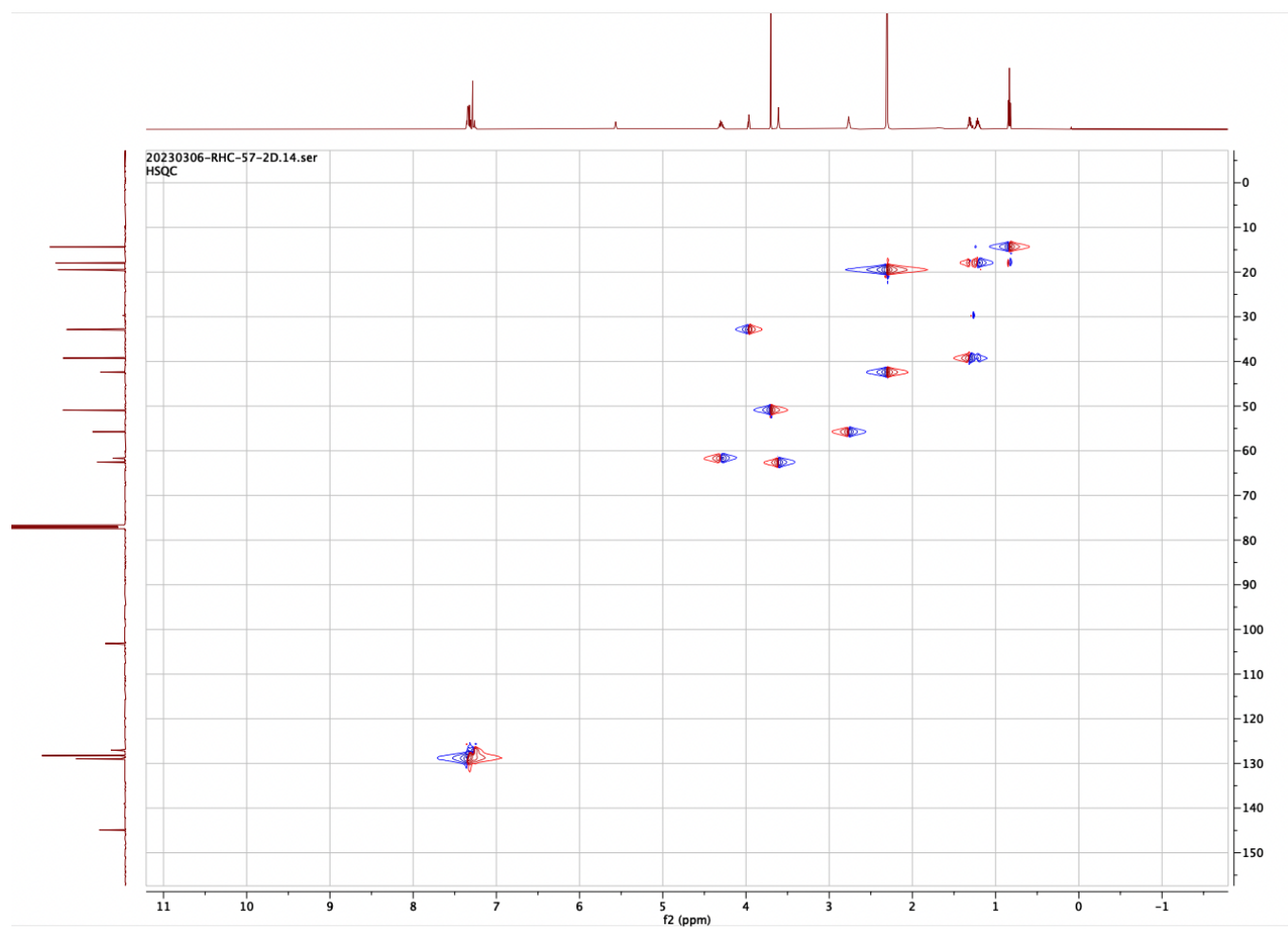


Figure 13. HSQC NMR (600 MHz, CDCl₃)



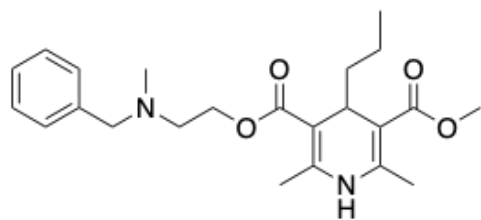
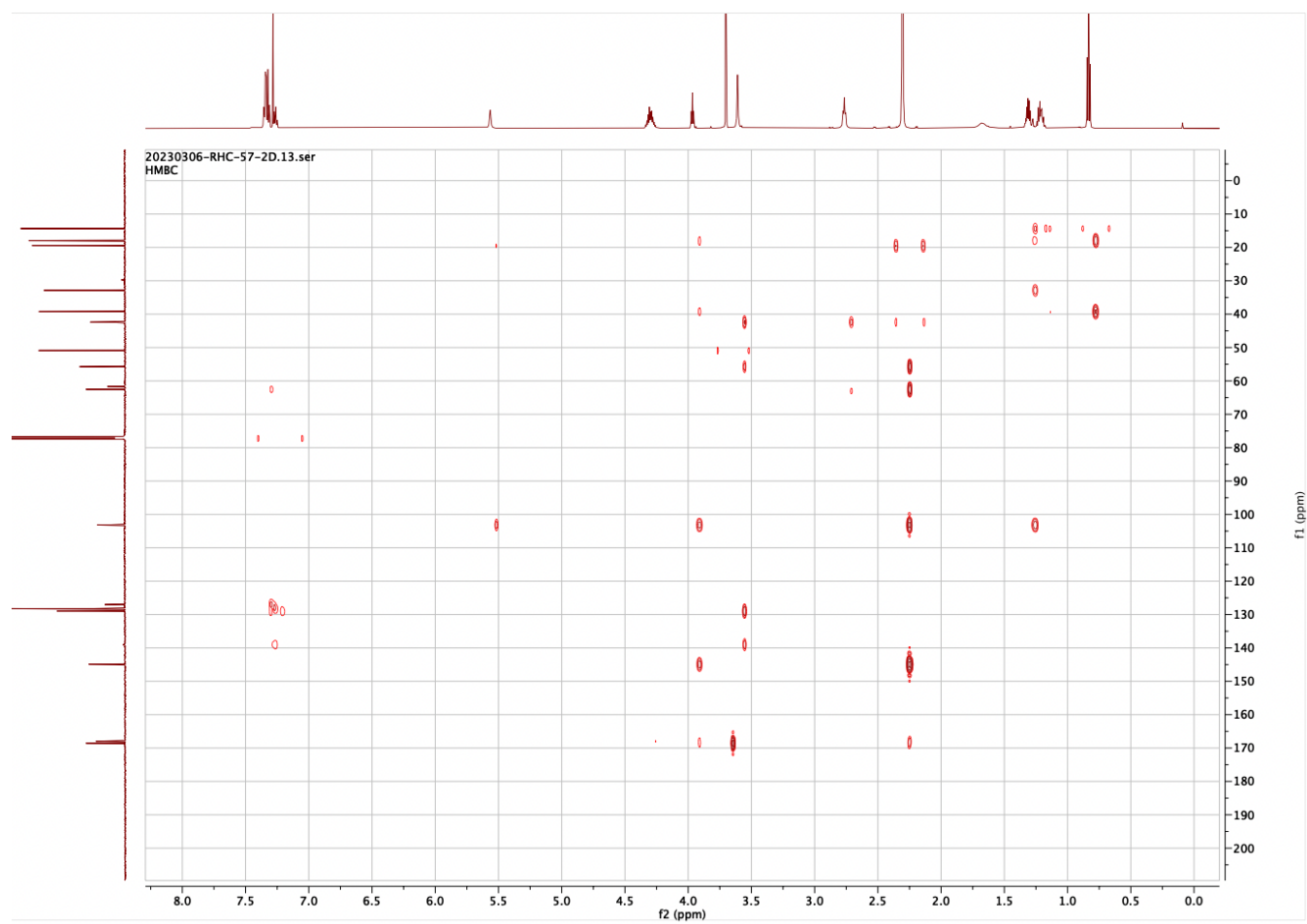


Figure 14. HMBC NMR (600 MHz, CDCl₃)



3-(2-(benzyl(methyl)amino)ethyl) 5-methyl 4-cyclohexyl-2,6-dimethyl-1,4-dihydropyridine -3,5-dicarboxylate (RHC-58).

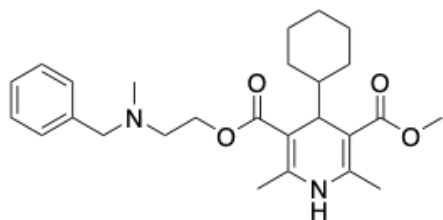


Figure 15. ^1H NMR (600 MHz, CDCl_3)



3-(2-(benzyl(methyl)amino)ethyl) 5-methyl 2,6-dimethyl-4-phenyl-1,4-dihydropyridine- 3,5-dicarboxylate (RHC-59).

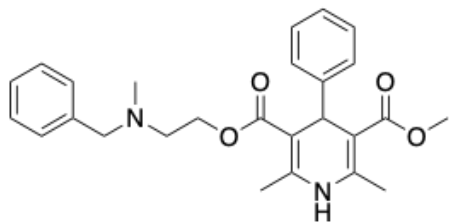
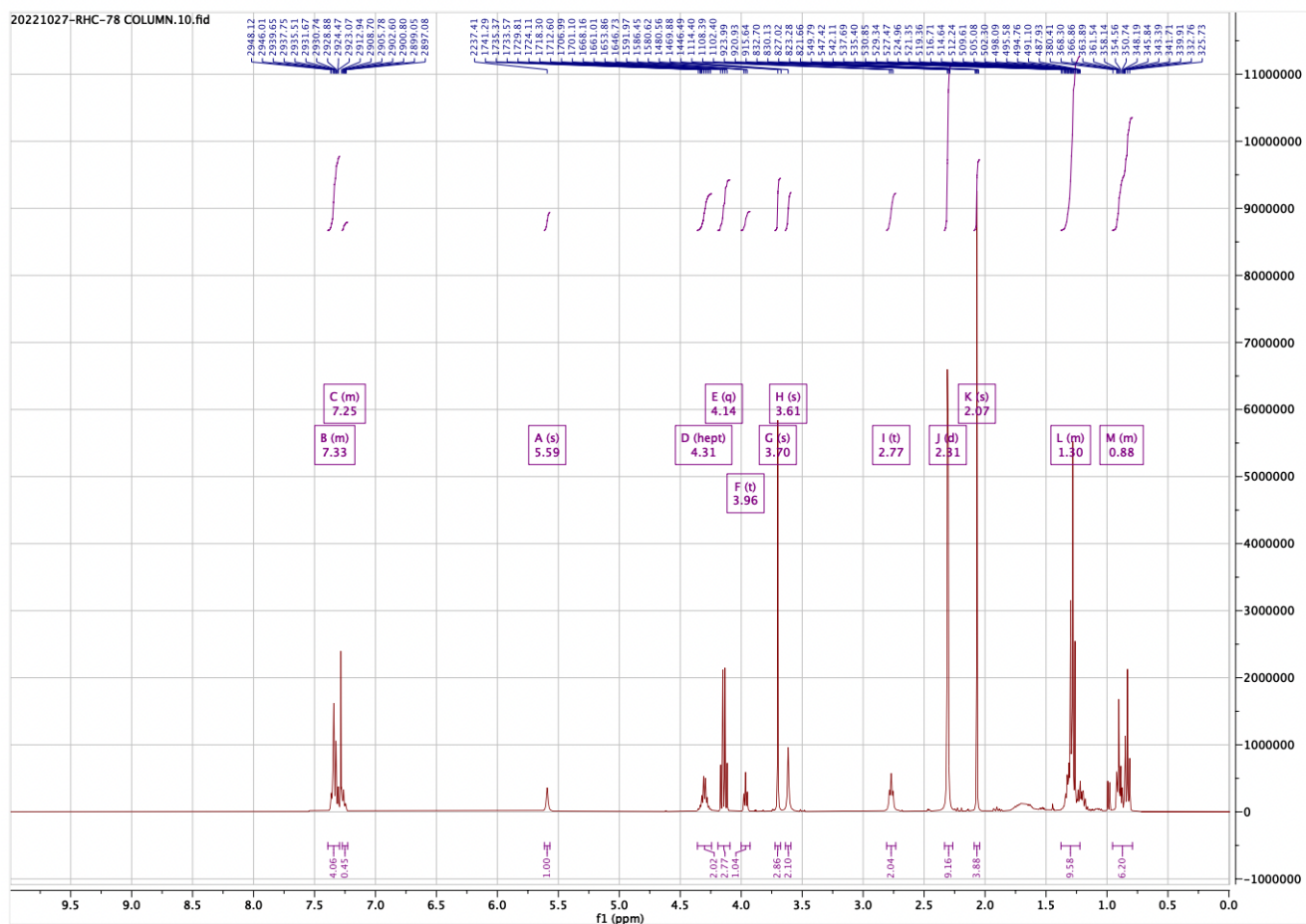


Figure 16. ¹H NMR (600 MHz, CDCl₃)



3-(2-(benzyl(methyl)amino)ethyl) 5-methyl 4-cyclopropyl-2,6-dimethyl-1,4-dihydropyridine-3,5-dicarboxylate (RHC-71).

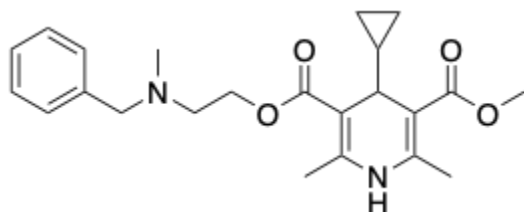
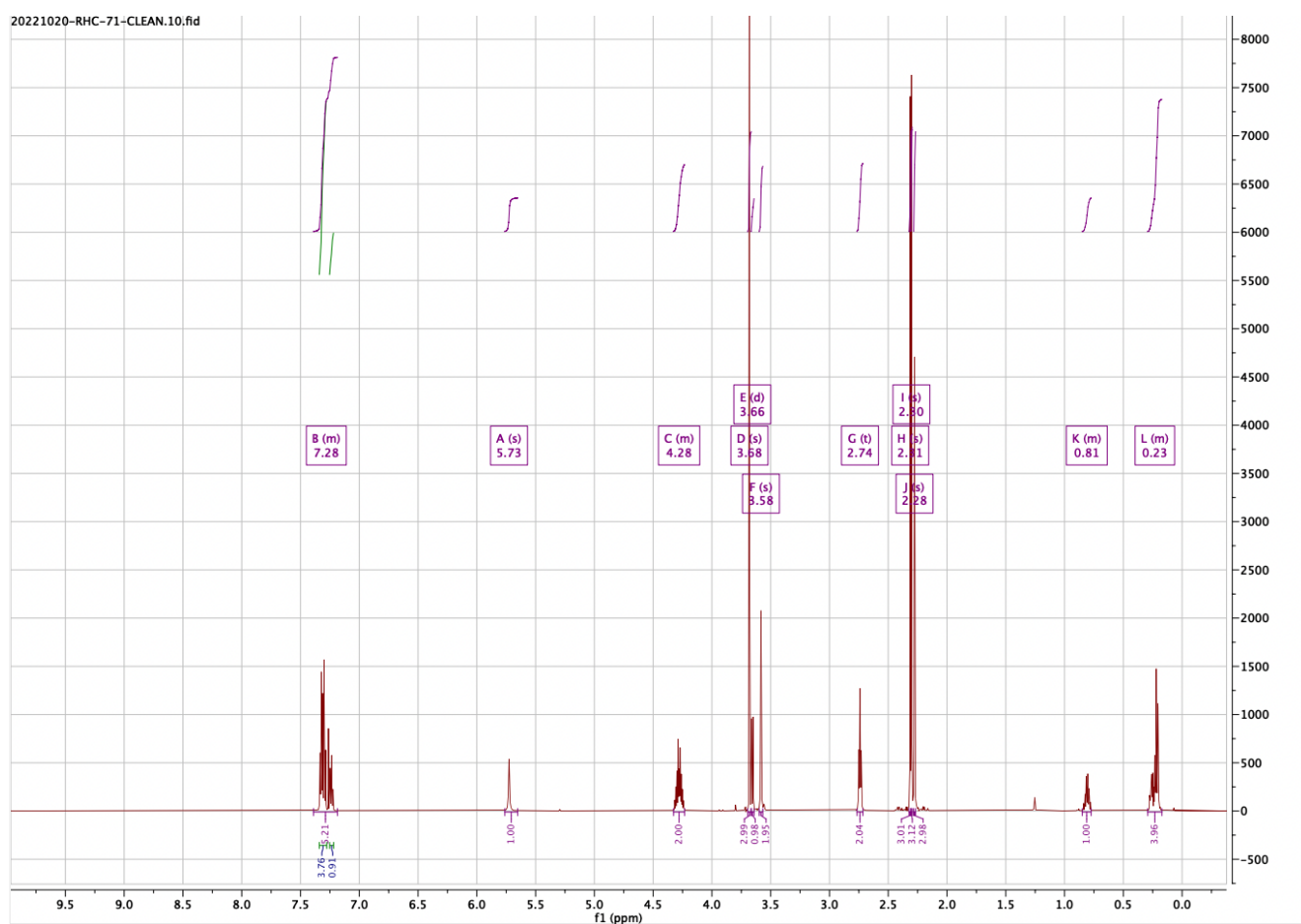


Figure 17. ^1H NMR (600 MHz, CDCl_3)



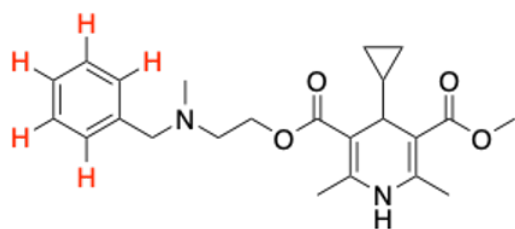
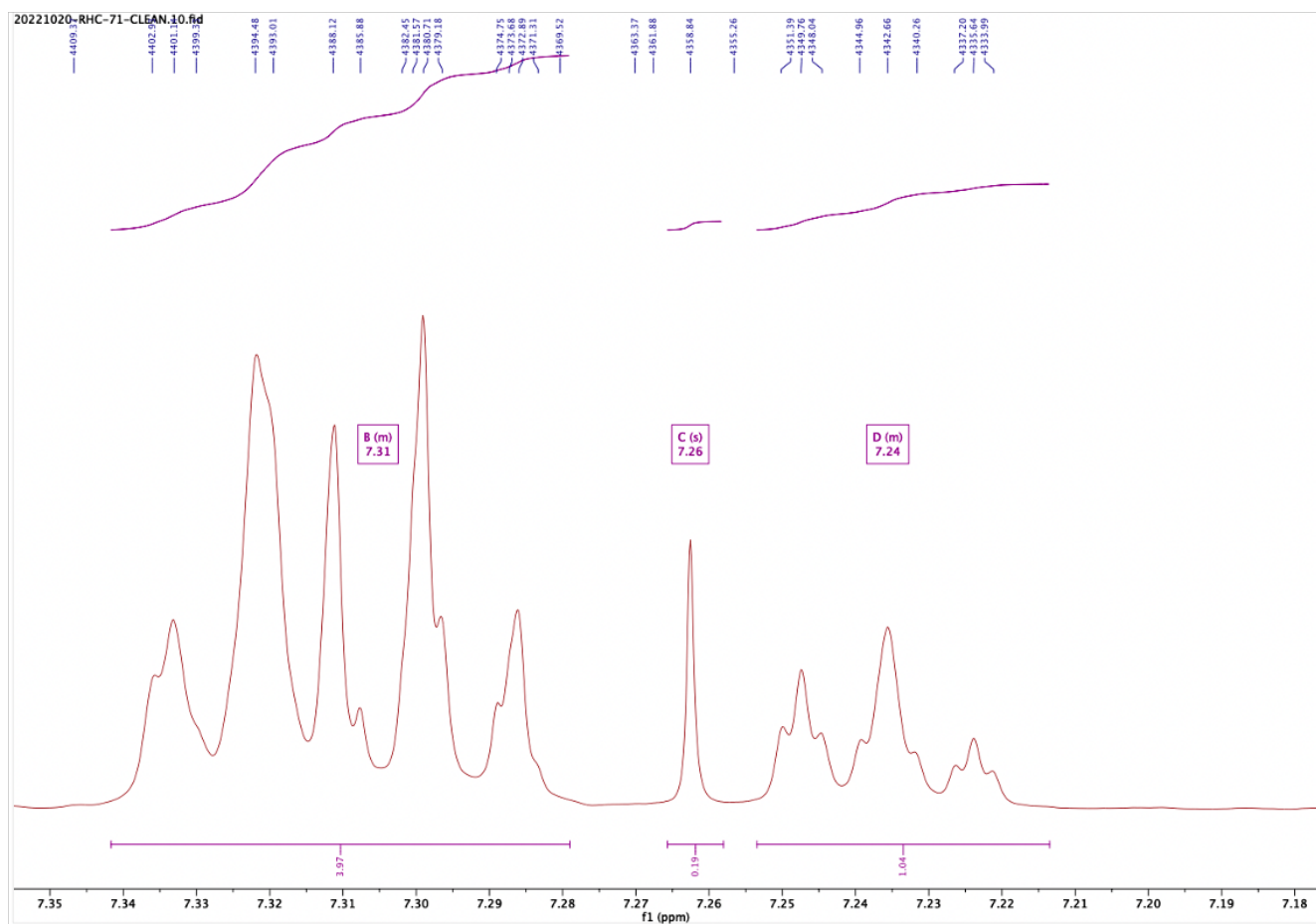


Figure 18. ^1H NMR (600 MHz, CDCl_3), aromatic region expansion (RHC-76).



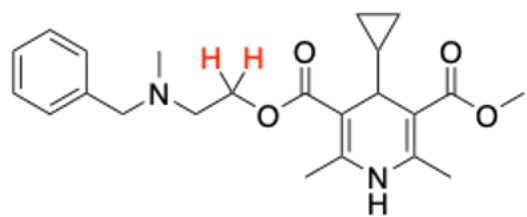
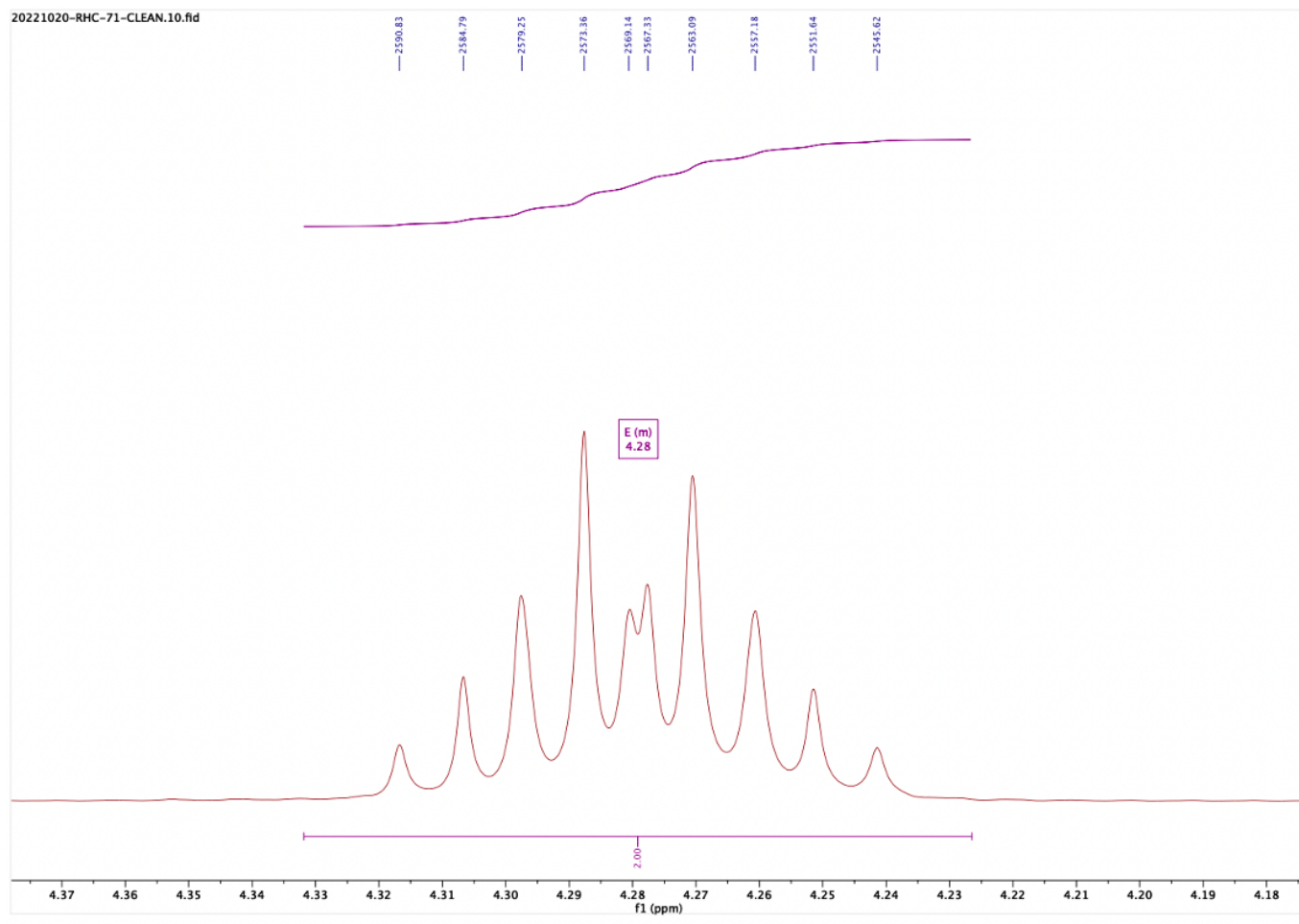


Figure 19. ^1H NMR (600 MHz, CDCl_3), 4.29 ppm expansion (RHC-76).



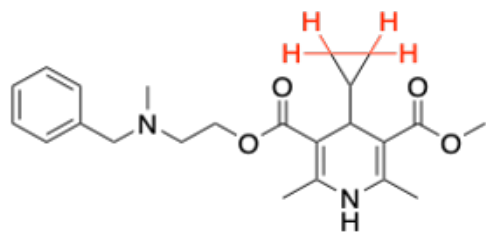
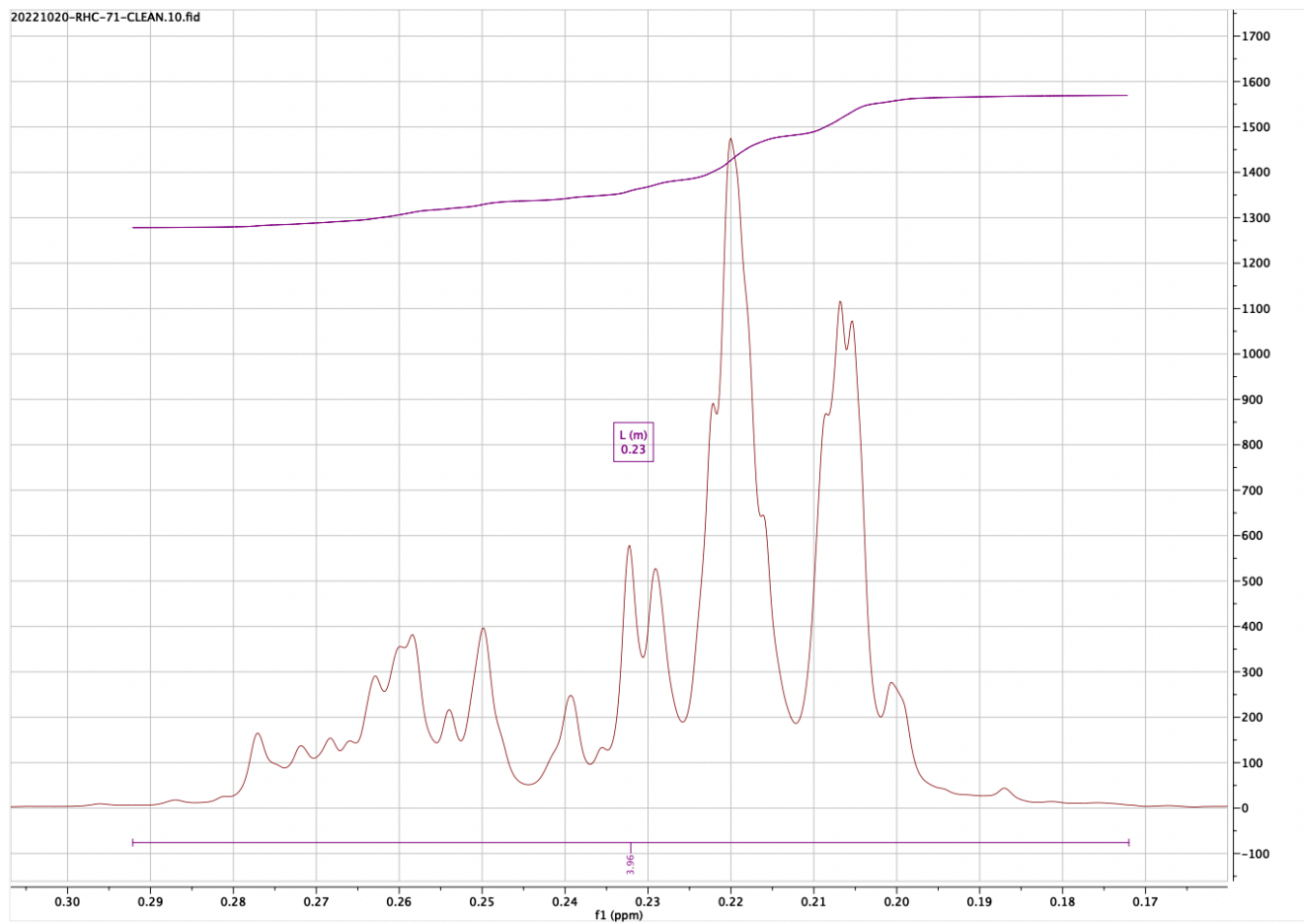


Figure 20. ^1H NMR (600 MHz, CDCl_3), 0.23 ppm expansion (RHC-76).



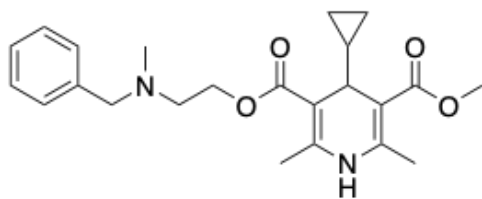
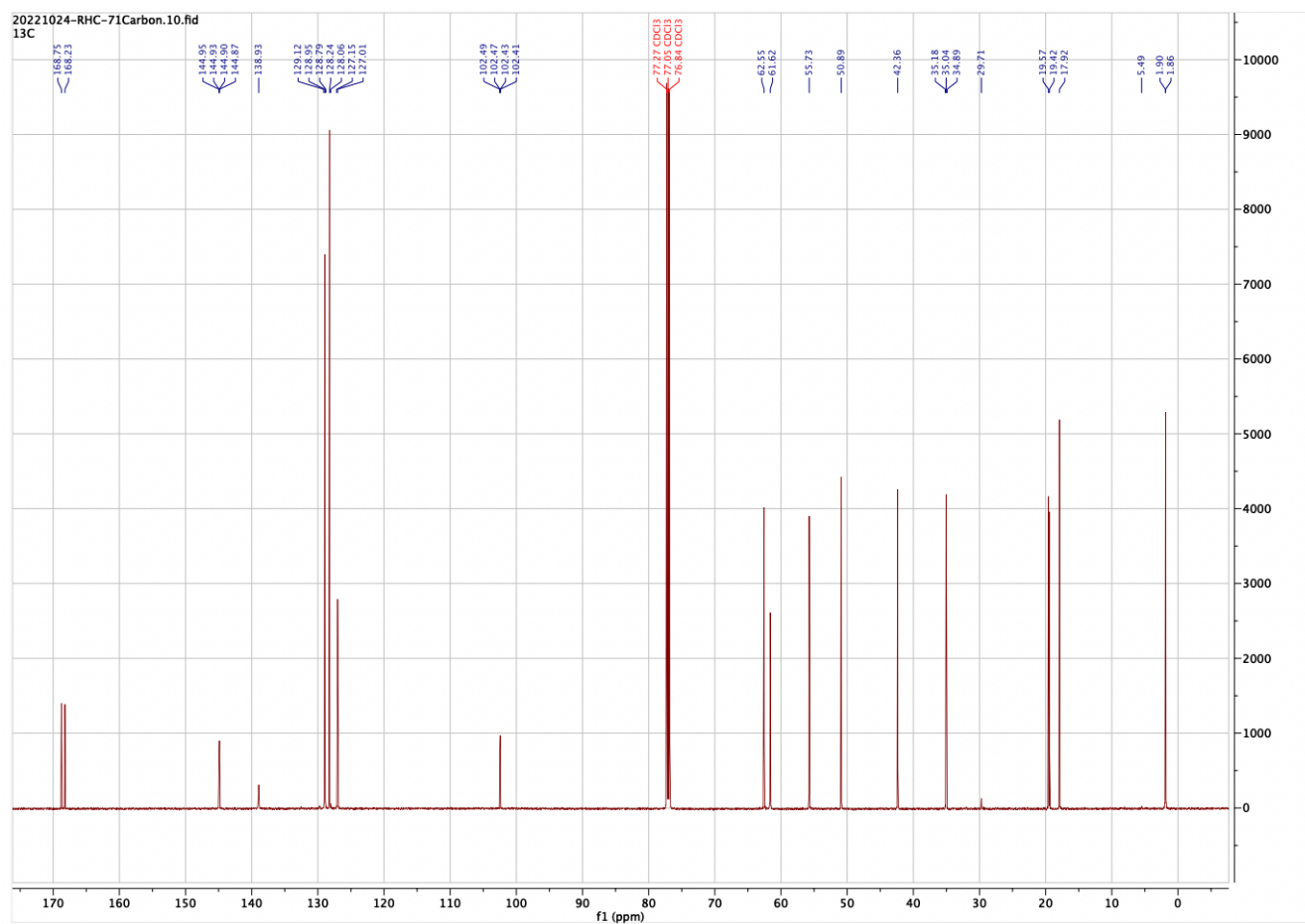


Figure 21. ^{13}C NMR (600 MHz, CDCl_3)



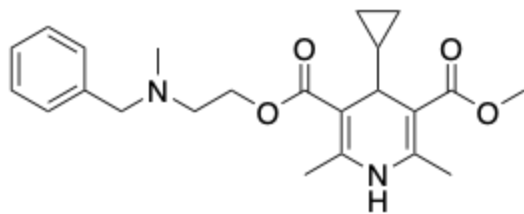
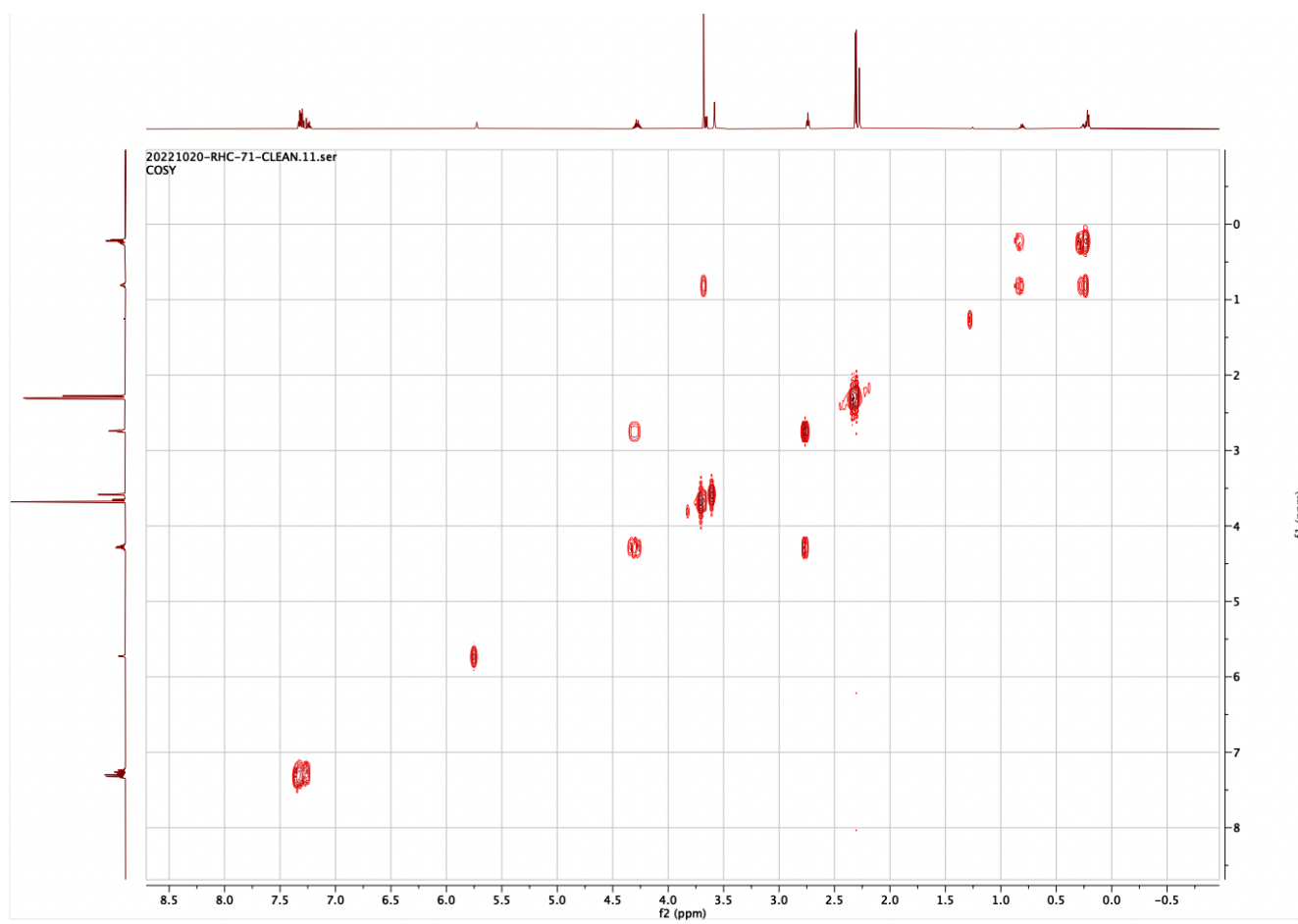


Figure 22. COSY NMR (600 MHz, CDCl₃)



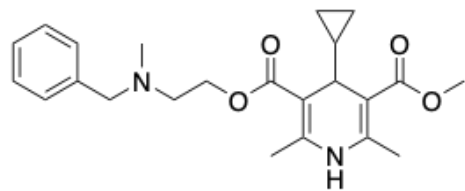
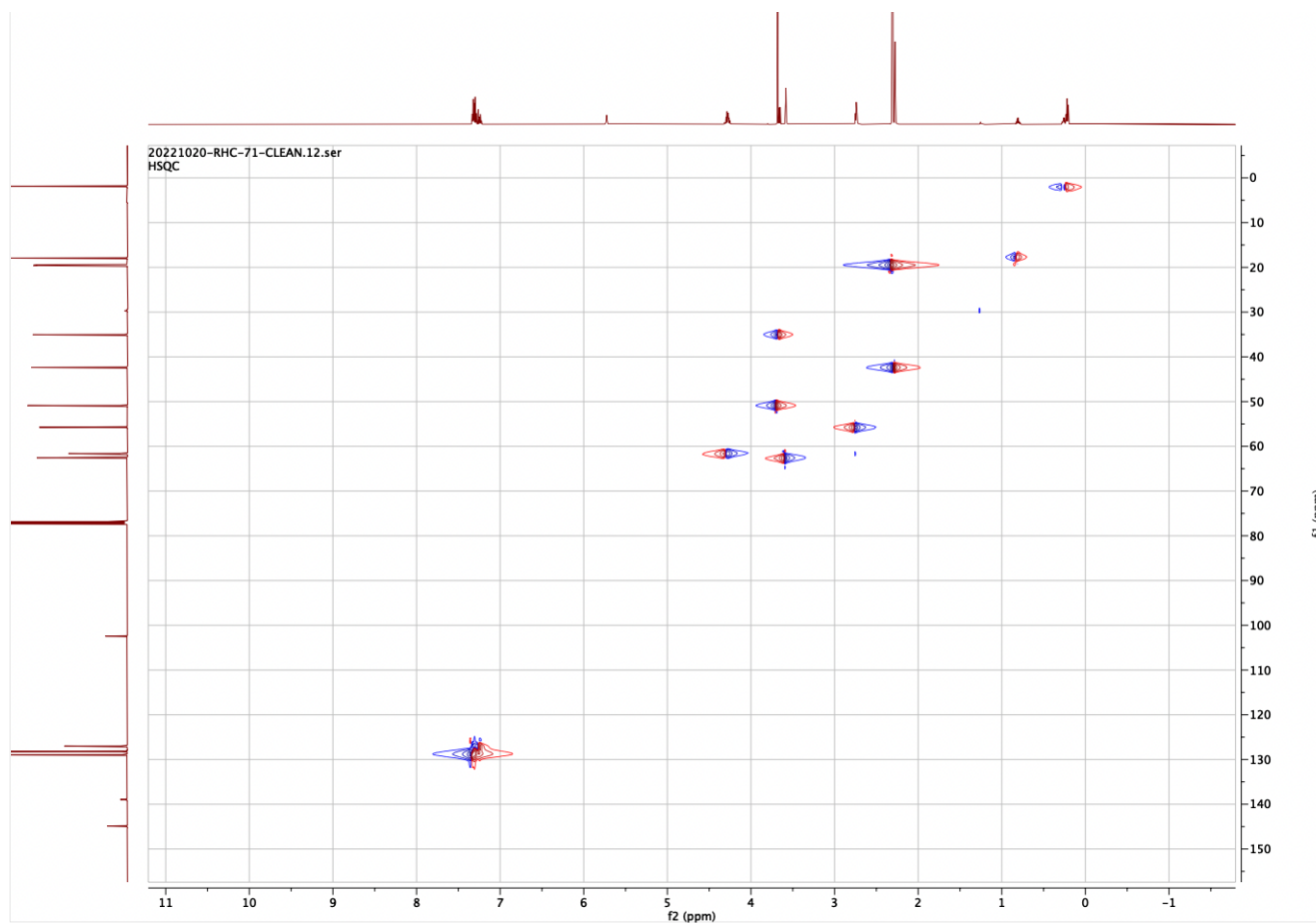


Figure 23. HSQC NMR (600 MHz, CDCl₃)



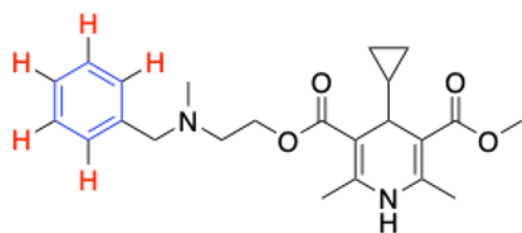
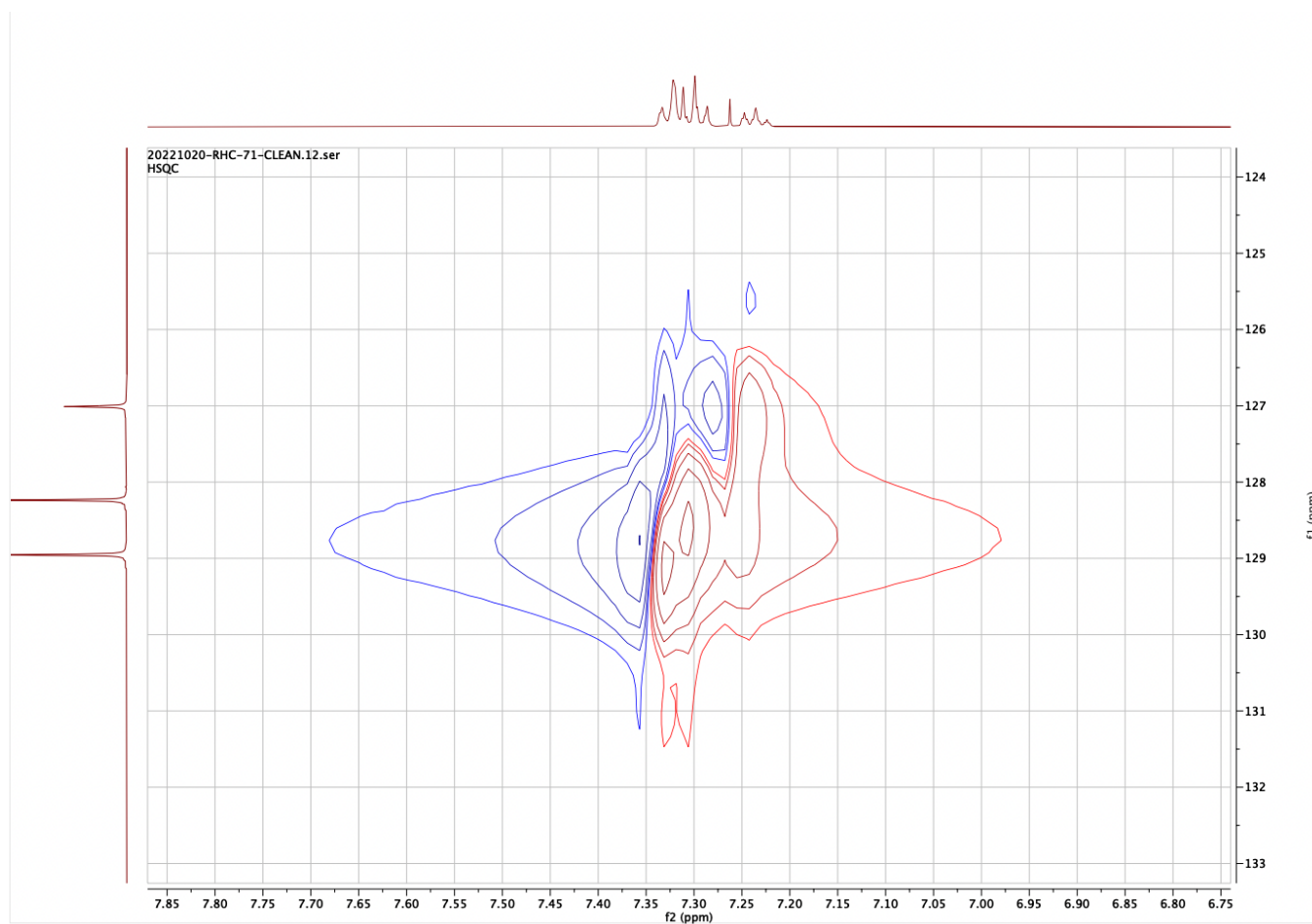


Figure 24. HSQC NMR (600 MHz, CDCl₃), aromatic region expansion.



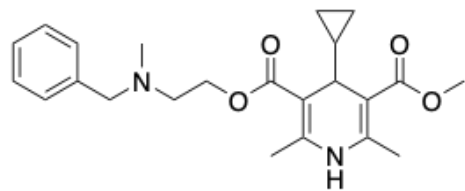
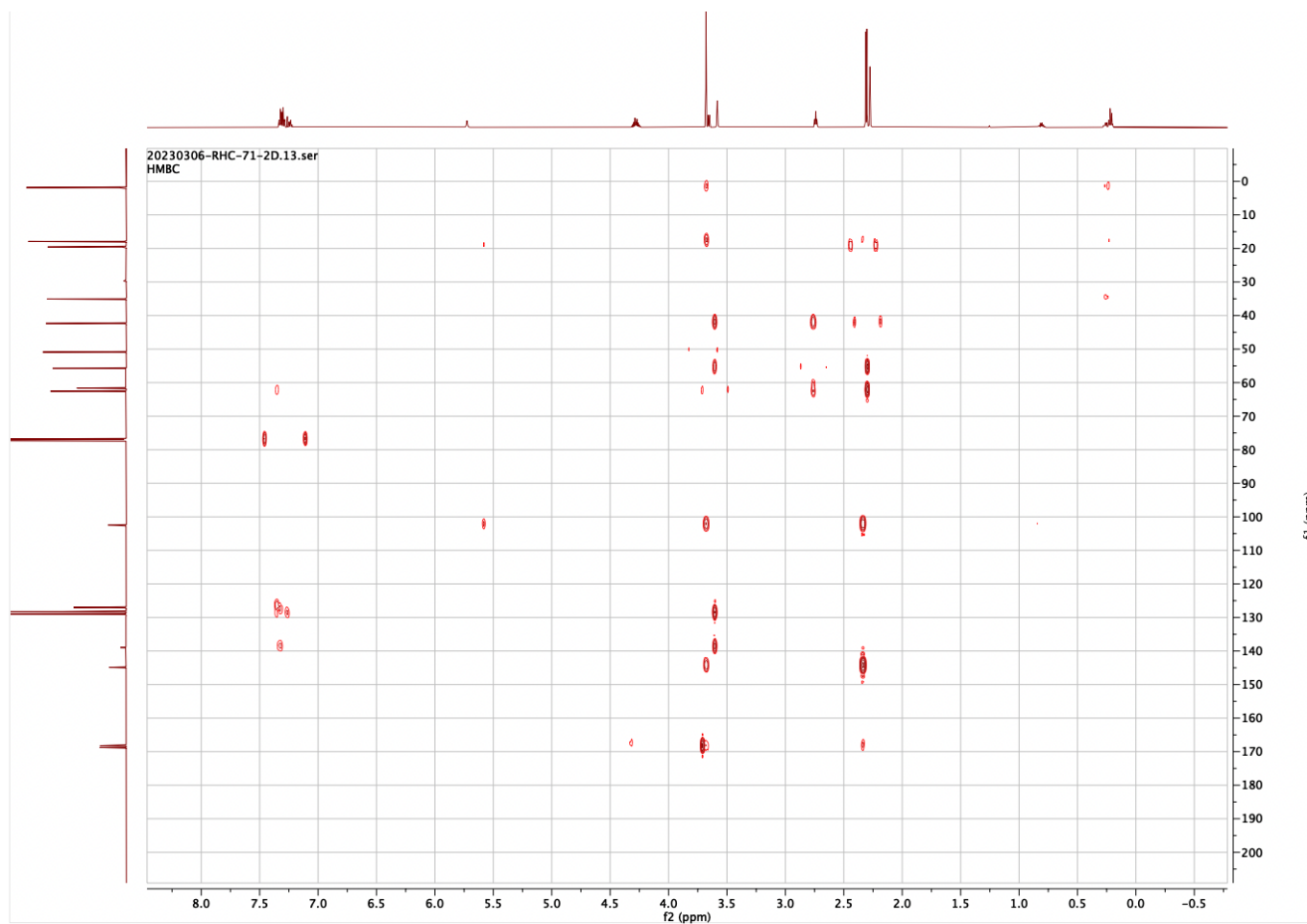


Figure 25. HMBC NMR (600 MHz, CDCl₃)



3-(2-(benzyl(methyl)amino)ethyl) 5-methyl 4-cyclopentyl-2,6-dimethyl-1,4-dihydropyridine-3,5-dicarboxylate (RHC-72).

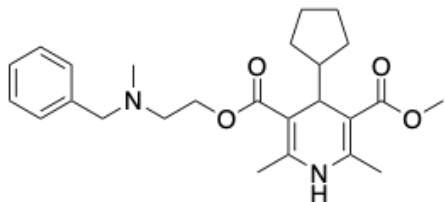
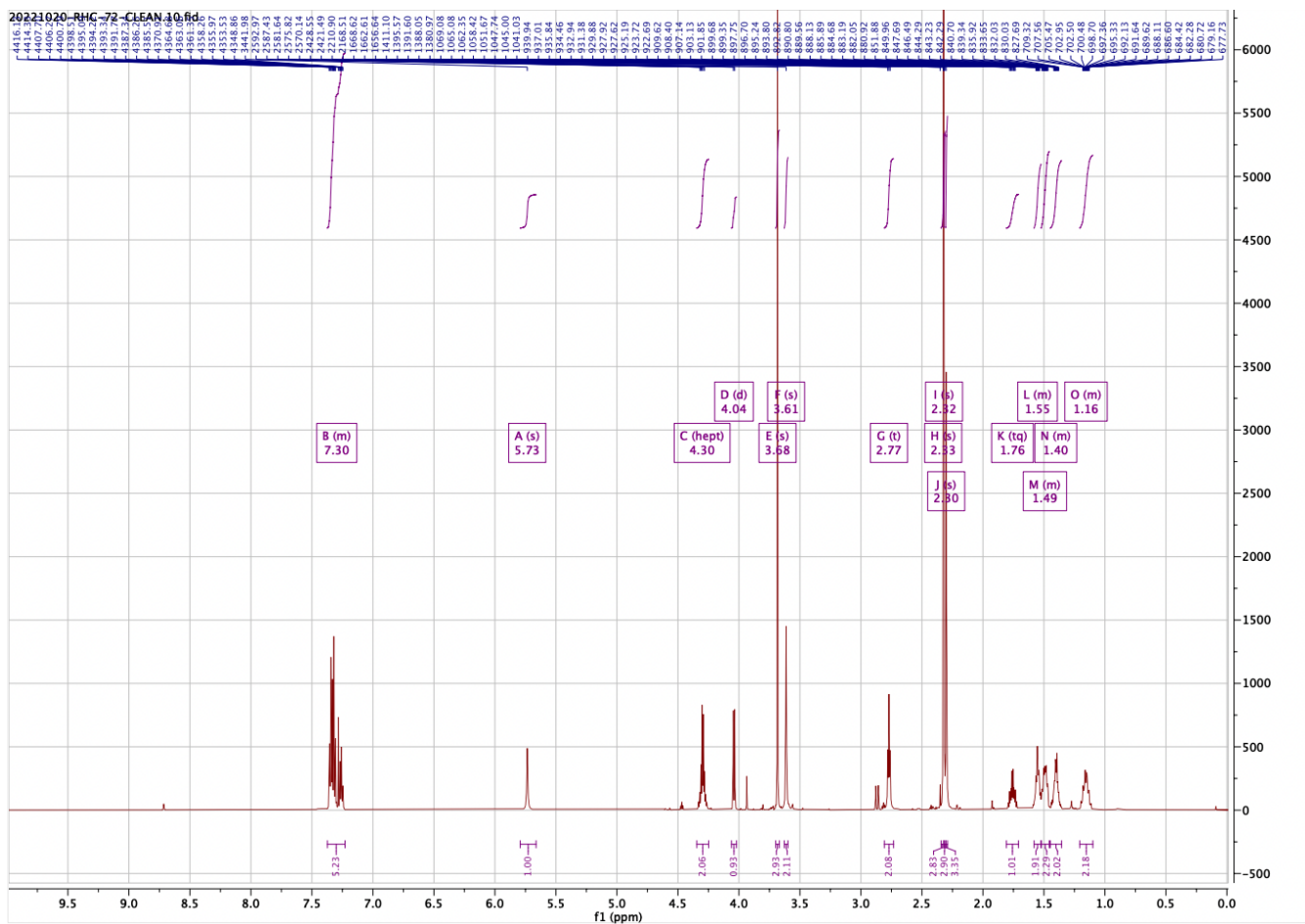


Figure 26. ¹H NMR (600 MHz, CDCl₃)



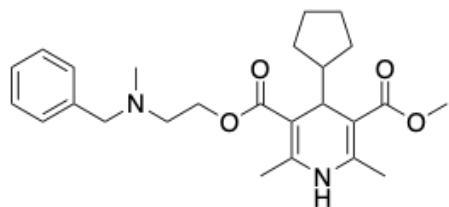
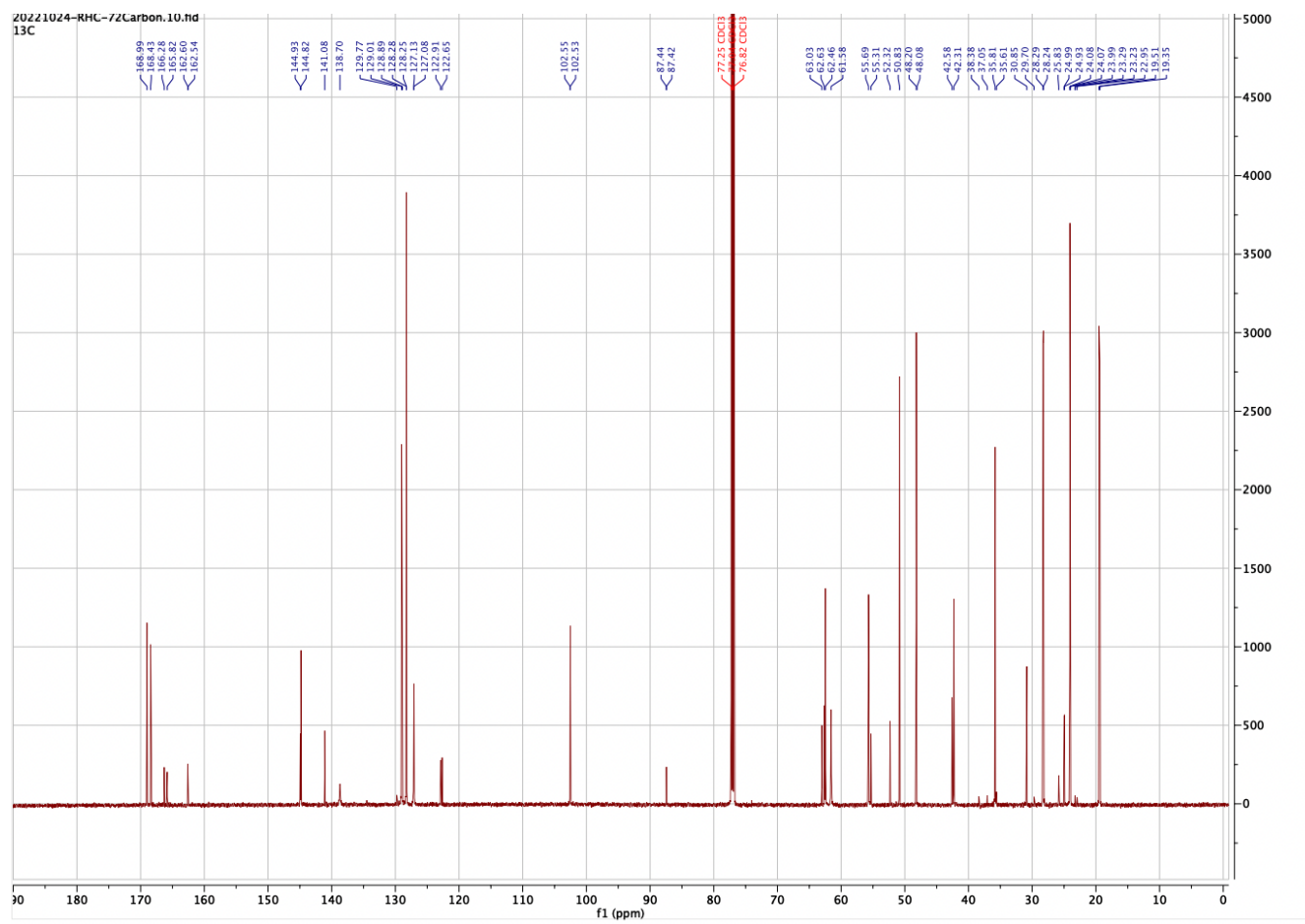


Figure 27. ^{13}C NMR (600 MHz, CDCl_3)



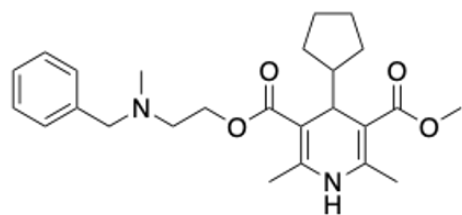
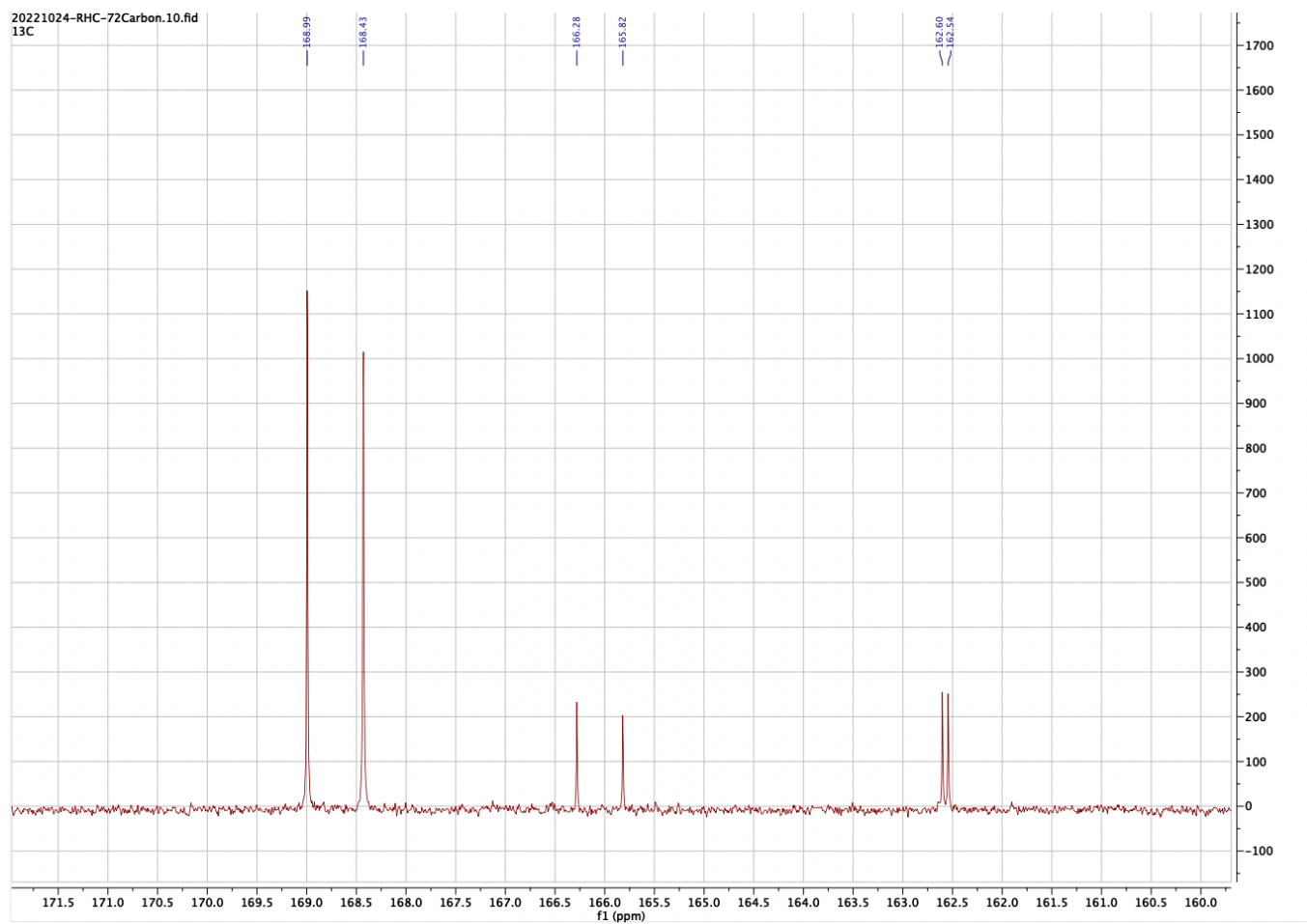


Figure 28. ^{13}C NMR (600 MHz, CDCl_3), 170 ppm region expansion (RHC-72).



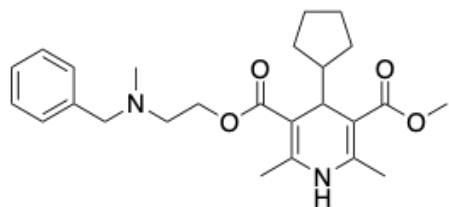
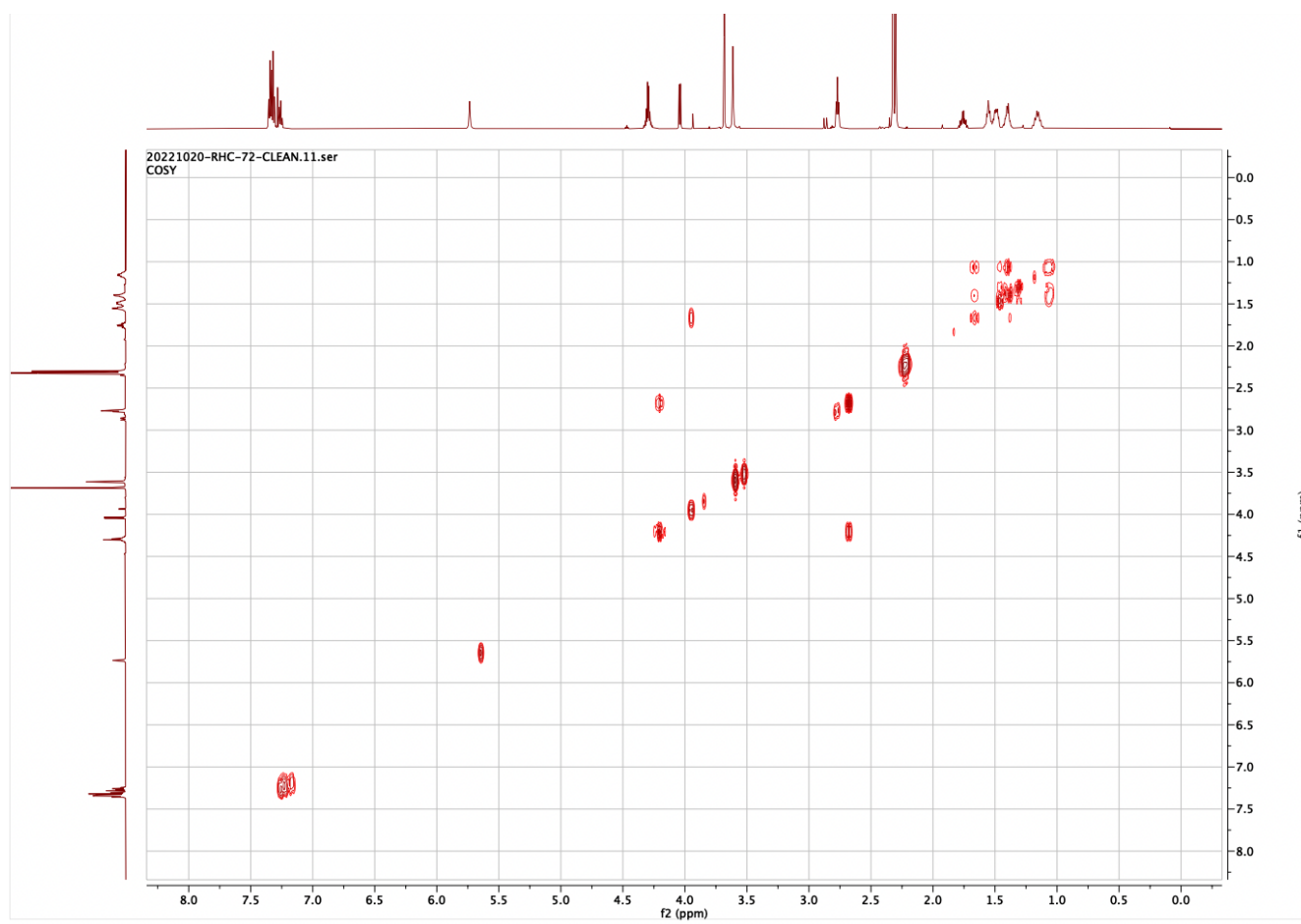


Figure 29. COSY NMR (600 MHz, CDCl₃)



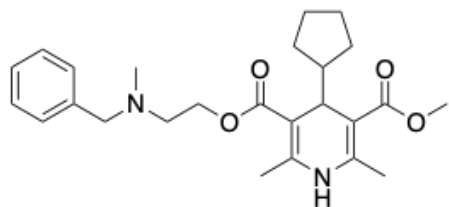
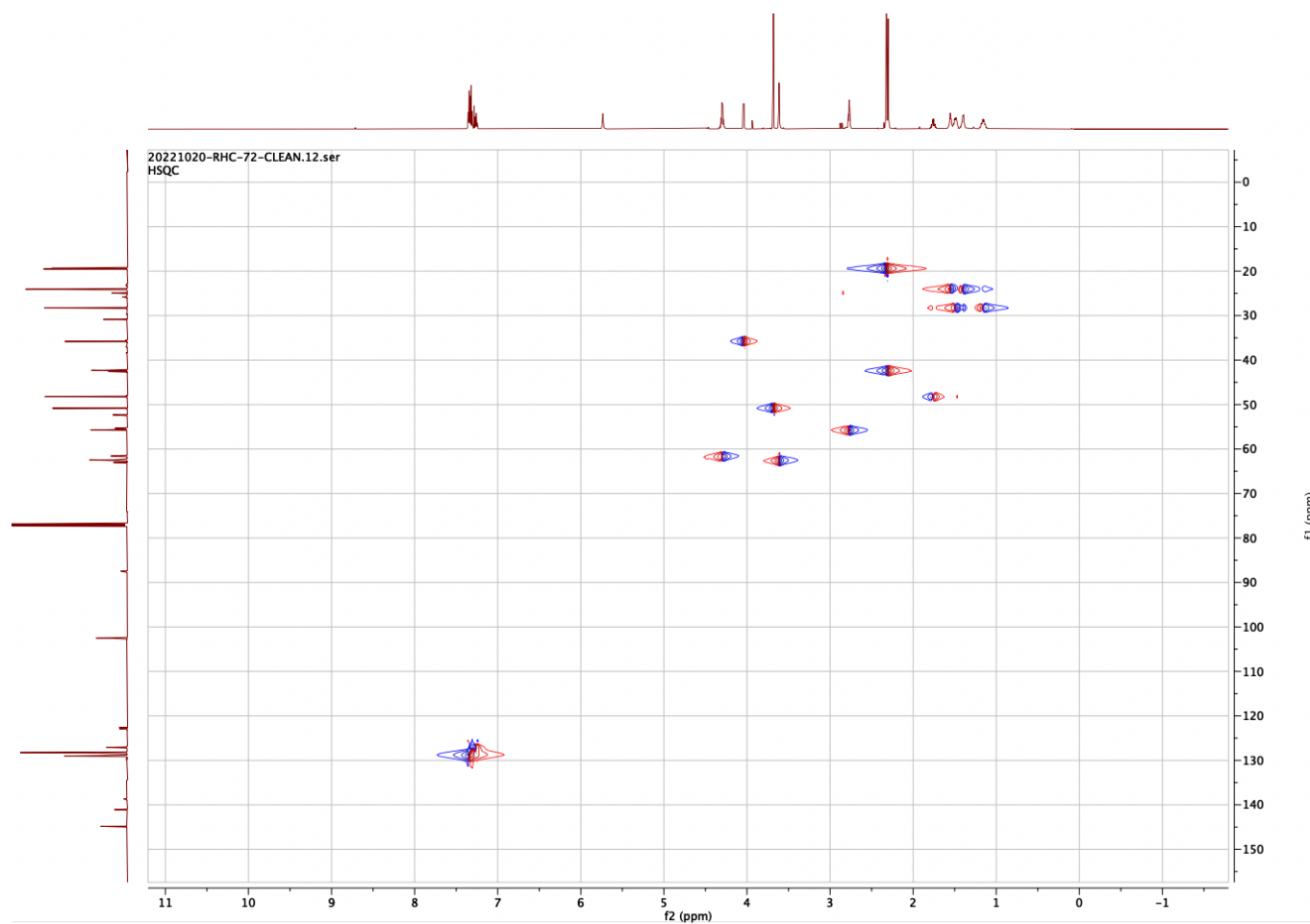


Figure 30. HSQC NMR (600 MHz, CDCl₃)



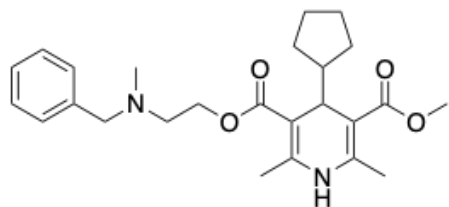
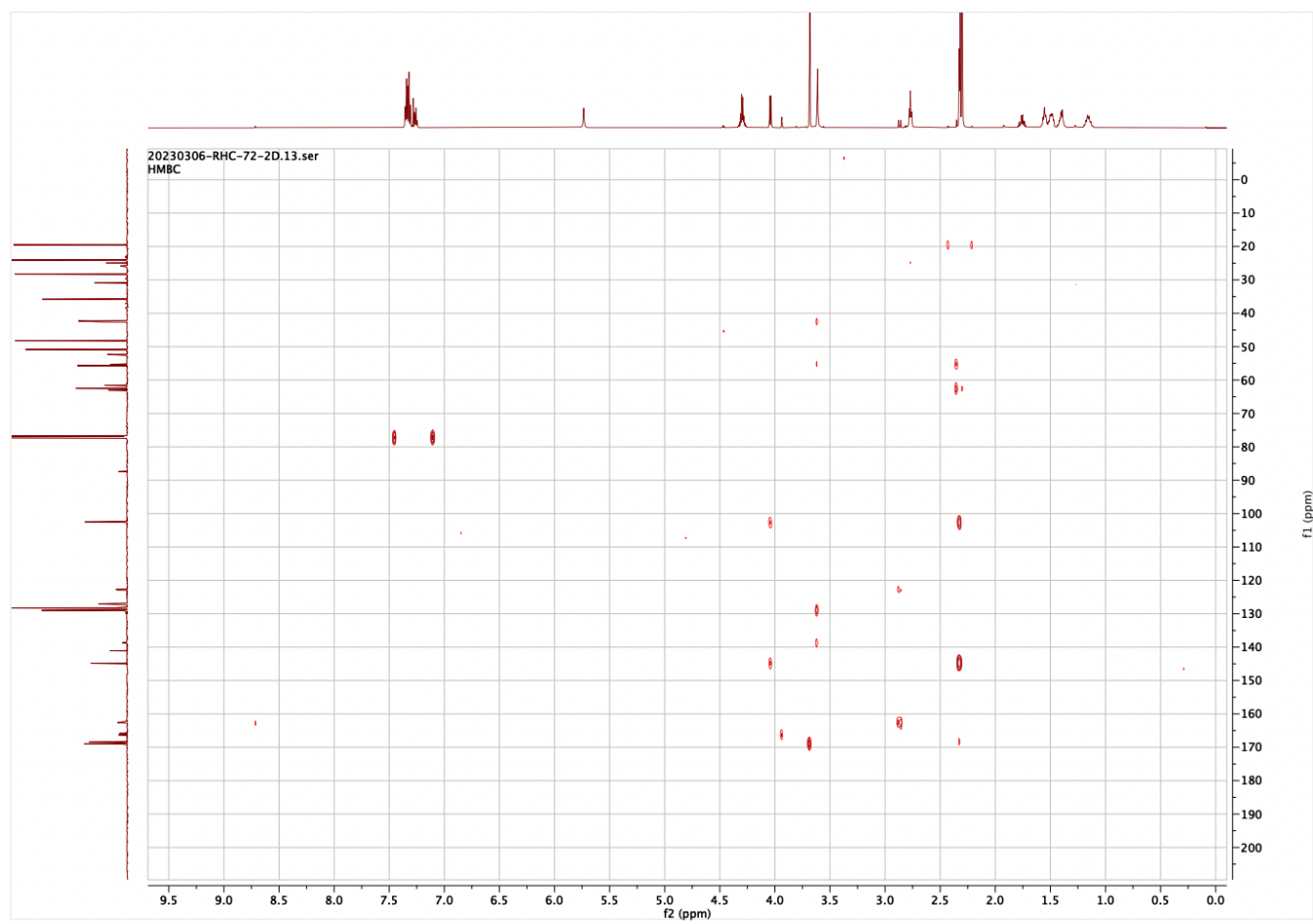


Figure 31. HMBC NMR (600 MHz, CDCl₃)



3-(2-(benzyl(methyl)amino)ethyl) 5-methyl 4-isopropyl-2,6-dimethyl-1,4-dihydropyridine- 3,5-dicarboxylate (RHC-73).

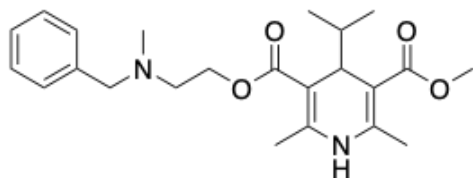
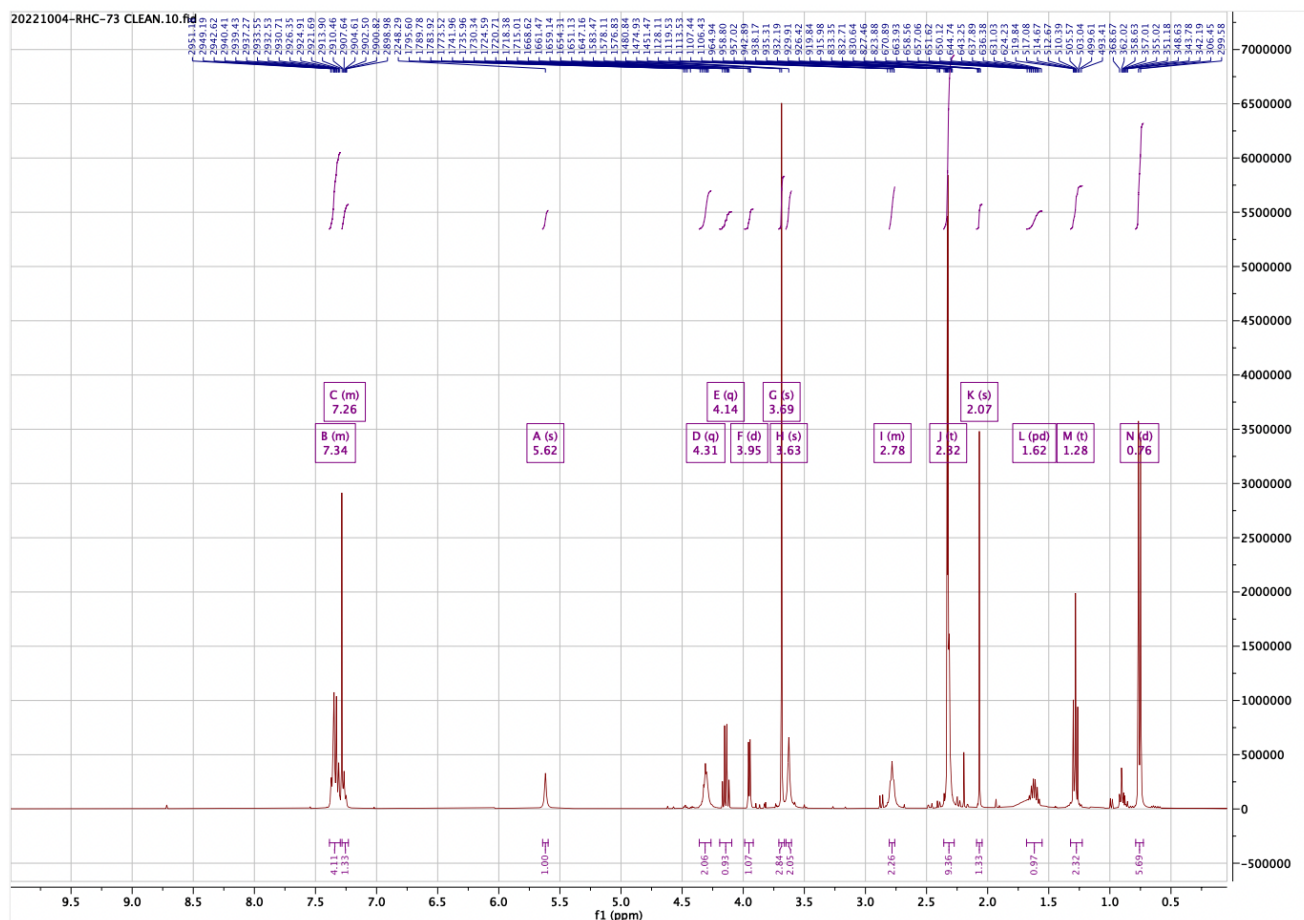


Figure 32. ¹H NMR (600 MHz, CDCl₃)



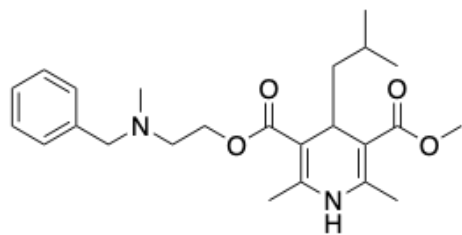
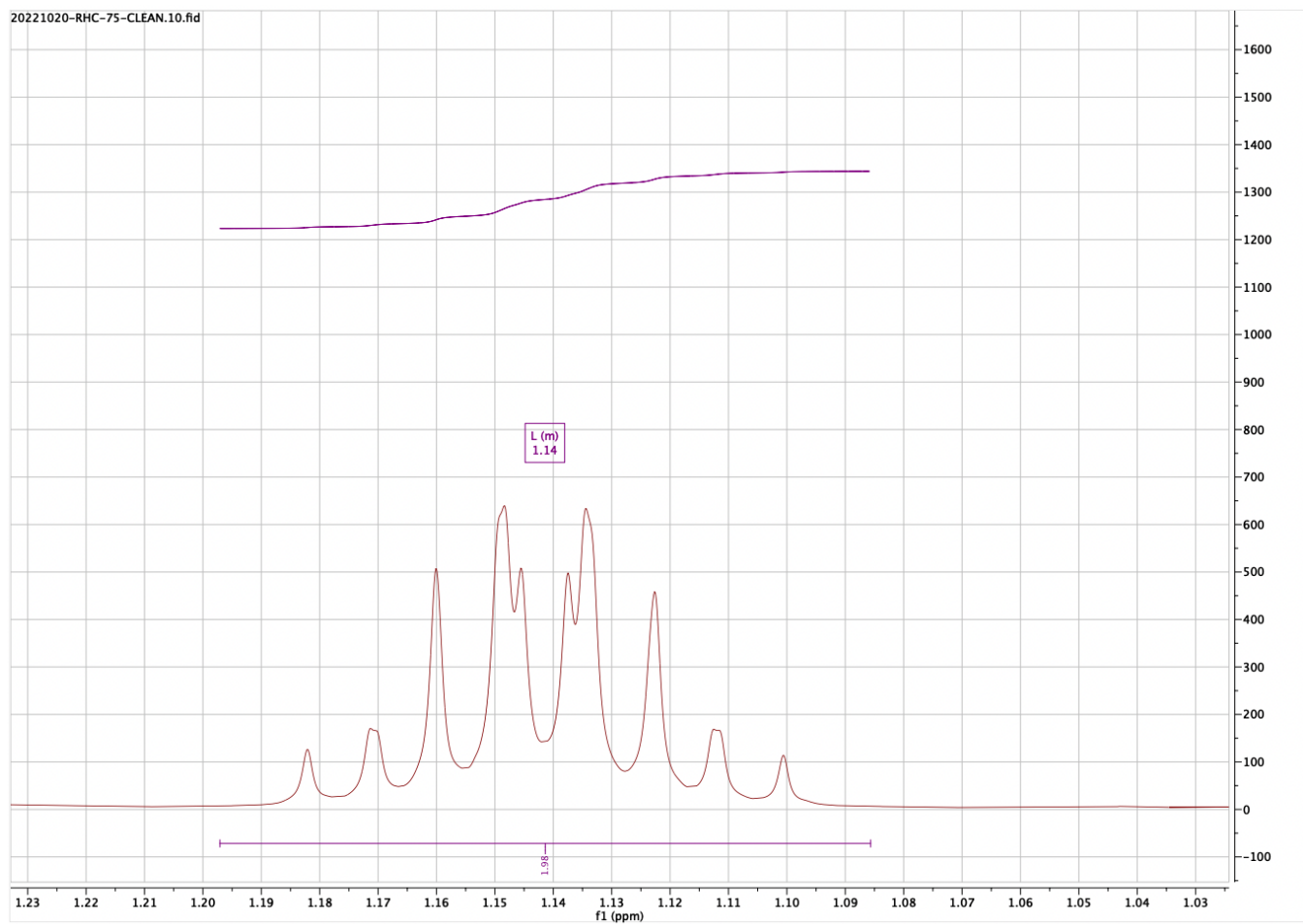


Figure 34. ^1H NMR (600 MHz, CDCl_3), 1.14 ppm region expansion.



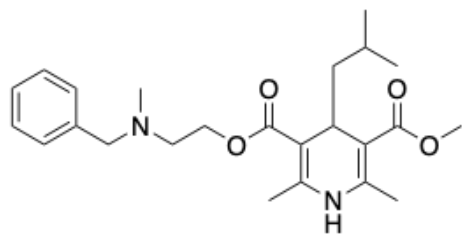
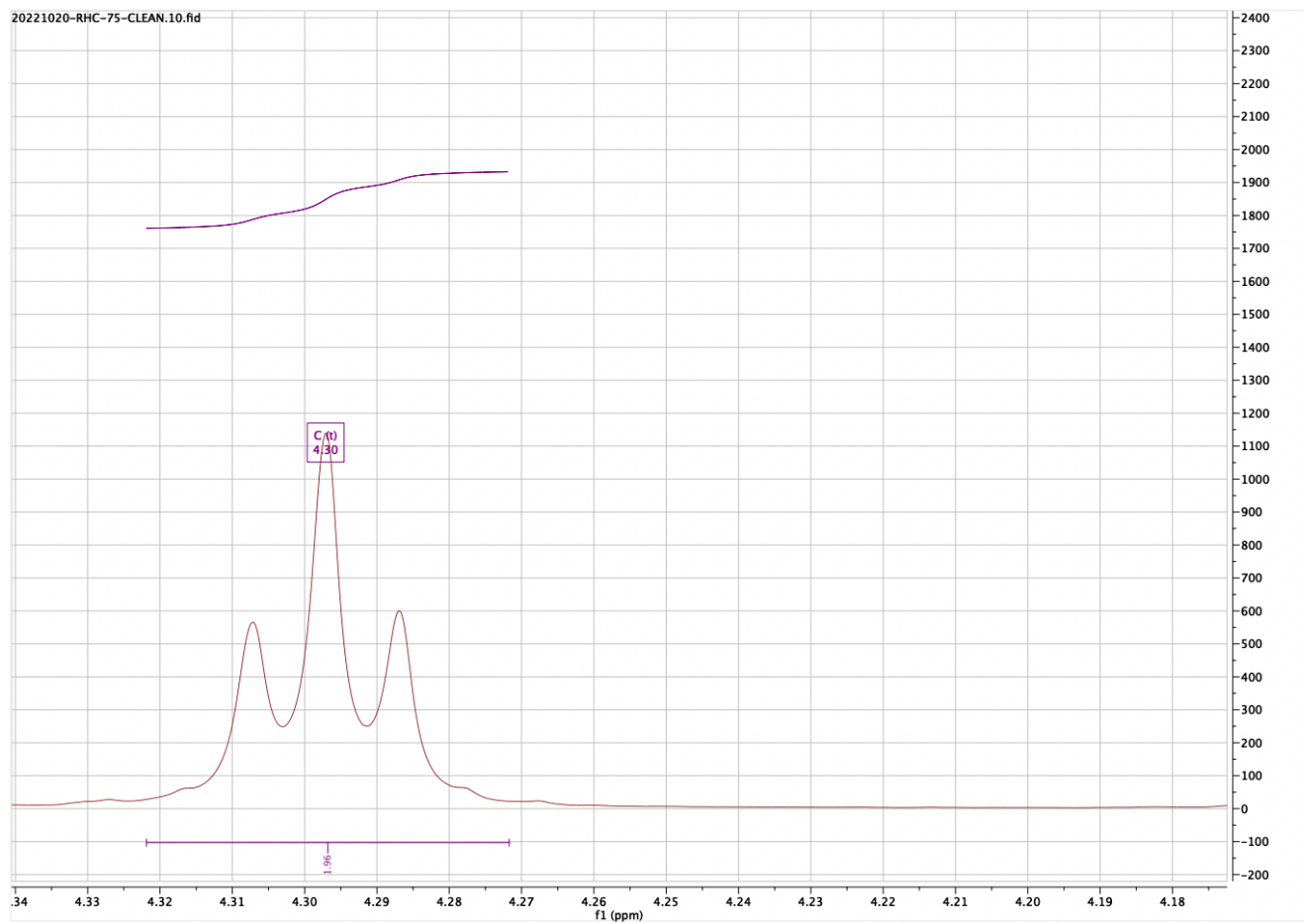


Figure 35. ^1H NMR (600 MHz, CDCl_3), 4.30 ppm region expansion.



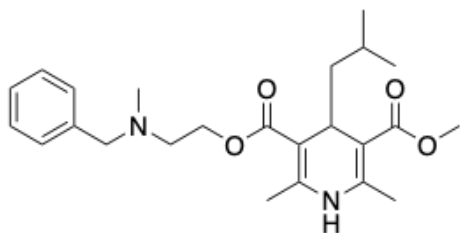
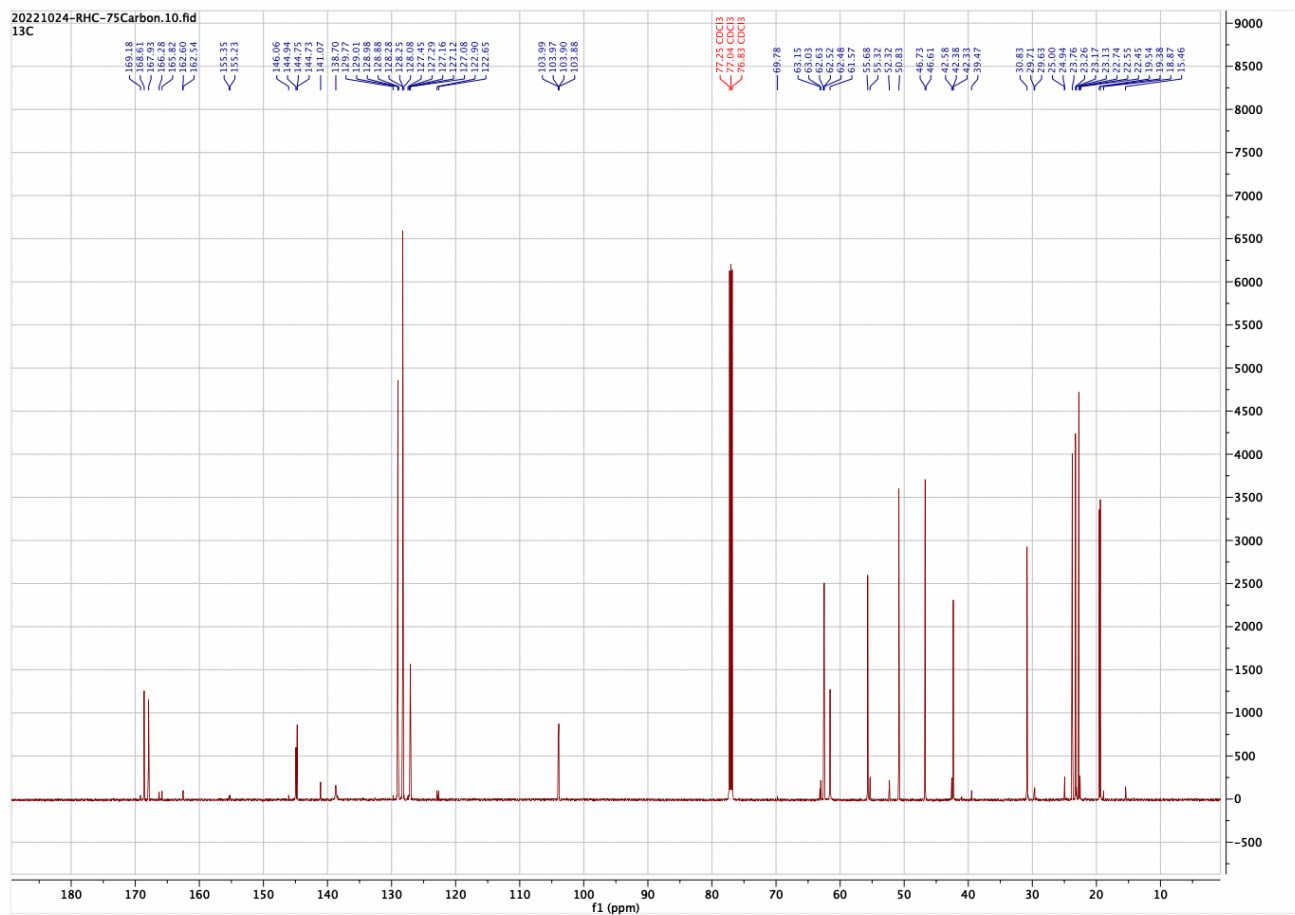


Figure 36. ^{13}C NMR (600 MHz, CDCl_3)



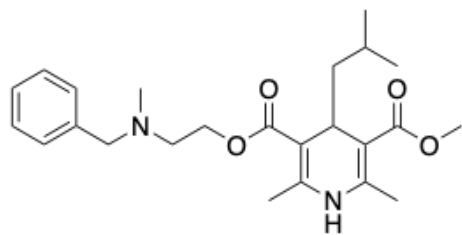
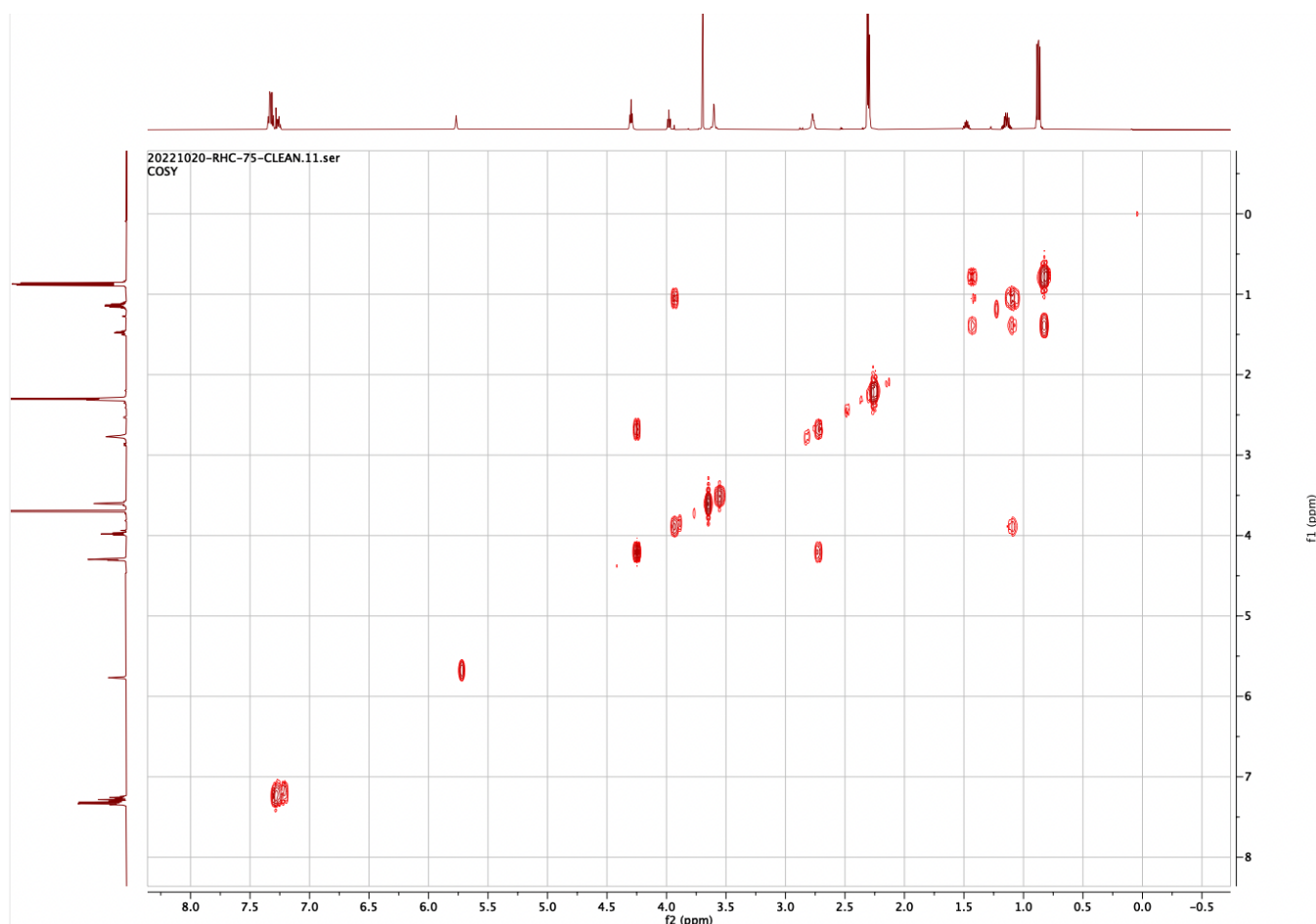


Figure 37. COSY NMR (600 MHz, CDCl₃)



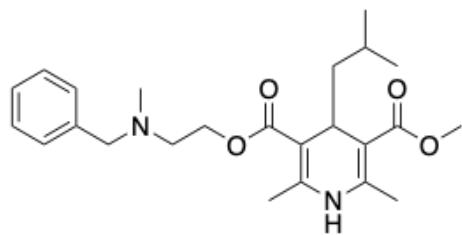
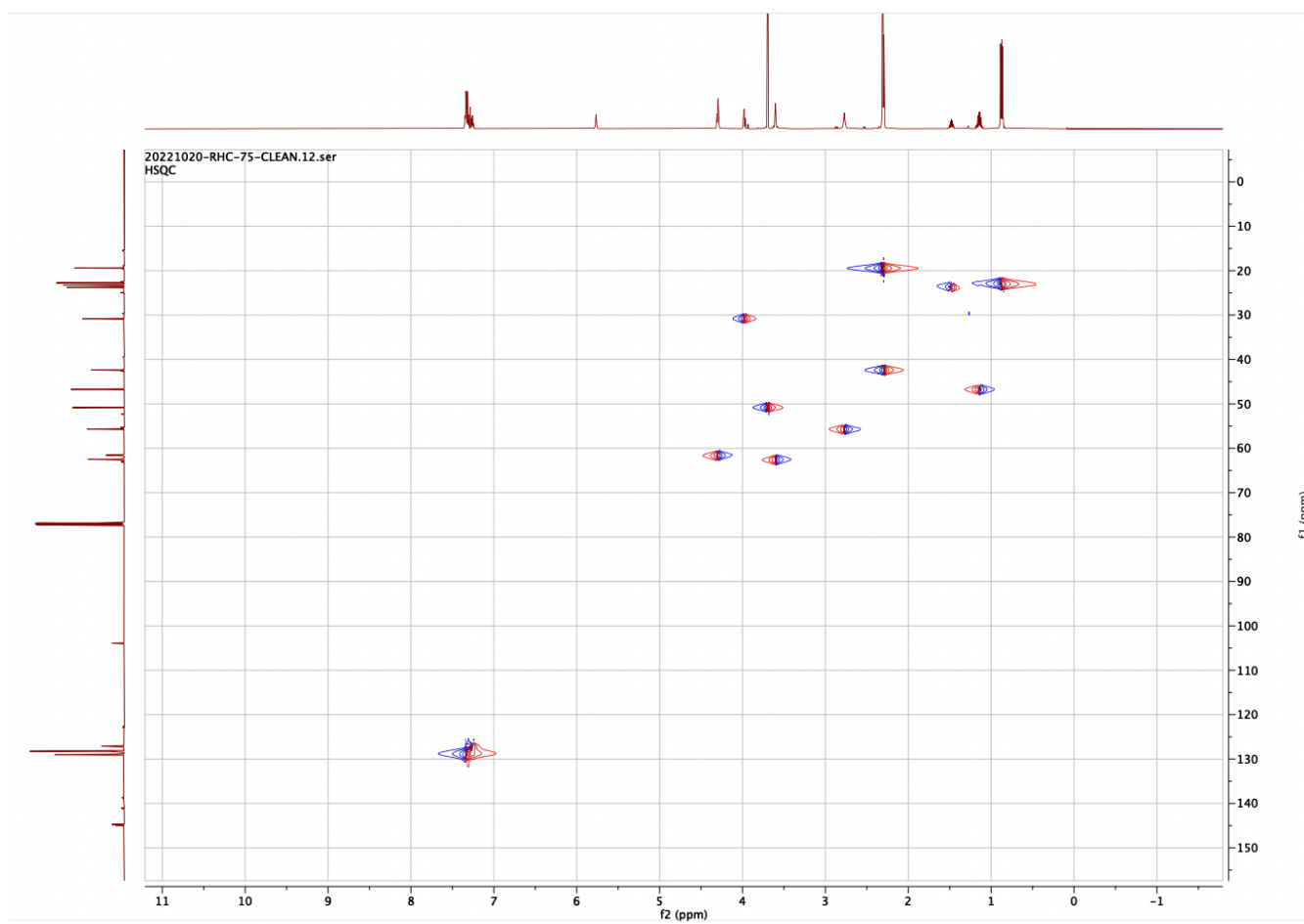


Figure 38. HSQC NMR (600 MHz, CDCl₃)



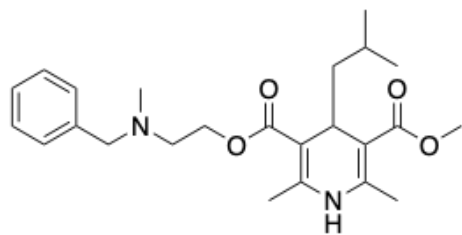
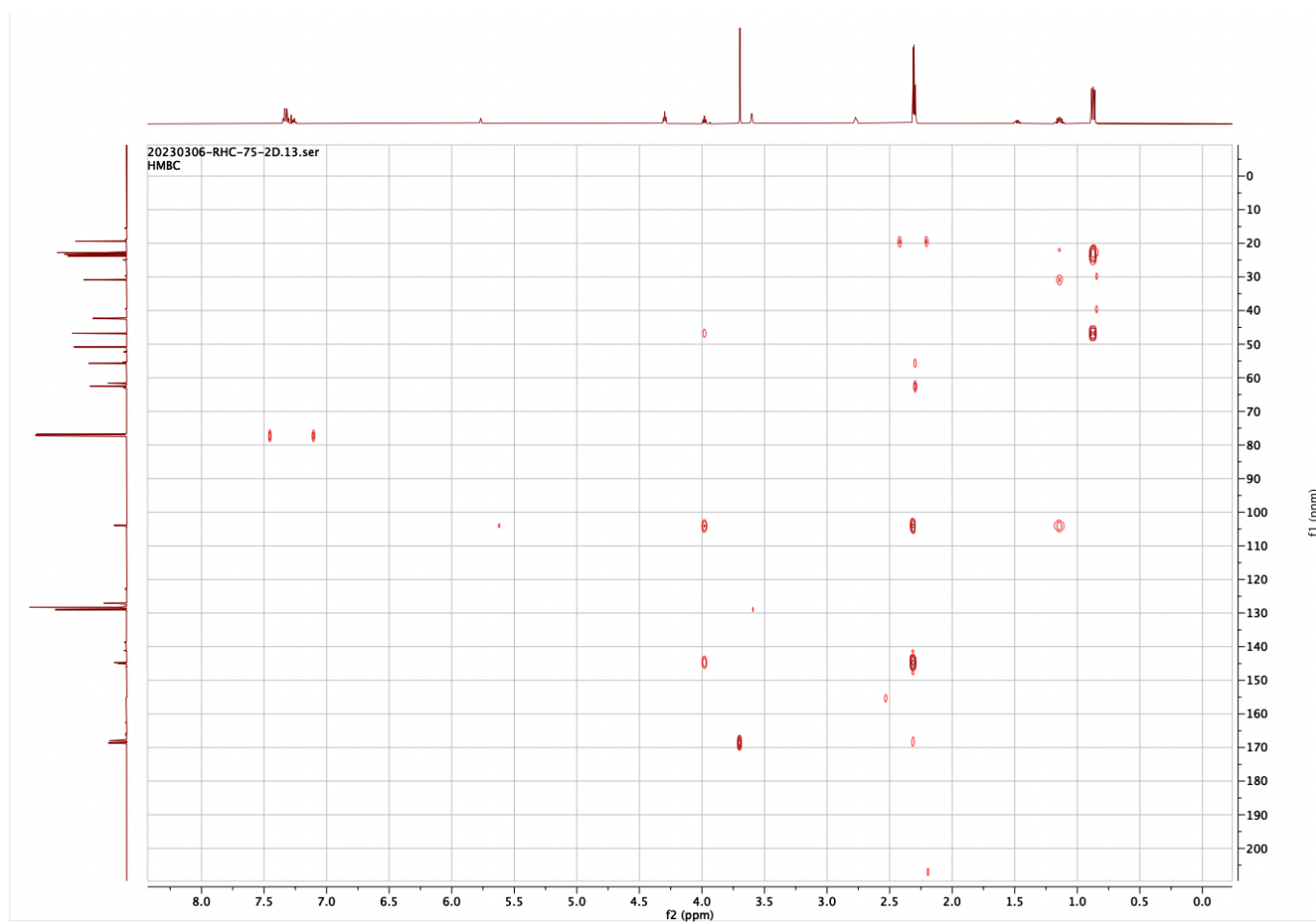


Figure 39. HMBC NMR (600 MHz, CDCl₃)



3-(2-(benzyl(methyl)amino)ethyl) 5-methyl 4-cyclopropyl-2,6-dimethylpyridine-3, 5-dicarboxylate (RHC-76).

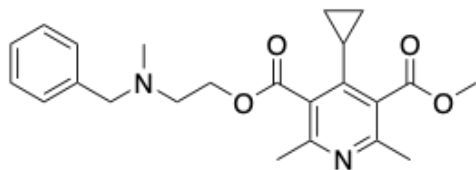


Figure 40. ^1H NMR (600 MHz, CDCl_3)



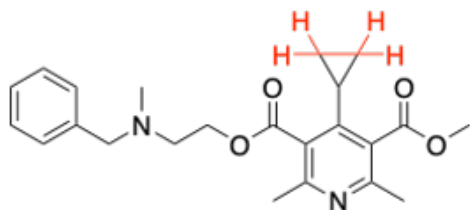
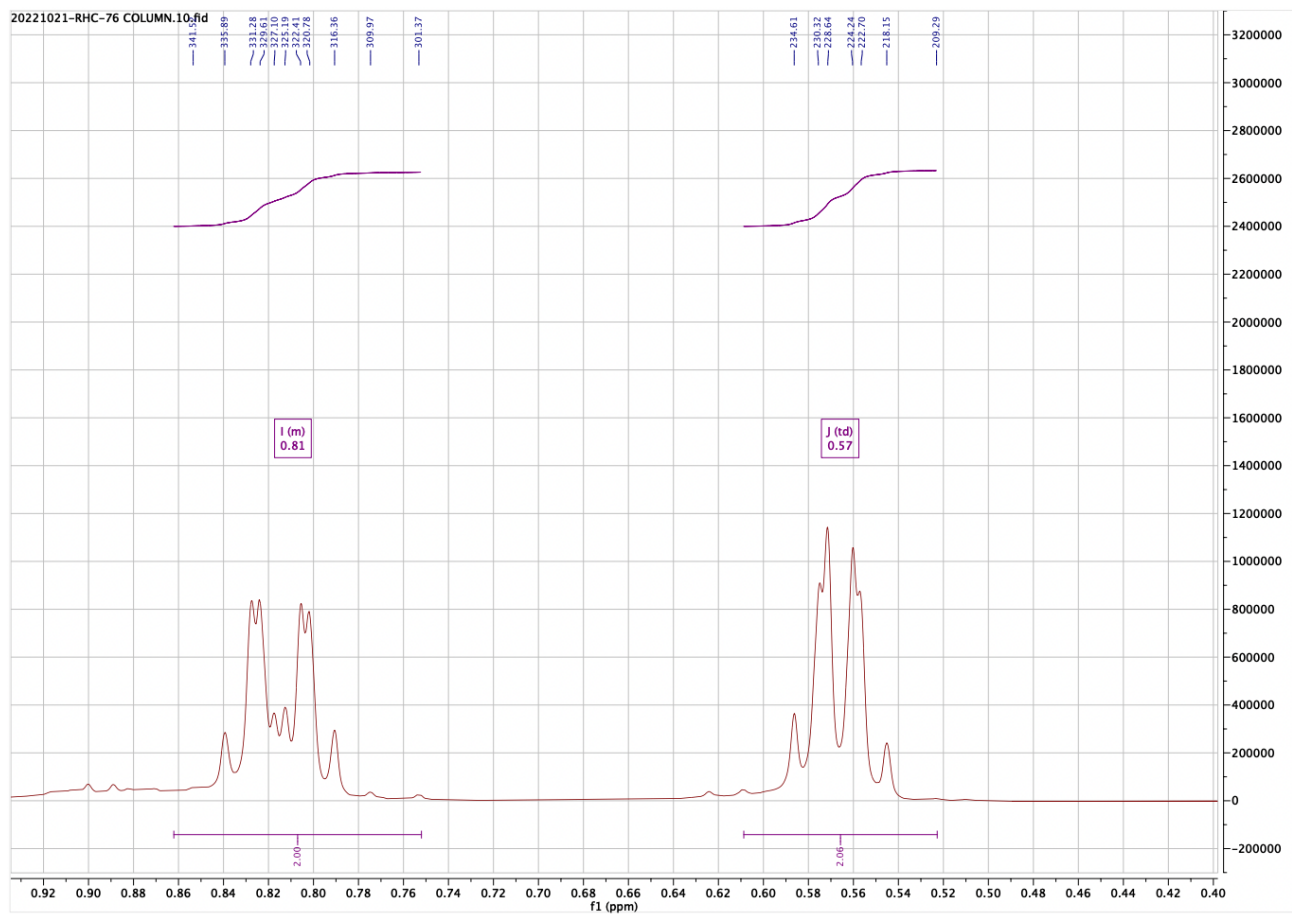


Figure 41. ^1H NMR (600 MHz, CDCl_3), alkyl region expansion in the 0.81 ppm and 0.57 ppm.



3-(2-(benzyl(methyl)amino)ethyl) 5-methyl 4-(cyclopentylmethyl)-2,6-dimethyl-1,4-dihydropyridine-3,5-dicarboxylate (RHC-88).

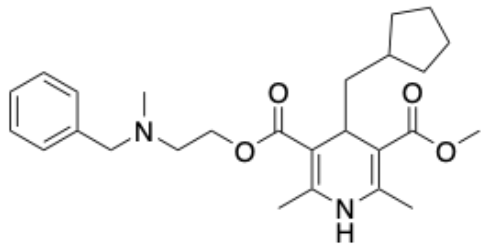
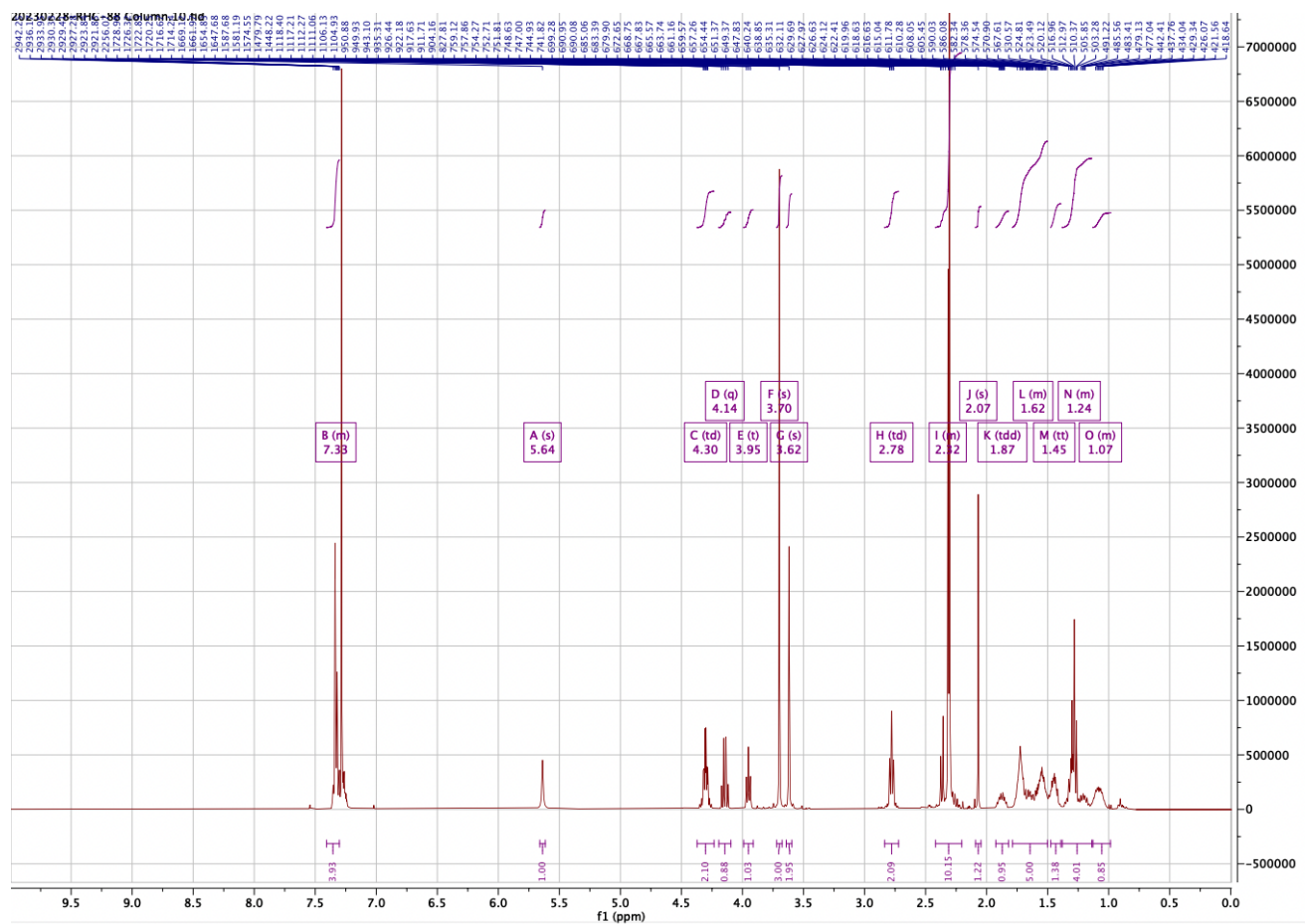


Figure 42. ^1H NMR (600 MHz, CDCl_3)



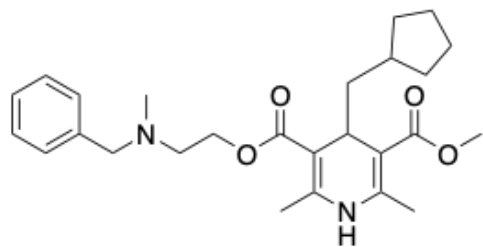
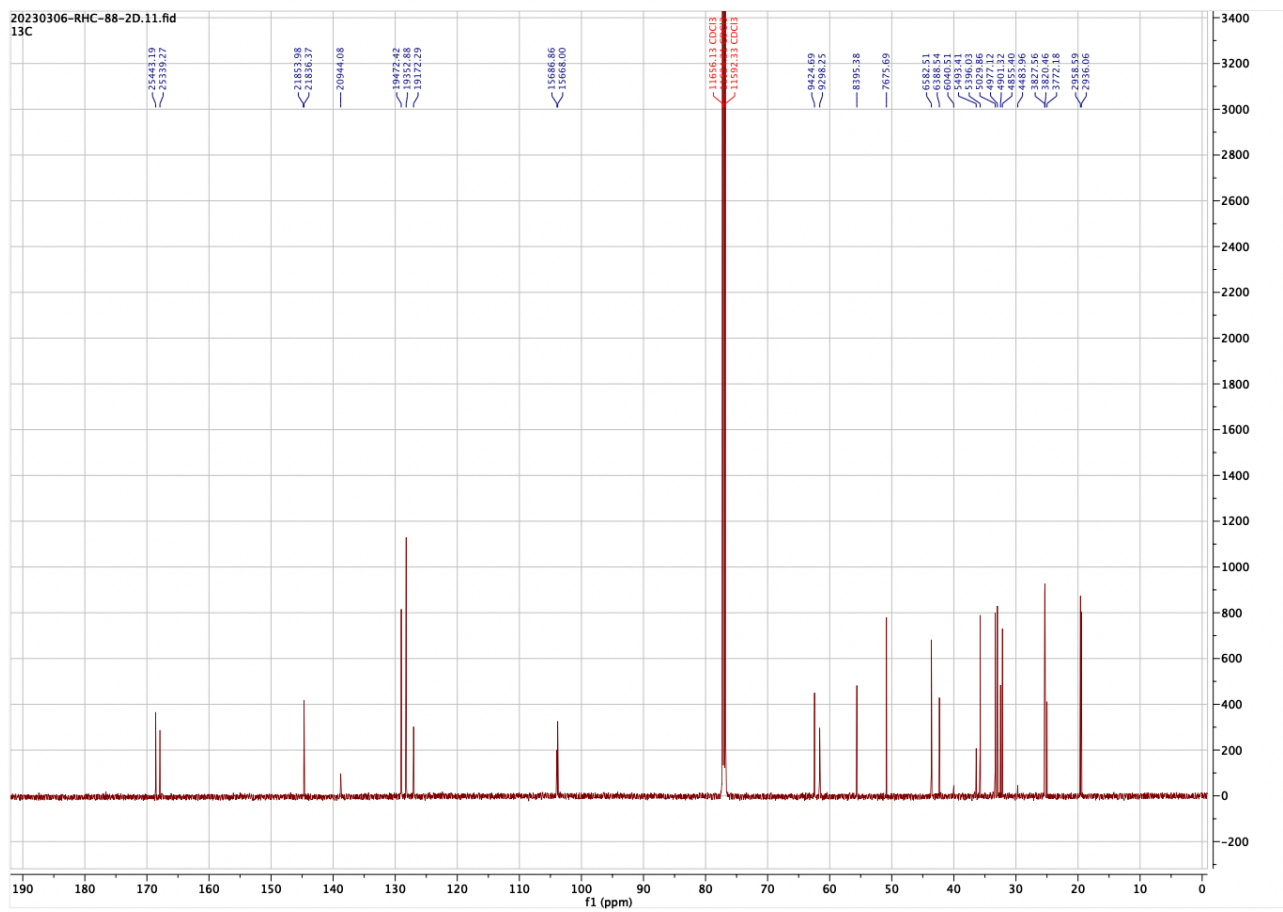


Figure 43. ^{13}C NMR (600 MHz, CDCl_3)



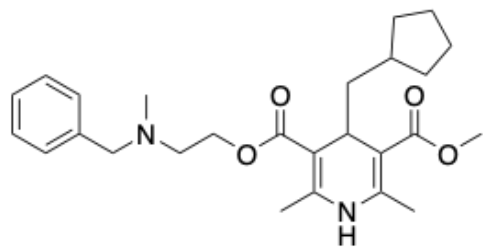
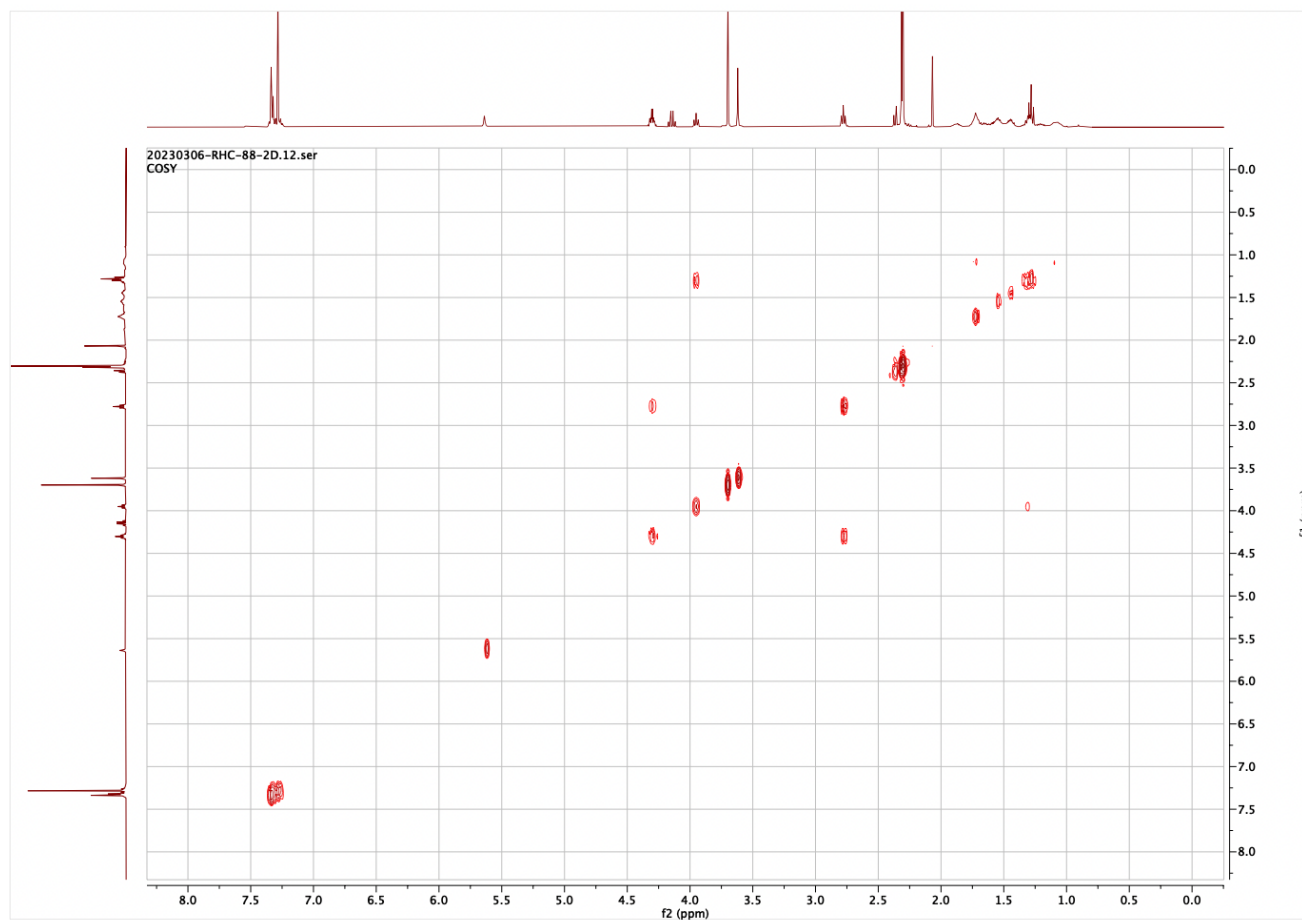


Figure 44. COSY NMR (600 MHz, CDCl₃)



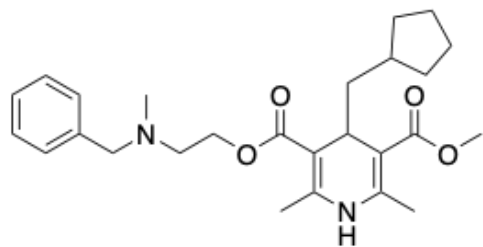


Figure 45. HSQC NMR (600 MHz, CDCl₃)



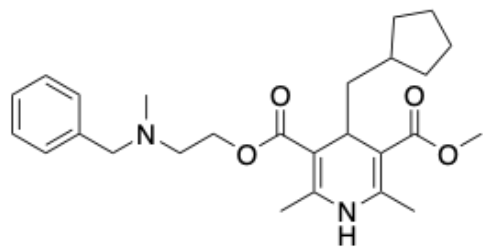
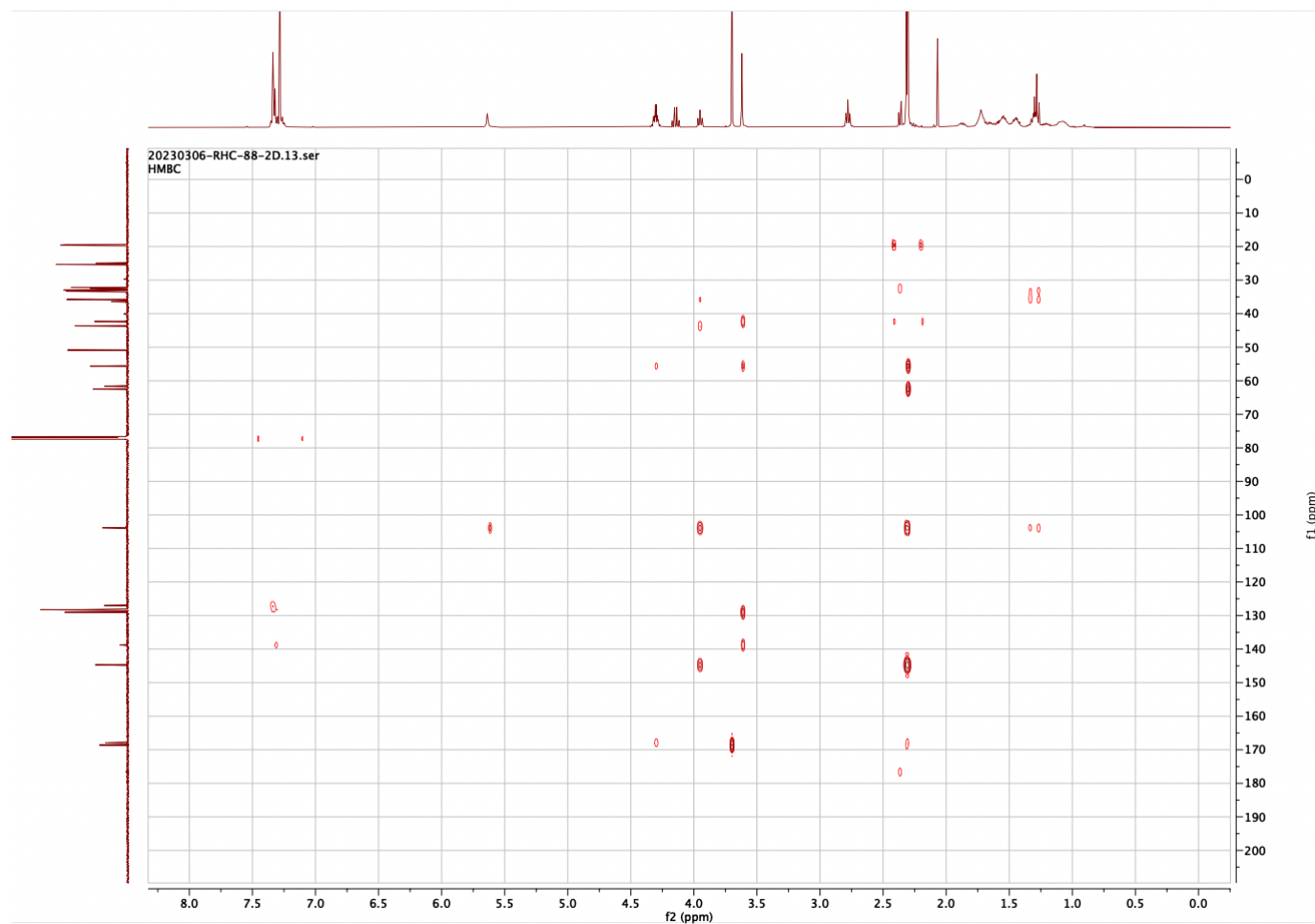


Figure 46. HMBC NMR (600 MHz, CDCl₃)



3-(2-(benzyl(methyl)amino)ethyl) 5-methyl 2,6-dimethyl-4-(pentan-3-yl)-1,4-dihydropyridine - 3,5-dicarboxylate (RHC-89).

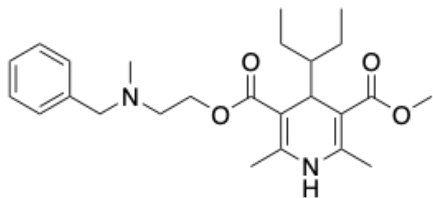
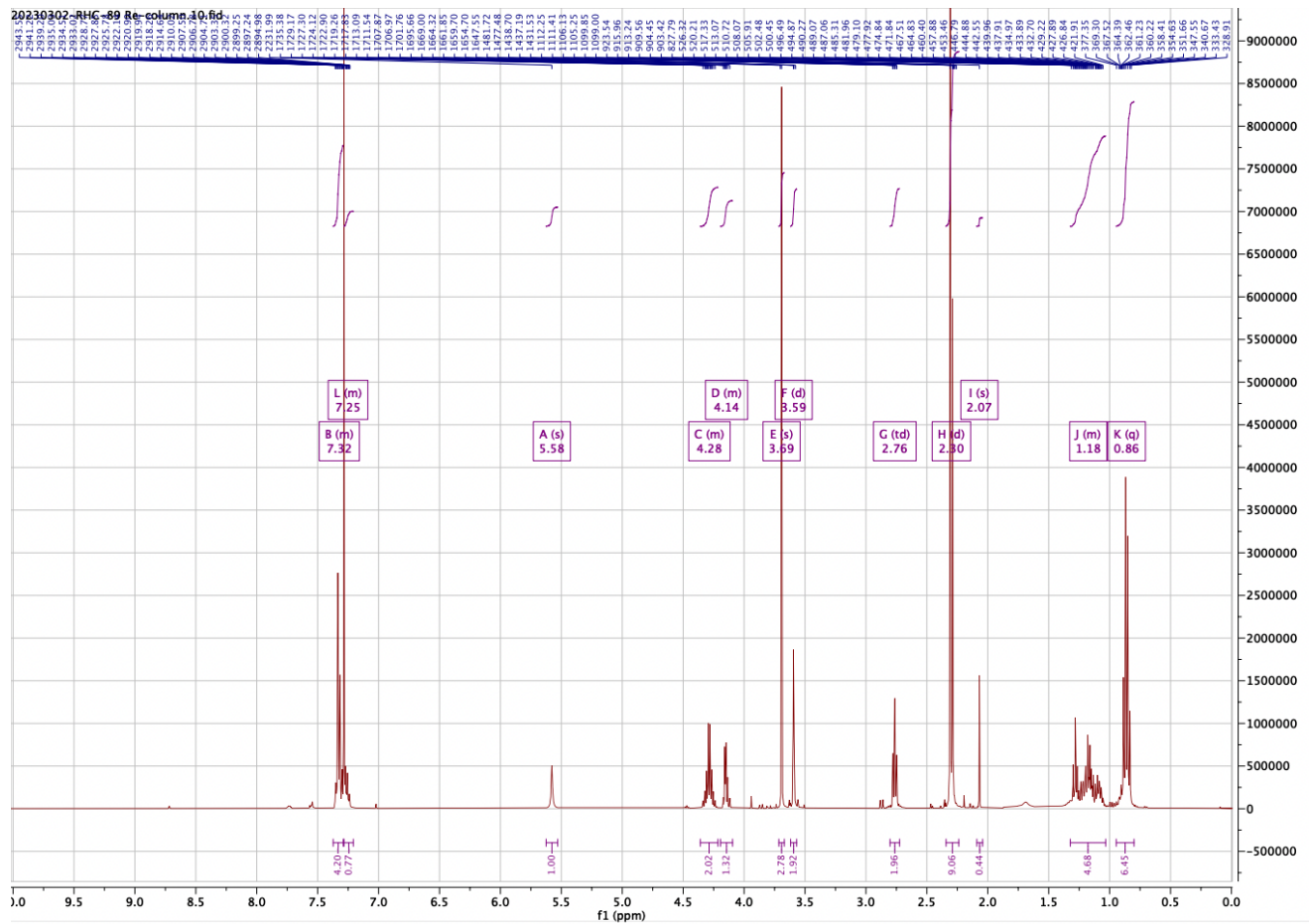


Figure 47. ^1H NMR (600 MHz, CDCl_3)



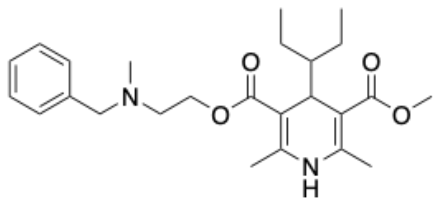
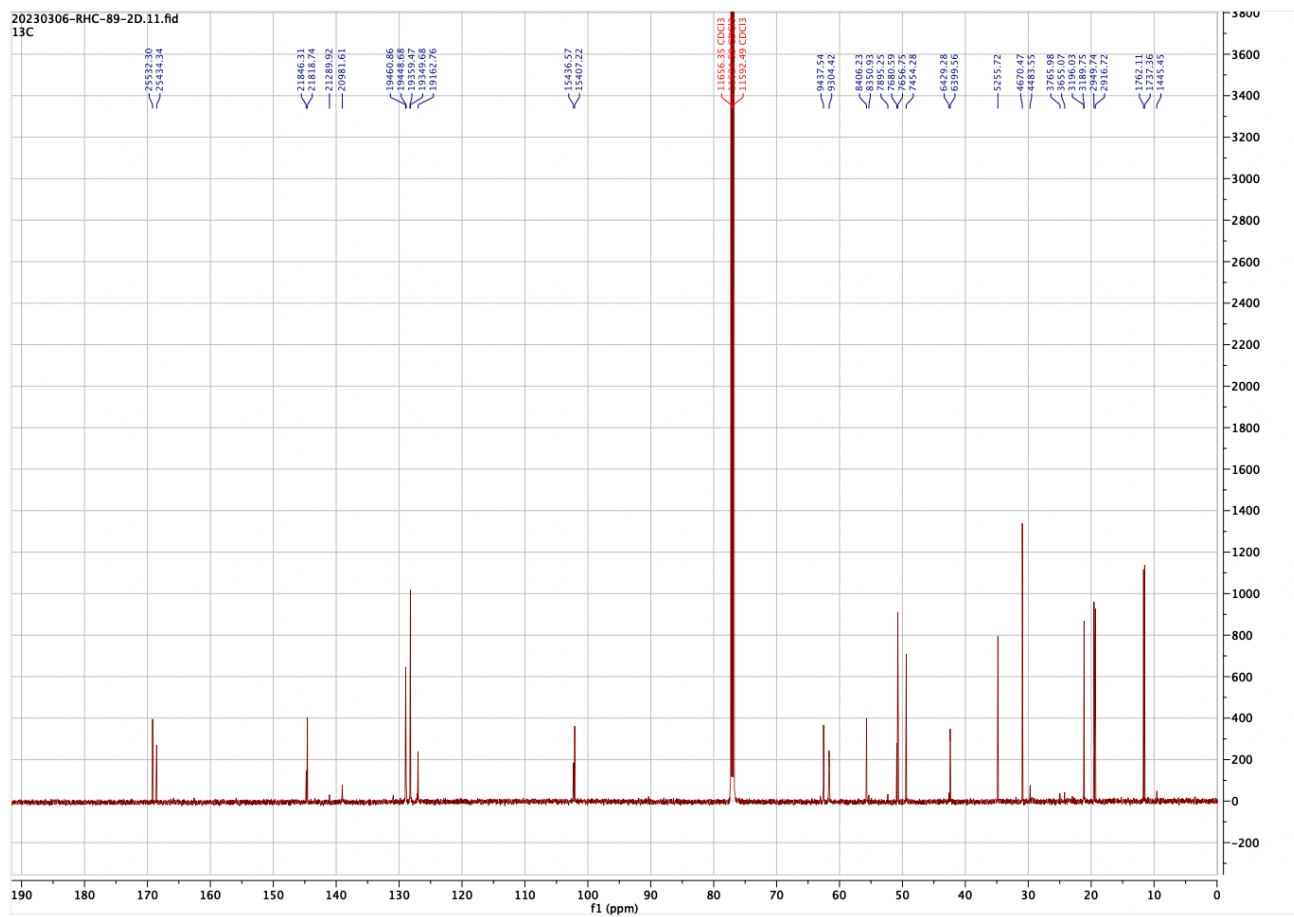


Figure 48. ^{13}C NMR (600 MHz, CDCl_3)



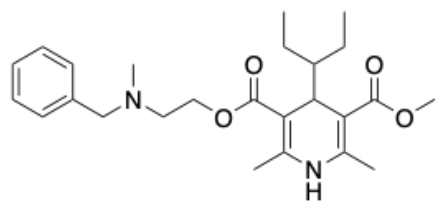
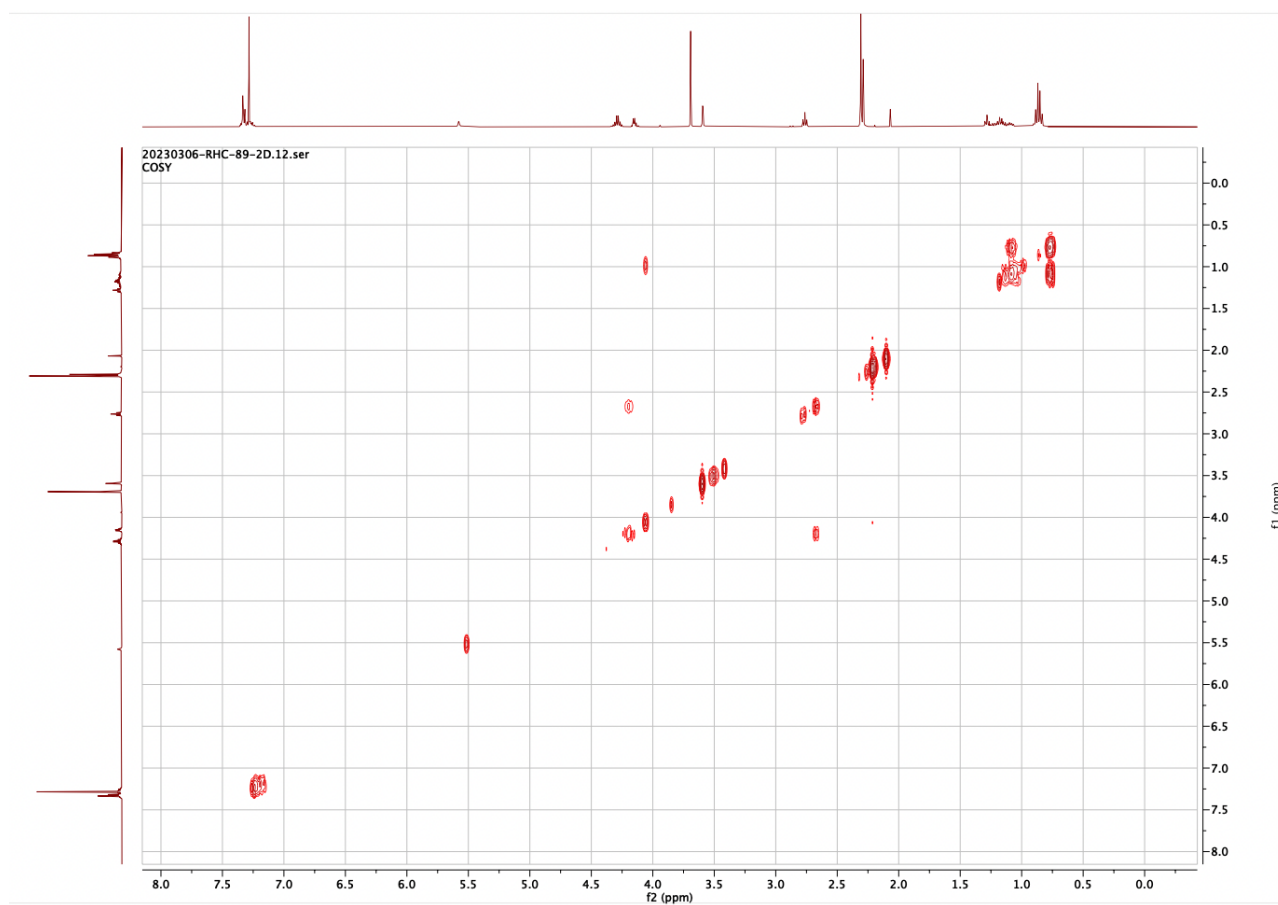


Figure 49. COSY NMR (600 MHz, CDCl₃)



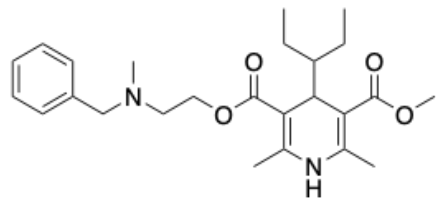
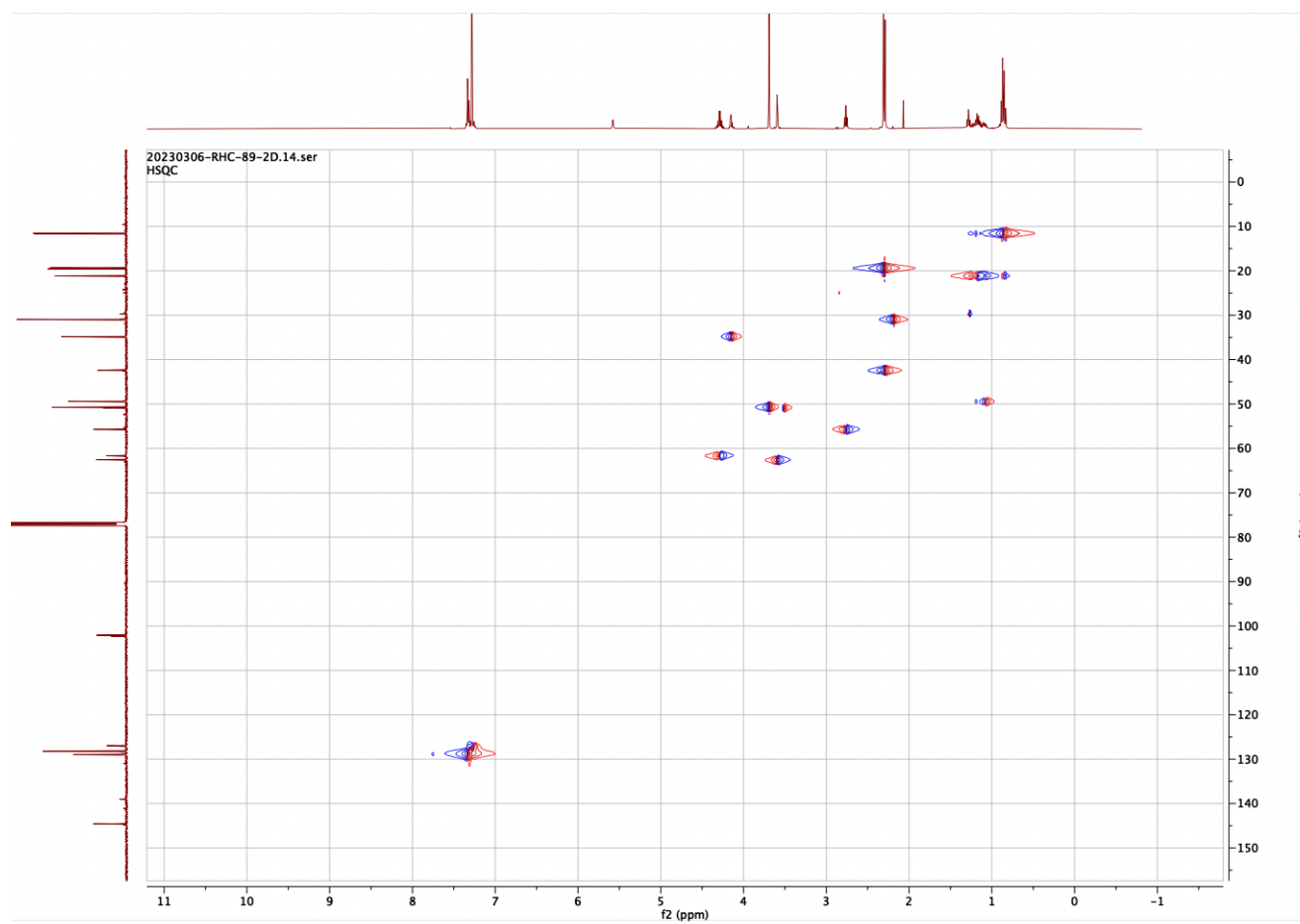


Figure 50. HSQC NMR (600 MHz, CDCl₃)



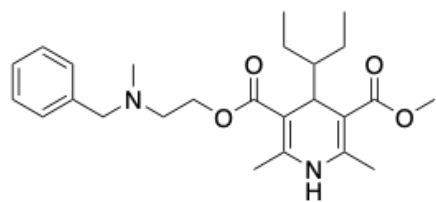
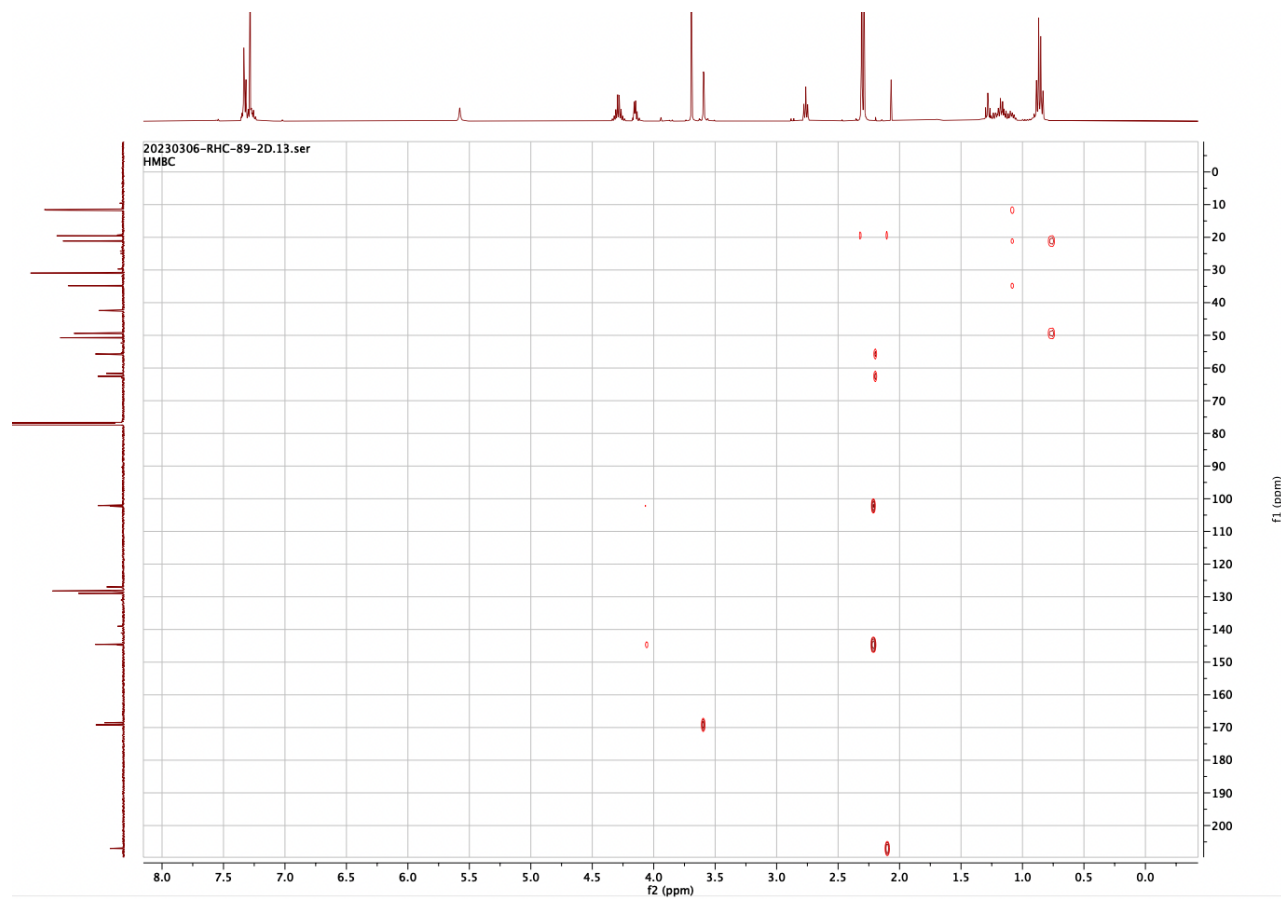


Figure 51. HMBC NMR (600 MHz, CDCl₃)



2-(Benzylmethylamino) ethyl acetoacetate

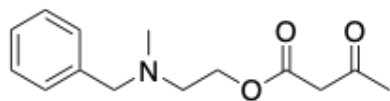
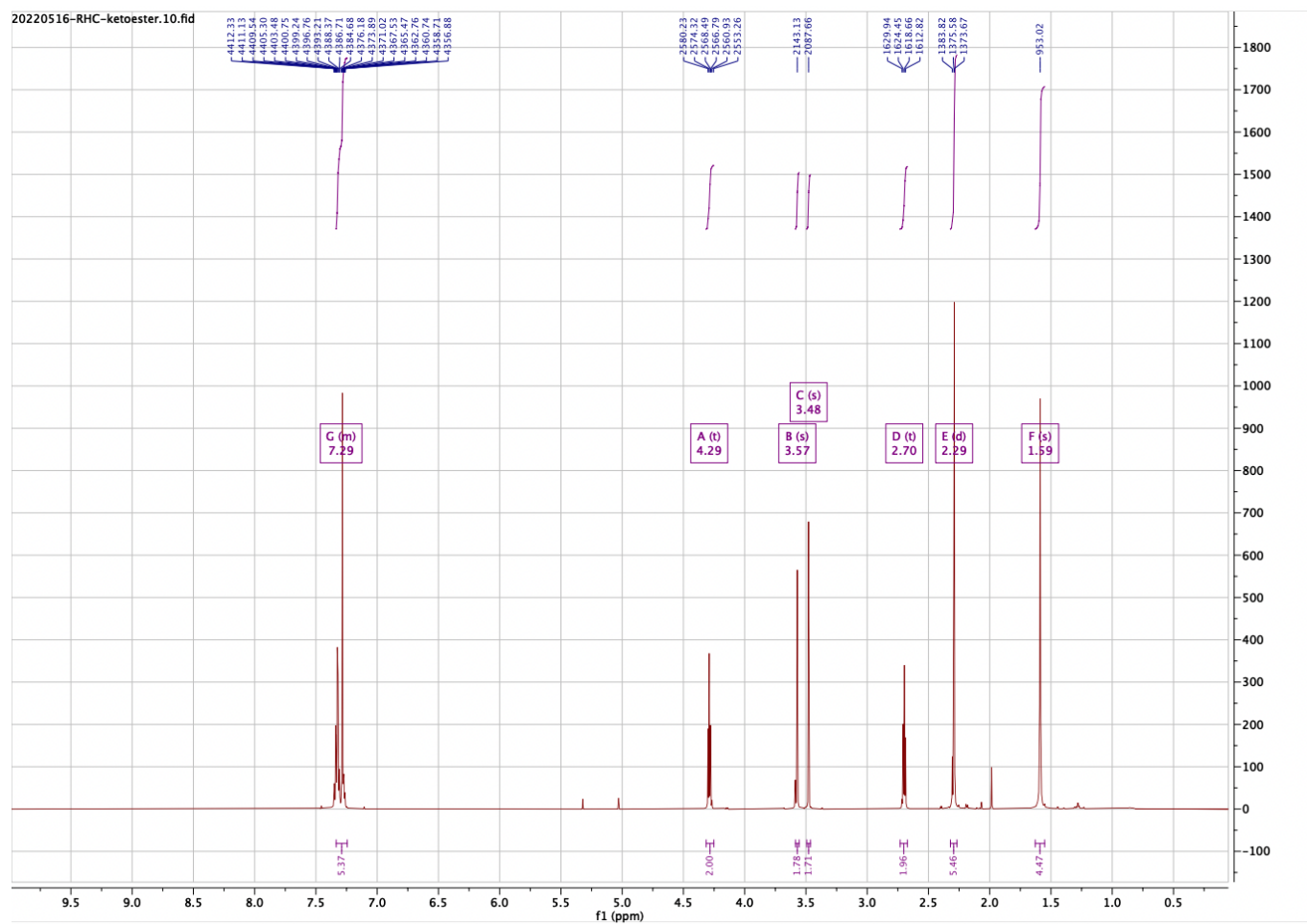


Figure 52. ^1H NMR (400 MHz, CDCl_3)



Cyclobutanecarbaldehyde (crude from DMP oxidation).

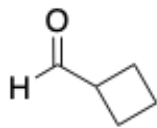


Figure 54. ^1H NMR (400 MHz, CDCl_3)

